DEVELOPMENT AND IMPLEMENTATION OF AN AUTOMATED SEM-EDX ROUTINE FOR CHARACTERIZING RESPIRABLE COAL MINE DUST

Victoria Anne Johann

Thesis submitted to the faculty of the Virginia Polytechnic Institute and State University in partial fulfillment of the requirements for the degree of

Master of Science
In
Mining Engineering

Emily Sarver, Chair

Nino Ripepi
Cigdem Keles

September 8, 2016
Blacksburg, VA

Keywords: Scanning Electron Microscopy (SEM), Computer-Automated SEM-EDX, Respirable Dust, Particle Cross-Sectional Diameter, Aspect Ratio, Chemical Composition, Coal Workers' Pneumoconiosis (CWP), Silicosis

DEVELOPMENT AND IMPLEMENTATION OF AN AUTOMATED SEM-EDX ROUTINE FOR CHARACTERIZING RESPIRABLE COAL MINE DUST

Victoria Anne Johann

ACADEMIC ABSTRACT

This thesis describes the development and use of a computer-automated microscopy routine for characterization of respirable dust particles from coal mines. Respirable dust in underground coal mining environments has long been known to pose an occupational health hazard for miners. Typically following years of exposure, coal workers' pneumoconiosis (CWP) and silicosis are the most common disease diagnoses. Although dramatic reductions in CWP and silicosis cases were achieved across the US between about 1970-1999 through a combination of regulatory dust exposure limits, improved ventilation and dust abatement practices, a resurgence in disease incidence has been noted more recently – particularly in parts of Appalachia. To shed light on this alarming trend and allow for better understanding of the role of respirable dust in development of disease, more must be learned about the specific characteristics of dust particles and occupational exposures.

This work first sought to develop an automated routine for the characterization of respirable dust using scanning electron microscopy with energy dispersive x-ray (SEM-EDX). SEM-EDX is a powerful tool that allows determination of the size, shape, and chemistry of individual particles, but manual operation of the instrument is very time consuming and has the potential to introduce user bias. The automated method developed here provides for much more efficient analysis – with a data capture rate that is typically 25 times faster than that of the manual method on which it was based – and also eliminates bias between users. Moreover, due to its efficiency and broader coverage of a dust sample, it allows for characterization of a larger and more representative number of particles per sample. The routine was verified using respirable dust samples generated from known materials commonly observed in underground coal mines in the central Appalachian region, as well as field samples collected in this region. This effort demonstrated that particles between about 1-9μm were accurately classified with respect to defined chemical categories, and suggested that analysis of 500 particles across a large area of a sample filter generally provides representative results.

The automated SEM-EDX routine was then used to characterize a total of 210 respirable dust samples collected in eight Appalachian coal mines. The mines were located in three distinct regions (i.e., northern, mid-central and south-central Appalachia), which differed in terms of primary mining method, coal seam thickness and mining height, and coal and/or rock mineralogy. Results were analyzed to determine whether number distributions of particle size, aspect ratio, and chemistry classification vary between and within distinct mine regions, and by general sampling location categories (i.e., intake, feeder, production, return). Key findings include:

1) Northern Appalachian mines have relatively higher fractions of coal, carbonate, and heavy mineral particles than the two central Appalachian regions, whereas central Appalachian mines have higher fractions of quartz and alumino-silicate particles.

2) Central Appalachian mines tended to have more mine-to-mine variations in size, shape, and chemistry distributions than northern Appalachian mines.

3) With respect to particle size, samples collected in locations in the production and return categories have the highest percentages of very small particles (i.e., 0.94-2.0μm), followed by the feeder and then the intake locations.

4) With respect to particle shape, samples collected in locations in the production and return categories have higher fractions of particles with moderate (i.e., length is 1.5 to 3x width) to relatively high aspect ratios (i.e., length is greater than 3x width) compared to feeder and intake samples.

5) Samples with relatively high fractions of alumino-silicates have higher fractions of particles with moderate aspect ratios than samples with low alumino-silicate fractions.

6) Samples with relatively high fractions of quartz particles have higher fractions of particles with moderate aspect ratios and higher percentages of very small particles than samples with no identified quartz particles.

7) Samples with high fractions of carbonates have higher percentages of particles with relatively low aspect ratios (i.e., length and width are similar) than samples with no identified carbonate particles.

DEVELOPMENT AND IMPLEMENTATION OF AN AUTOMATED SEM-EDX ROUTINE FOR CHARACTERIZING RESPIRABLE COAL MINE DUST

Victoria Anne Johann

PUBLIC ABSTRACT

This thesis describes the development and use of a computer-automated microscopy routine for characterization of respirable dust particles from coal mines. Overexposure to respirable dust has long been known to pose an occupational health hazard for miners, leading to the development of lung diseases such as coal workers' pneumoconiosis (CWP, commonly called "black lung") and silicosis. Incidence of such diseases amongst US coal miners declined for many years following regulation and development of mining best practices. However, a recent resurgence in disease incidence, particularly in parts of Appalachia, demonstrates a real need for greater understanding of the respirable dust in underground coal mines.

This work first sought to develop an automated routine for characterizing coal mine dust using scanning electron microscopy with energy dispersive x-ray (SEM-EDX). SEM-EDX is a powerful tool that allows the size, shape and chemistry of individual particles to be determined. The developed routine is not only much faster than an analogous manual method, but it also reduces the possibility of user bias and provides for more representative results by examining more particles across a wider area of a sample. The method was verified using laboratory-generated dust samples from known materials commonly observed in underground coal mines, as well as field samples collected in central Appalachia. This effort indicated that the method produces accurate and representative results.

Next, the automated SEM-EDX method was used to scan 210 respirable dust samples. These were collected in eight mines in three different regions of Appalachia (i.e., northern, mid-central and south-central Appalachia), which differed by primary mining method, coal seam thickness and mining height, and coal and/or rock mineralogy. Results were analyzed to determine whether particle size, shape, and chemistry number distributions vary between and within distinct mine regions, and by general sampling location categories (i.e., intake, feeder, production, return). Key findings include:

1) Northern Appalachian mines have relatively higher fractions of coal, carbonate, and heavy mineral particles than the two central Appalachian regions, whereas central Appalachian mines have higher fractions of quartz and alumino-silicate particles.

2) Central Appalachian mines tended to have more mine-to-mine variations in size, shape, and chemistry distributions than northern Appalachian mines.

3) With respect to particle size, samples collected in locations in the production and return categories have the highest percentages of very small particles (i.e., 0.94-2.0μm), followed by the feeder and then the intake locations.

4) With respect to particle shape, samples collected in locations in the production and return categories have higher fractions of particles with moderate (i.e., length is 1.5 to 3x width) to relatively high aspect ratios (i.e., length is greater than 3x width) compared to feeder and intake samples.

5) Samples with relatively high fractions of alumino-silicates have higher fractions of particles with moderate aspect ratios than samples with low alumino-silicate fractions.

6) Samples with relatively high fractions of quartz particles have higher fractions of particles with moderate aspect ratios and higher percentages of very small particles than samples with no identified quartz particles.

7) Samples with high fractions of carbonates have higher percentages of particles with relatively low aspect ratios (i.e., length and width are similar) than samples with no identified carbonate particles.

ACKNOWLEDGEMENTS

Foremost, I would like to thank my advisor Dr. Emily Sarver for all the support and guidance she has given me throughout my graduate career. I am sincerely grateful for all of the time and effort she has dedicated to helping me achieve my goals.

I would also like to thank my committee members, Dr. Cigdem Keles and Dr. Nino Ripepi for their support and encouragement. Data collection could not have occurred in such a timely manner without Dr. Cigdem Keles conducting some of the SEM analysis.

Also, I want to thank Steve McCartney of the Virginia Tech ICTAS-NCFL for his assistance with my SEM training, Ted Juzwak of Bruker Corporation for assistance in learning the automation software capabilities, and Dan Baxter of Environmental Analysis Associates for his professional expertise to help speed up the automated routine.

I want to extend a special thanks to my research colleague Meredith Scaggs. Without her extensive efforts to collect and prepare samples, this project would not have been possible.

I would also like to express my thanks to the Alpha Foundation for the Improvement of Mine Safety and Health for providing funding for this work.

Finally, I want thank my family and friends for supporting me through my graduate experience. I am especially appreciative of my parents, Peyton and Sally Johann, my sister, Madeline Johann, brother, Peyton Johann Jr., and my fiancé, Erik Essex, for their encouragement over the past year and a half.

TABLE OF CONTENTS

LIST OF FIGURES

LIST OF TABLES

Chapter 1. Considerations for an Automated SEM-EDX Routine for Characterizing Respirable Coal Mine Dust

Victoria Johann[a], *Emily Sarver*[a]
[a]*Virginia Tech, Blacksburg, Virginia, USA*

This paper was peer reviewed and originally published in the proceedings of the 15th North American Mine Ventilation Symposium, June 20-25, 2015. Blacksburg, Virginia, preprints no. 15-47. It is reproduced here with permission from the publisher.

Abstract

Respirable dust in coal mining environments has long been a concern for occupational health. Over the past several decades, much effort has been devoted to reducing dust exposures in these environments, and rates of coal workers' pneumoconiosis (CWP) have dropped significantly. However, in some regions, including parts of Central Appalachia it appears that incidence of CWP has recently been on the rise. This trend is yet unexplained, but a possible factor might be changes in specific dust characteristics, such as particle composition, size or shape.

Prior work in our research group has developed a standardized methodology for analyzing coal mine dust particles on polycarbonate filter media using scanning electron microscopy with energy dispersive x-ray (SEM-EDX). While the method allows individual particles to be characterized, it is very time-intensive because the instrument user must interrogate each particle manually; this limits the number of particles that can practically be characterized per sample. Moreover, results may be somewhat user-dependent since classification of particle composition involves some interpretation of EDX spectra.

To overcome these problems, we aim to automate the current SEM-EDX method. The ability to analyze more particles without user bias should increase reproducibility of results as well as statistical confidence (i.e., in applying characteristics of the analyzed particles to the entire dust sample.) Some challenges do exist in creating an automated routine, which are primarily related to ensuring that the available software is programmed to differentiate individual particles from anomalies on the sample filter media, select and measure an appropriate number of particles across a sufficient surface area of the filter, and classify particle compositions similarly to a trained SEM-EDX user following a manual method. This paper discusses the

benefits and challenges of an automated routine for coal mine dust characterization, and progress to date toward this effort.

Keywords: Coal Workers' Pneumoconiosis (CWP), Respirable Dust, Particle Analysis, Scanning Electron Microscopy (SEM), Automated SEM

1. Introduction

Coal mining operations generate dust which can be respired into the lungs of workers to cause occupational health diseases such as coal workers' pneumoconiosis (CWP). The mining industry saw dramatic reductions in CWP cases as dust standards and ventilation regulations in underground coal have improved over the past few decades under the Federal Coal Mine Health and Safety Act of 1969 [1]. The Act also established the Coal Workers' Health Surveillance Program through which NIOSH has witnessed first-hand the increase in CWP rates in the eastern United States, particularly Central Appalachia, since the mid-1990s [1-3]. This is of particular concern because the majority of cases have been reported in young coal miners and many of the cases are advanced [1-2]. Further research should be aimed toward determining the cause of increased incidence of CWP in Central Appalachia in order to improve miner health and safety [3]. Little is definitively known regarding the effects of specific dust characteristics (such as size, shape, and chemical composition) on lung disease occurrences in underground miners. Analyzing these dust particle characteristics using scanning electron microscopy (SEM) may be a good place to start. Automated SEM analysis could be particularly advantageous in collecting data from more dust samples at a faster rate.

Automated SEM-EDX analysis has historically been used for applications such as industrial process control and forensics [4]. However, SEM automated analysis hardware and software advancements have made it applicable to a variety of other applications, including mineral samples [4]. Automated SEM is able to analyze features such as inclusions in metals; porosity of geological samples, and samples containing wear debris from combustion engines [4]. Another application for mineral samples is the detection of an anomalous particle within a grouping of thousands of particles of other compositions [4]. This application might be particularly useful to the occupational health field for the analysis of dust samples containing atypical or hazardous particles.

Some work has been conducted in the realm of automated dust particle analysis. Deboudt et al. [5] performed automated SEM-EDX particle analysis on dust samples collected on the Atlantic coast of Africa. As in our project, this group collected airborne particulate samples on polycarbonate filters and ran an SEM at an accelerating voltage of 15kV. Using the Link ISIS Series 300 Microanalysis system developed by Oxford Instruments, this group was able to collect spectral data for individual particles with a 20 second acquisition time [5]. Even faster rates of data collection can be achieved though. Ritchie and Filip [6] recently undertook an effort to optimize the speed of automated particle analysis by SEM-EDX and demonstrated data collection at approximately three particles per second. They employed a structured query language database that stores millions of particle records and is able to simultaneously classify multiple particles to multiple categories [6]. The authors' research group does not necessarily need to be analyzing particles at that rate, though aiming to speed up analysis time by a few seconds and perhaps creating a comprehensive particle database could be beneficial toward research efforts.

Other researchers have also worked on multi-frame particle analysis using the SEM. Fritz, Camus, and Rohde [7] have done work with automated microscope stage analysis that can cover hundreds of frames in one run to ensure total sample coverage. For applications in the mining industry, this ability is particularly attractive for particle sizing and the analysis of respirable dust particles. Collecting data for particles over the entire sample can be necessary for statistical significance [7]. The authors' research group also plans to employ automated multi-frame analysis.

2. Previously Developed Standard Dust Characterization Method

Prior work in the authors' research group has developed a standardized methodology for analyzing coal mine dust particles on a polycarbonate filter [8-10]. This method was developed using an FEI Quanta 600 FEG environmental scanning electron microscope (ESEM) (FEI, Hillsboro, OR) equipped with a Bruker Quantax 400 EDX spectroscope (Bruker, Ewing, NJ). The ESEM is operated under high vacuum conditions at a voltage of 15kV with a spot size of 5.0μm and at the optimal working distance of 12-13mm. Bruker Esprit software is used to collect spectra results for the classification of individual particles. The "spot" analysis function of the ESEM software is used in conjunction with the EDX software to generate elemental spectra.

Six compositional classification schemes were developed for coal mine dust particles based on peak elemental spectra heights of aluminum, calcium, carbon, copper, iron, magnesium, oxygen, potassium, silicon, sodium, sulfur, and titanium. The six classifications are "alumino-silicate," "carbonaceous," "carbonate," "heavy mineral," "mixed carbonaceous," and "quartz." Any particles that do not fit into these categories are termed "other." Data on particle size and shape is also collected in this dust characterization method. The long and intermediate dimensions of each particle are measured using the line measurement tool provided in the ESEM imaging software. The shape is qualitatively classified based on user interpretation as either "angular," "rounded," or "transitional."

The sample analysis routine begins by focusing the SEM at 10,000x magnification to provide optimal resolution for analyzing particles in the desired size range of 0.5-8.0µm in diameter. Two horizontal lines are drawn 2µm apart, centered on the screen and spanning the width of the screen, using a line measurement tool, as depicted in Figure 1.1.

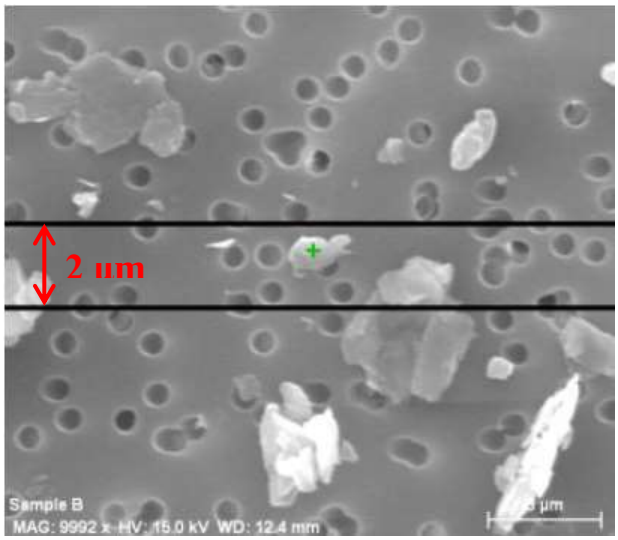

Figure 1.1. *Example of the horizontal lines drawn 2 µm apart for particle selection. Only particles touching this region are to be selected for analysis [8].*

The stage is moved so that the first field to be analyzed is three screen shifts from the outer, left edge of the filter, 2.25mm (one quarter of the filter diameter) down from the top of the filter. Moving from left to right and top to bottom each particle with a long dimension greater than 0.5µm intersecting the space between the two horizontal lines and falling completely within the field of view is analyzed. Up to ten particles meeting the specifications are characterized per field in order to ensure that at least ten fields are analyzed and increase the representativeness of

the results. Figure 1.2 shows a backscatter detector image of a typical field of ten particles that would be analyzed.

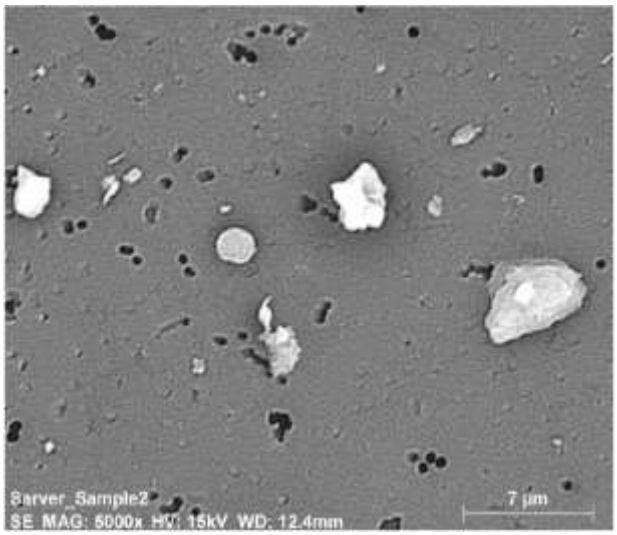

Figure 1.2*. Example of a typical field of particles to be analyzed (at 10,000x magnification).*

Once the first field has been analyzed, the next field of view to the right is analyzed. If fewer than 100 particles have been analyzed upon reaching the edge of the first row, the stage is shifted so that the field of view is 4.5mm (one half of the filter diameter) from the top of the filter and the same procedure for the previous row is followed. If fewer than 100 particles have been analyzed upon reaching the edge of the second row, the stage is shifted once more so that the field of view is 6.75mm (three quarters of the filter diameter) from the top of the filter, following the previous procedure. Figure 1.3 depicts this analysis routine in terms of filter navigation under the SEM.

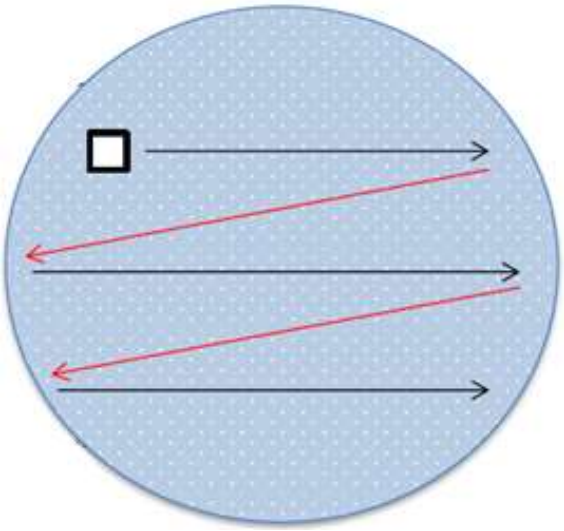

Figure 1.3*. Illustration of a 9 mm diameter polycarbonate filter and navigation routing for SEM-EDX analysis.*
The box represents the first frame in which particles are selected for characterization; the black arrows define the directions for successive screen shifts between characterization frames. When one horizontal line of analysis is complete (black arrows), the red arrows define shifting back to the left side of the filter to continue analysis on the next horizontal line [8].

The manual method has the capacity to analyze 100 particles on one sample in 75-90 minutes, depending on user experience and sample characteristics (e.g., particle density); despite the wealth of information that can be obtained, the method is clearly too time-consuming to be practical for a large number of samples.

3. Automation of the Standard Dust Characterization Method

Considering the need to significantly speed up particle characterization, efforts to automate the above routine have recently been initiated. This work is being developed using the same ESEM-EDX system previously mentioned, and several special features available for add-on to Bruker's Esprit software. A major benefit to automation is that the software can characterize particles at a magnification that is ten times lower than the magnification required for the standard dust characterization method. Figure 1.4 shows a backscatter detector image of a typical field of particles that would be analyzed using the automated routine.

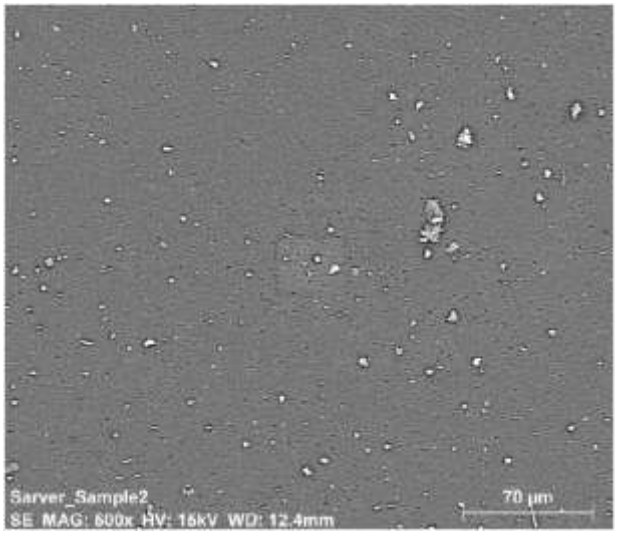

Figure 1.4. *Example of a typical field of particles (at 1,000x magnification).*

This image comes from the same sample as Figure 1.2; however, by being able to analyze particles at 1,000x versus 10,000x magnification, many more particles can be analyzed per frame. Once the first frame is selected, the imaging tool in the Esprit software is used to pull the image of the frame from the SEM software and import it for analysis. A special feature in Esprit allows for rules and filters to be applied to the image so that the software is programmed to identify dust particles. Here, a binary image can be created and settings can be adjusted so that the software distinguishes particles as white and the filter as black. Figure 1.5 depicts the binary imaging process in Esprit.

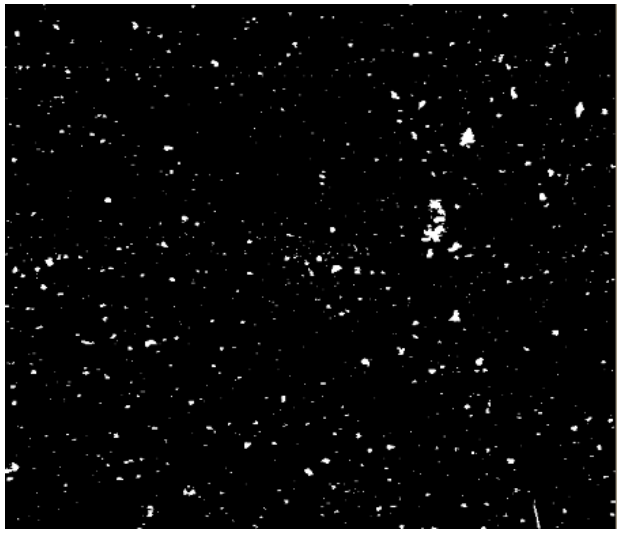

Figure 1.5. *Example of a binary image of a typical particle field (at 1,000x magnification). This is the same particle field as in Figure 1.4.*

Once all settings have been adjusted for particle identification, particle sizing can be conducted. Figure 1.6 depicts the particle field once all the particles have been sized. The software outputs data such as length, width, and shape factor to characterize the particles by size and shape, as shown in Figure 1.7.

This single frame contains 171 particles that can be analyzed, 71 more particles than would have been analyzed in up to ten frames using the standard dust characterization method. This particle sizing routine minimizes user interpretation of the long and intermediate particle dimensions which was required for the standard dust characterization method.

Once sizing is completed, the particle classification scheme can be implemented. The Esprit software allows for particle classification based on the weight percent of elements detected in spectral analysis. Therefore, rules can be set for the maximum or minimum elemental weight percentages required for various particle classification categories. We have currently developed rudimentary rules and particle classification categories to demonstrate the utility of automated analysis and its potential for respirable dust particles from coal mining environments. The preliminary categories are based on typical elemental weight percentages observed for particles classified using the manual method. Figure 1.8 displays chemistry results for some particles identified in Figure 1.6, showing the weight percentages of specific elements considered by the classification rules. Figure 1.9 shows particle classification results in a bar chart as a useful visual tool.

It should be noted that the chemistry classification categories are not currently developed enough to accurately classify every particle (i.e., as it would be classified manually). This is especially true for carbonaceous particles because they can contain small weight percentages of elements other than carbon and oxygen. This does not allow them to be classified under the original carbonaceous category that only sets parameters for carbon and oxygen weight percentages. Therefore, in this preliminary work, a second carbonaceous classification category was created with additional elemental weight percentage rules (i.e., “carbonaceous II” in Figure 1.9). By doing this, carbonaceous particles that were previously not classified are classified in the second carbonaceous category. A particle chemistry analysis feature in the Esprit software can classify each particle detected in the frame.

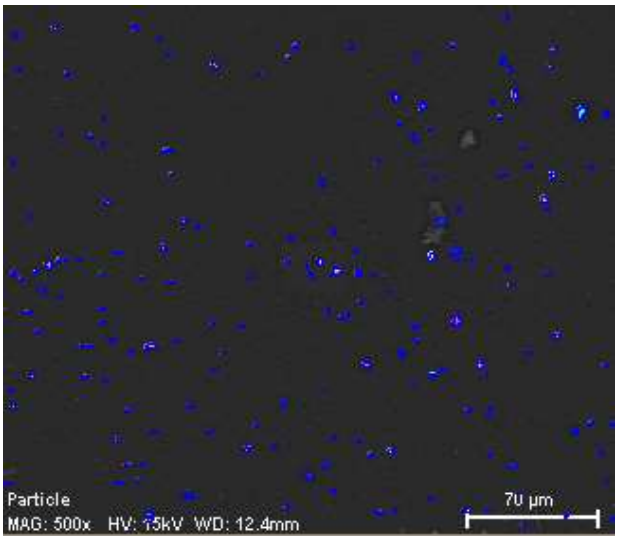

Figure 1.6*. Example of the particle sizing process in Esprit.*
This is the same particle field as in Figure 1.4. Each particle found that is accepted for analysis is outlined in blue while undergoing size classification.

Accepted	Area	Length	Width	Average Diameter	Pos X	Pos Y	Aspect Ratio	Feret Std Dev	Perimeter	Orientation	On Border	Shape Factor	Max Circle Rad
P162	3.4	2.88	1.78	2.54	3701	24858	1.62	0.28	8.1	2	0	0.661	1.02
P163	2.5	2.71	1.33	2.19	3808	24856	2.03	0.44	6.5	8	0	0.738	0.72
P164	2.7	3.69	0.89	2.73	3757	24855	4.15	0.88	8.2	176	0	0.511	0.51
P165	4.3	3.82	1.78	3.00	3796	24855	2.15	0.63	9.3	13	0	0.627	1.02
P166	4.1	3.69	1.78	2.96	3627	24854	2.07	0.62	9.0	11	0	0.632	1.02
P167	4.8	3.55	2.15	2.95	3751	24854	1.65	0.45	8.9	159	0	0.758	1.02
P168	3.4	2.71	2.05	2.45	3850	24852	1.32	0.17	7.5	58	0	0.757	1.02
P169	3.0	2.88	1.33	2.30	3876	24850	2.16	0.45	6.8	16	0	0.801	1.02
P170	7.5	4.75	3.12	3.88	3628	24850	1.52	0.51	12.7	145	0	0.590	1.14
P171	3.0	2.71	1.78	2.35	3827	24847	1.52	0.32	7.1	0	0	0.740	0.72
Min	2.3	2.35	0.89	1.98	3552	24847	1.09	0.08	5.8	0	0	0.364	0.51
Max	20.7	7.99	5.34	6.23	3876	25119	4.15	1.84	20.3	179	0	0.929	2.11
Average	5.0	3.62	2.06	2.98	3713	24973	1.86	0.50	9.2	83	0	0.701	1.04
Std Dev	3.3	1.13	0.76	0.88	96	75	0.53	0.27	3.0	74	0	0.119	0.30

Figure 1.7*. Example of the particle sizing results for some particles shown in Figures 1.4-1.6.*
The accepted particles are all numbered and listed in order in the first column. Other particle properties are provided for each particle in subsequent columns. At the bottom of the results page, minimum, maximum, average, and standard deviation values are provided for each particle property.

Alle	cps/eV	Results [Atom-% (norm.)]						Sort: Element
P1	0.06	Pd	Au	C	O 92.27	Al 0.48	Si 1.43	Na 5.82
P2	0.22	Pd	Au	C	O 86.11	Al 7.85	Si 6.04	
P3	0.16	Pd	Au	C	O 88.42	Al 6.33	Si 5.25	
P4	0.17	Pd	Au	C	O 90.81	Al 0.42	Si 0.31	Ca 8.46
P5	0.06	Pd	Au	C	O 90.53	Al 4.63	Si 4.84	
P6	0.09	Pd	Au	C	O 91.18	Al 1.53	Si 0.93	Ca 6.35
P7	0.03	Pd	Au	C	O 90.79	Al 3.34	Si 3.39	Fe 2.49
P8	0.06	Pd	Au	C	O 92.64	Al 1.24	Si 0.19	Ca 5.93
P9	0.06	Pd	Au	C	O 90.80	Al 2.57	Si 6.63	
P10	0.25	Pd	Au	C	O 97.71	Al 1.23	Si 1.06	
P11	0.14	Pd	Au	C	O 86.58	Al 6.62	Si 4.64	Ti 2.17
P12	0.13	Pd	Au	C	O 92.41	Al 3.12	Si 4.47	
P13	0.06	Pd	Au	C	O 85.51	Al 7.23	Si 7.26	
P14	0.10	Pd	Au	C	O 83.65	Al 7.98	Si 8.37	
P15	0.20	Pd	Au	C	O 89.33	Al 6.66	Si 4.01	
P16	0.22	Pd	Au	C	O 93.24	Al 1.50	Si 1.63	Fe 3.63
P17	0.10	Pd	Au	C	O 92.24	Al 1.36	Si 0.55	Ca 5.85
P18	0.09	Pd	Au	C	O 86.45	Al 7.39	Si 6.16	

Figure 1.8*. Example of the particle chemistry results for some particles shown in Figures 1.4-1.6. Each analyzed particle is listed in order in the first column. Information regarding the counts and weight percentages of detected elements are provided for each particle in subsequent columns.*

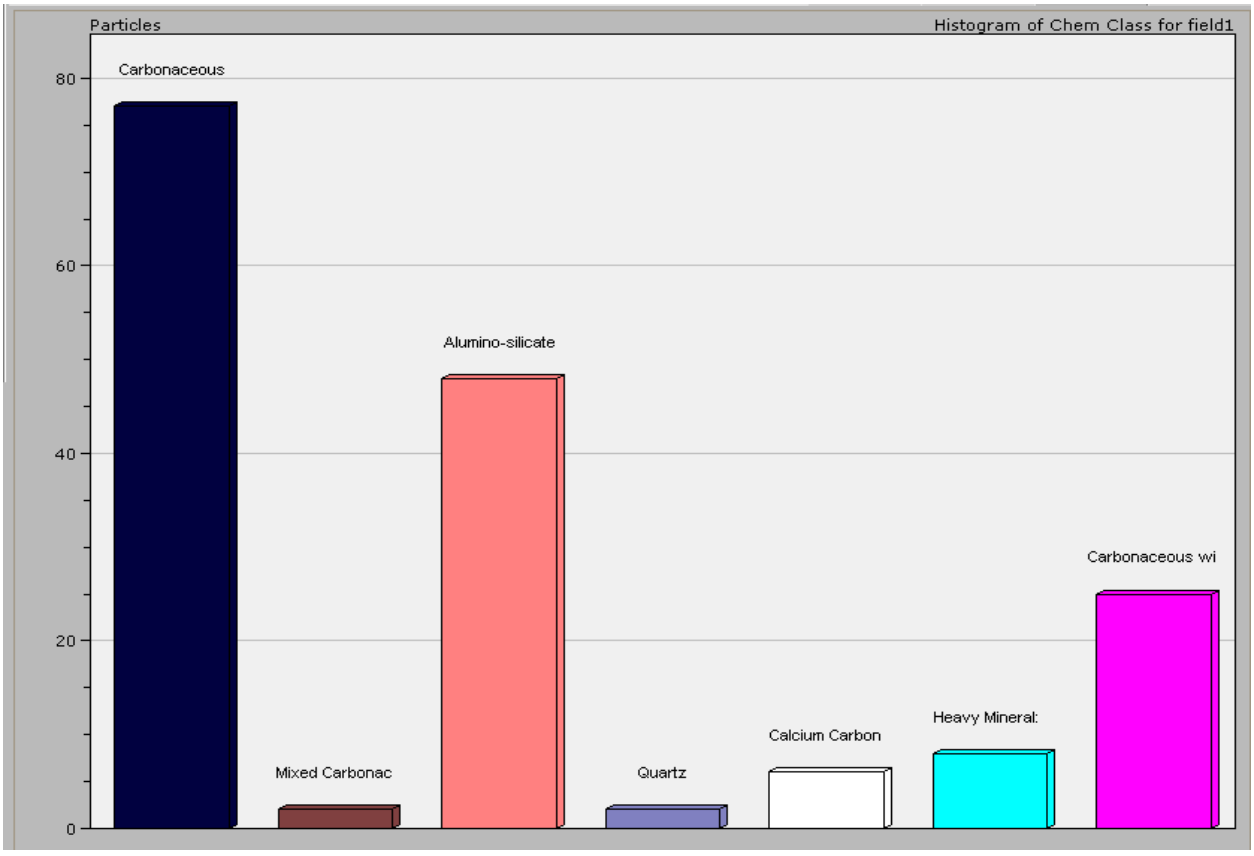

Figure 1.9*. Example of the particle classification results for particles shown in Figures 1.4-1.6. Once each particle is classified based on the specified chemical classification parameters, the Esprit software outputs a histogram with the particle frequency for each class (carbonaceous, mixed carbonaceous, alumino-silicate, quarts, carbonate, heavy mineral, and carbonaceous II).*

The automated analysis at the particle density demonstrated in Figure 1.4 takes just over ten seconds per particle which allows for total analysis of this frame of 171 particles in approximately 30 minutes. At this rate, 171 dust particles are being analyzed two or three times faster than just 100 dust particles using the standard dust characterization method. It is expected that with several modifications in basic operating parameters of the SEM-EDX system, the efficiency can be greatly increased. The majority of particles in this frame were classified as carbonaceous while many particles were classified as alumino-silicates and fewer were classified as heavy minerals, carbonates, mixed carbonaceous, and quartz.

Another special feature in the Esprit software allows for the automation of the microscope stage movement from frame to frame. The user is able to designate the starting frame position and the ending frame position along the sample filter. Once the entire area of the filter to be analyzed is determined, particle sizing and chemistry can be run frame by frame and the software will export the data after completion. This tool can even be used to run multiple samples consecutively so that up to 16 samples could be analyzed in one run.

4. Discussion

It seems as though developing an automated particle analysis routine is a step in the right direction for our research. The standard dust characterization method is too time-intensive for the amount of particles that can practically be analyzed per sample because the user must interrogate each particle manually. A major advantage to automated particle analysis is the amount of time saved in the lab due to quick, electronic characterization of particles. This is also applied to data entry where automated analysis automatically exports data into Microsoft Excel while data obtained from the standard method must be manually entered. Moreover, results from the standard dust characterization method may be somewhat user-dependent since classification of particle composition and shape currently involves some interpretation of EDX spectra. Other benefits of an automated particle analysis routine are a significant increase in the number of particles than can be analyzed per sample and minimization of user interpretation to acquire results. The ability to analyze more particles without user bias should increase reproducibility of results as well as statistical confidence in obtaining results from a representative portion of the sample.

However, some challenges do exist in creating an automated routine, including training the available software to appropriately make multiple decisions such as those involving differentiation of individual particles from anomalies on the filter media, selection of particles for analysis, and classification of particle composition. Another challenge arises due to the filter media being comprised of carbon and carbon being a key element in the classification of carbonaceous, mixed carbonaceous, and carbonate minerals. We are working to determine whether or not carbon should be deconvoluted for proper mineral identification and other key elements be used to classify these particles in its place. We have determined that gold and palladium should definitely be deconvoluted before spectral analysis because the sample coating is comprised of these elements and can interfere with the chemical identification of the dust particles.

5. Conclusions

There is much work still to be done to refine the particle classification parameters in order to properly automate the particle analysis. Our goal is to determine and implement the correct particle classification categories and their appropriate rules for our samples. To do this, we plan to:

- collect spectral data on many particles from our samples
- determine the appropriate elemental weight percentage thresholds for the classification parameters
- determine which elements should be deconvoluted
- modify the currently developed particle classification categories so that they are able to classify all particles encountered
- ensure that the software is properly classifying all particles

We aim to program the software to classify particles in the same manner that the user would classify them, but without the human error.

6. Acknowledgements

The authors acknowledge the Alpha Foundation for the Improvement of Mine Safety and Health for funding this work. We would also like to thank Steve McCartney of Virginia Tech

ICTAS-NCFL for operational assistance with SEM-EDX analysis, Ted Juzwak of Bruker Corporation for assistance in learning the Esprit software capabilities, and Patrick Wynne for countless hours of SEM work. We are also grateful to Meredith Scaggs for her efforts to collect and prepare dust samples.

References

[1] Centers for Disease Control (CDC). Advanced Cases of Coal Workers' Pneumoconiosis-Two Counties, Virginia. MMWR, 55.33 (2006) 909-913.

[2] D. Blackley, C. Halldin, and A.S. Laney, Resurgence of a Debilitating and Entirely Preventable Respiratory Disease among Working Coal Miners, American Journal of Respiratory and Critical Care Medicine 190.6 (2014) 708-709.

[3] E. Suarthana et al, Coal workers' pneumoconiosis in the United States: regional differences 40 years after implementation of the 1969 Federal Coal Mine Health and Safety Act, Occupational and Environmental Medicine 68.12 (2011) 908-913.

[4] C. Lang et al., Automated SEM Analysis in Industrial Process Control and Scientific Research, Microscopy Society of America, 2014.

[5] K. Deboudt et al., Mixing state of aerosols and direct observation of carbonaceous and marine coatings on African dust by individual particle analysis, Journal of Geophysical Research 115 (2010) 1-14.

[6] N. Ritchie and V. Filip, SEMantics for High Speed Automated Particle Analysis by SEM/EDX, Microscopy and Microanalysis 17.S2 (2011) 896-897.

[7] G. Fritz, P. Camus, and D. Rohde, Consideration for Automated Multi-Frame Particle Sizing in the SEM, Microscopy and Microanalysis 12.S02 (2006) 210-211.

[8] R. Sellaro, Development and Demonstration of a Standard Methodology for Respirable Coal Mine Dust Characterization Using SEM-EDX, Virginia Polytechnic Institute and State University, 2014.

[9] R. Sellaro and E. Sarver, Preliminary investigation of SEM-EDX as a tool for characterization of coal mine dusts, Mining Engineering 66.8 (2014) 16-40.

[10] R. Sellaro and E. Sarver, Characterization of respirable dust in an underground coal mine in Central Appalachia, Transactions of the Society for Mining, Metallurgy & Exploration 336 (2014) 457-466.

Chapter 2. Development of an Automated SEM-EDX Routine for Characterizing Respirable Coal Mine Dust

Victoria Johann[a], *Emily Sarver*[a], *Cigdem Keles*[a]

[a]*Virginia Tech, Blacksburg, Virginia, USA*

Abstract

Recently, incidence rates of coal workers' pneumoconiosis (CWP) and other related respiratory illnesses appear to be on the rise in central Appalachia. Changes in specific dust characteristics, such as particle size, shape or chemical composition, may offer insights regarding causal factors. SEM-EDX analysis of coal mine dust samples can be used to estimate these particle characteristics. If conducted manually, such work can be very time intensive, which limits the number of particles that can be analyzed. Moreover, potential exists for user bias in interpretation of EDX spectra. A computer-automated scanning routine, on the other hand, can allow similar analysis at a much faster rate, increasing total particle counts and reproducibility of results. In order to develop a reliable routine, automation software must be programmed to consistently detect all particles in the size range of interest, properly "cut" agglomerated particles, and appropriately classify particles by chemistry. In short, the automated routine must be able to characterize dust particles in the same manner that a manual user would. This paper examines the reproducibility (between users) of a previously developed manual SEM-EDX dust characterization method, and then presents verification of a newly developed computer-automated routine.

Keywords: Coal Workers' Pneumoconiosis (CWP), Scanning Electron Microscopy (SEM), Computer-Automated SEM-EDX, Respirable Dust, Particle Size, Shape, and Chemistry

1. Introduction

Respirable dust in underground coal mining environments has long been known to pose an occupational health hazard for miners [1]. Particulates with an aerodynamic diameter less than 10μm are generally considered respirable [2-5]. Coal workers' pneumoconiosis (CWP, commonly referred to as "black lung") and silicosis are the most prevalent occupational respiratory diseases affecting coal miners, usually after chronic exposures to respirable dust [1].

These diseases generally cause scarring of lung tissue, leading to difficulty breathing amongst other symptoms, and can eventually lead to premature death [6-7]. Across the US, dramatic reductions in CWP and silicosis cases have been achieved via a combination of regulatory dust exposure limits, improved ventilation and development of dust abatement technologies [8-11].

After passage of the Coal Mine Health and Safety Act in 1969, the Coal Workers' Health Surveillance Program (CWHSP) was established in 1970 to detect early stages of CWP and prevent development of progressive massive fibrosis (PMF) [12]. This program collects and reports the results from miner chest X-rays. The percentages of miners with detected CWP of any level of severity (i.e., levels 1-3, and observed PMF) are publically available through the CWHSP Data Query System [12]. Between 1970 and 1999, a decreasing trend in CWP incidence rates was generally observed amongst CWHSP participants across the US. But since 1999, trends in some regions have unexpectedly reversed [11, 13-15]. In particular, mid-central and south-central Appalachia (i.e., MSHA districts 4 and 12, respectively) appear to have dramatically increased incidence rates – nearing or exceeding the 1970 rates in these regions [12]. Moreover, CWP and PMF appear to be affecting relatively younger miners than before [10-13, 15]. While these alarming trends have not been fully explained, a number of causal factors have been suggested (e.g., see [13-22]), including exposure conditions and specific dust characteristics.

Many have noted that mines in the regions with the most apparent recent increases in lung disease incidence are mining increasingly thinner coal seams, and thus also cutting more roof and floor rock [e.g., 16-19]. The roof rock in many of these mines is comprised of sandstone; therefore, higher concentrations of crystalline silica (quartz) may be expected in dust, which could be affecting miner health [18, 20]. Many mines in parts of central Appalachia are also relatively small and accordingly have small labor forces, which means that miners may also be working longer hours and/or in a variety of job roles. In this case, individuals may be exposed to relatively high or variable dust concentrations and a range of dust characteristics [4, 11, 17]. Advances in mining equipment have also yielded more powerful cutting tools for production activities, which are likely to generate relatively smaller dust particle sizes; and it has been suggested that small particles can be more harmful to health than larger respirable dust particles [21]. Indeed, particle size as well as shape (e.g., elongation, angularity, roughness) can affect the degree of dust particle deposition in the lungs [23]. Considering all of the above, a more

thorough grasp of specific characteristics of dust particles and occupational exposures may allow for better understanding of the role of respirable dust in development of disease.

Prior work in the authors' research group led to the development of a standardized methodology for characterizing respirable coal mine dust samples by particle size, shape and chemistry distributions. It involves manual analysis with a scanning electron microscope equipped with energy dispersive x-ray (SEM-EDX), and has been described in detail elsewhere [25-27]. SEM-EDX is a very powerful tool for particulate characterization, and is well established for both chemical identification of particles (e.g., see [29-35]) as well as determination of size and shape parameters (e.g., see [34,36]). On a limited basis, SEM-EDX has been used specifically for analysis of mine dust mineralogy and size characterization in the context of occupational health (e.g., see [37-40]); however, it has not seen widespread use in this domain – probably due to the fact that it is relatively time and cost intensive.

Although the previously developed manual SEM-EDX method provides in-depth data on individual particles, it is very time intensive – requiring up to 90 minutes to analyze 100 particles. Therefore, it is generally only feasible to analyze a relatively small number of particles per sample. The potential for user bias and/or error in interpretation of EDX chemical spectra also represent a limitation of manual analysis. A computer-automated routine, on the other hand, could allow for more efficient, unbiased sample analysis. Automated SEM-EDX has the ability to analyze on a frame-by-frame basis and gather particle size, shape and elemental (i.e., chemical) characteristics for individual particles. Computer-automated SEM analysis of particulates has been developing since the mid-1970s (e.g., see [41-42]). Much progress has been made over the years to increase the speed and efficiency of such analysis, as well as the abundance of data that can be collected on a particulate level (e.g., see [24, 43-44]). A routine programmed to scan particles frame-by-frame and covering a relatively large percentage of the filter area is not only more efficient than an analogous manual method, but it should also increase the reproducibility of results and statistical confidence in the data collected [24, 43-44].

The objectives of the work described here were to: 1) evaluate the reproducibility (between multiple users) of the previously developed manual SEM-EDX dust characterization method; and 2) develop an automated method, and verify it based on accuracy of results obtained on known samples, and reproducibility of results between multiple scans of the same samples.

2. Materials and Methods

A total of ten respirable dust samples were used in this study (Table 2.1). The samples were collected in five mines in mid-central and south-central Appalachia. Sampling locations in the mines varied, but can be classified into one of four primary categories: in or near the intake, feeder or conveyor belt, production activities, and return.

Table 2.1. *Sampling Details of Ten Selected Samples*

Sample Number	Mine Region	Location Category	Specific Location
1	South-central Appalachia	Feeder	Belt Drive
2		Intake	Tram In
3		Production	Continuous Miner
4		Feeder	Behind Feeder
5		Intake	Tram In/Walk/Tram Out
6	Mid-central Appalachia	Production	Roof Bolter
7		Return	Return Entry
8		Production	Continuous Miner
9		Production	Continuous Miner
10		Feeder	Behind Feeder

All samples were collected by the research team using Escort ELF dust sampling pumps (calibrated to 1.7 L/min) with nylon Dorr-Oliver cyclones to discard particles larger than respirable size. Samples were collected directly onto 37-mm diameter polycarbonate (PC) filters in two-piece cassettes. Sample collection times ranged from about 2-4 hours. To prepare the samples for SEM-EDX analysis, clean tweezers were used to remove the filters from the cassettes, and then a circular sub-section (9-mm diameter) was carefully cut from the center of each filter using a stainless steel trephine. Each subsection was mounted to an aluminum stub using double-sided tape. The stubs were sputter coated with Au/Pd to render the surface of the sample electrically conductive for analysis by SEM.

Description of Developed Automated Dust Characterization Routine

Preliminary efforts to significantly reduce analysis time and normalize the dust characterization methodology via automation were described previously by the authors [28], and are summarized below. Both the manual and automated methods were developed using an FEI Quanta 600 FEG environmental scanning electron microscope (ESEM) (Hillsboro, OR), equipped with a backscatter electron detector (BSD) and a Bruker Quantax 400 EDX spectroscope (Ewing, NJ). Bruker's Esprit software version 1.9.4 (complete with DriftCorr,

ImageStitch, Feature, StageControl, and Jobs tools) was used to program and run the automated scanning routine. All automated work was conducted at a magnification of 1,000x (vs. 10,000x used for the manual method). Other key instrument settings for the automated routine are high vacuum mode, voltage of 15kV, working distance of 12.5mm, and spot size of 6.5μm. Using the manual method, samples were analyzed at a working distance anywhere between 12mm and 13mm and at a spot size of 5.0μm. The automated routine was developed to analyze approximately 500 particles per sample, whereas only 100 particles were analyzed per sample manually.

Particle Characteristics

Particle size and shape characteristics are determined from SEM image analysis, and are therefore dependent on image quality. The relatively low magnification level used for the automated dust characterization routine allows for efficient analysis (i.e. more particles are visible in a single frame), but limits image resolution. Therefore, only particles greater than about 1μm (longest visible dimension) are selected for analysis, and only basic size and shape parameters are currently considered. For particle sizing, the long dimension and intermediate (i.e., perpendicular to the long) dimension are reported; these are the same size parameters measured in the manual SEM-EDX dust characterization method. For particle shape, the aspect ratio (i.e., ratio of long to intermediate dimensions) is reported, and again this can be computed from the manual method data. The manual method additionally includes a qualitative assessment of particle shape, whereby the user classifies each particle as rounded, angular or transitional. No measure of angularity is currently made with the automated method given the relatively low magnification, though scanning at higher magnification may well allow for such assessment.

Regarding particle chemistry, in depth SEM-EDX analysis of respirable dust samples representative of Appalachian coal mines previously defined six distinct classification categories: carbonaceous, mixed carbonaceous, alumino-silicate, quartz, carbonate, and heavy mineral (Table 2.2). A category called “other” is used for any particle that does not fit in the six defined categories. Classification criteria were first defined and refined during development of the manual dust characterization method using both laboratory generated and field samples [25]. These criteria are based on raw peak heights of EDX elemental spectra, which can be observed in real-time and interpreted quickly by a manual user. For the automated method, The Esprit software allows for classification criteria based on atomic percentages derived from EDX

elemental spectra. Thus, to develop the automated routine, the manual criteria were adapted via an iterative process. In brief, the atomic percentage limits on the automated routine were gradually refined until automated and manual results agreed across a wide range of individual particles (i.e., between about 1-10μm and representing all six defined chemical composition categories shown in Table 2.2).

***Table 2.2**. Classification criteria for dust particle chemical composition. Criteria for manual method are taken from Sellaro et al., 2015 [25].*

Dust Particle Chemical Composition Category	**Example Mineralogy**	**Manual Classification Criteria [Raw Peak Heights, Cps/eV]**	**Automated Classification Criteria [Elemental Atomic, %]**
Carbonaceous (C)	Coal	Carbon ≥80 Oxygen ≤20	Carbon >80% Oxygen <29% Silicon <0.3% Aluminum <0.3% Calcium/Magnesium <0.3%
Mixed Carbonaceous (MC)	Biogenic/Organic Carbonaceous Clays	Silicon ≥10, <20 Aluminum ≥10, <20 Carbon ≥80 Oxygen ≤20	Carbon >78% Oxygen >13%, <20% Silicon >0.2%, <0.4% Aluminum >0.2%, <0.4% Calcium/Magnesium <0.4%
Alumino-silicate (AS)	Clays, Feldspars	Silicon ≥20 Aluminum ≥20 Oxygen >20	Carbon <85% Oxygen >15% Silicon >0.4% Aluminum >0.3%
Quartz (Q)	Crystalline Silica	Silicon ≥20 Oxygen >20	Carbon <86% Oxygen >15% Silicon >0.5% Aluminum <0.2%
Carbonate (CB)	Rock Dust, Calcite, Dolomite	Calcium/Magnesium ≥20 Oxygen >20 Carbon <80	Carbon <85% Oxygen >15% Calcium/Magnesium >0.5%
Heavy Mineral (HM)	Pyrite, Fe/Al/Ti Oxides	Iron/Titanium/Aluminum ≥20 Oxygen >20	Oxygen >12% Iron/Titanium/Aluminum>0.5%
Other (O)	DPM, etc.	Does not fit above conditions	Does not fit above conditions

To further verify the automated chemical classification criteria, respirable dust samples were generated from six known materials and analyzed using the automated dust characterization routine. The known materials were: washed coal, raw shale, a real rock dust product, high-grade quartz sand (Ward's Science, Rochester, NY) and kaolinite (Ward's Science, Rochester, NY) and calcite (Fisher Scientific, Fair Lawn, NJ) powders. These materials were chosen because their primary constituents should represent the primary chemical compositions of dust particles

found in Appalachian coal mines. Samples were pulverized in a fume hood (except for the kaolinite and calcite, which were already fine enough to contain significant respirable particles), and then further aerosolized using compressed air. At the same time, the ELF sampling pumps and cyclones described above were operated in the fume hood to collect respirable-sized particles on PC filters. Each piece of equipment was cleaned using compressed air before preparing the next sample in order to minimize contamination.

The washed coal sample was obtained from a float sink test to ensure that it was relatively clean. Raw shale pieces were handpicked from a run-of-mine coal sample cut from the Peerless seam in mid-central Appalachia, which were expected to be dominated by alumino-silicate minerals. The rock dust sample was generated from a rock dust product provided by a partner mine; it is known to contain approximately 92% carbonates (i.e., calcite and dolomite) per separate XRD analysis commissioned by the mine operator. Because these are not pure materials, it was expected that the coal would contain a minor fraction of non-carbonaceous material; the shale would have some coal content, and likely minor fractions of other materials such as carbonates; and the rock dust would contain some non-carbonate minerals. For samples with less expected impurities, kaolinite was chosen to represent a "pure" aluminio-silicate sample, and calcite was chosen to represent a "pure" carbonate sample. Finally, the quartz sample was prepared to verify that particles in this category are accurately classified.

Development of Multi-Frame Automation Routine

In order to ensure that particles are analyzed across a relatively large portion of the filter sub-sample (i.e., to increase probability of obtaining representative results), the automated routine was programmed so that at least ten frames (located relatively far from one another) must be scanned. At 1,000x magnification, each frame is approximately 15,048μm^2 (132μm x 114μm). Within each frame, particles must be consistently detected (i.e., discriminated from the filter background), and agglomerated particles must be "cut". A benefit of the Esprit software is that it can be programmed to run consecutive "jobs". Thus, a multi-frame routine was developed by creating and sequencing multiple single-frame jobs.

An array of 157 single-frame locations and the sequence of the first 10 frames is shown in Figure 2.1. The black square represents the center frame where the automated routine begins. From there, analysis proceeds through the red frames, starting with the first red frame to the left of the center frame, continuing to the left, then to the right of center frame. The same pattern

follows for the top and then the bottom rows of red frames. The analysis then proceeds in the same fashion through the orange, yellow, green, dark blue, light blue, purple, and finally pink frames. This sequence ensures that analysis is spatially dispersed across the sample. All jobs are programmed with respect to the x and y coordinates in reference to the center frame position.

Within each frame, the software was programmed to perform particle size, shape, and chemical analyses on up to 50 particles, export the data to an MS Excel file, and then navigate to the coordinates of the next frame. This process is repeated until at least 500 particles have been analyzed; the routine does not stop until it finishes all programmed tasks in a frame. Analysis time can range between about 15-60 minutes depending on the relative particle density on a sample. Figure 2.2 presents examples of very high and very low particle densities.

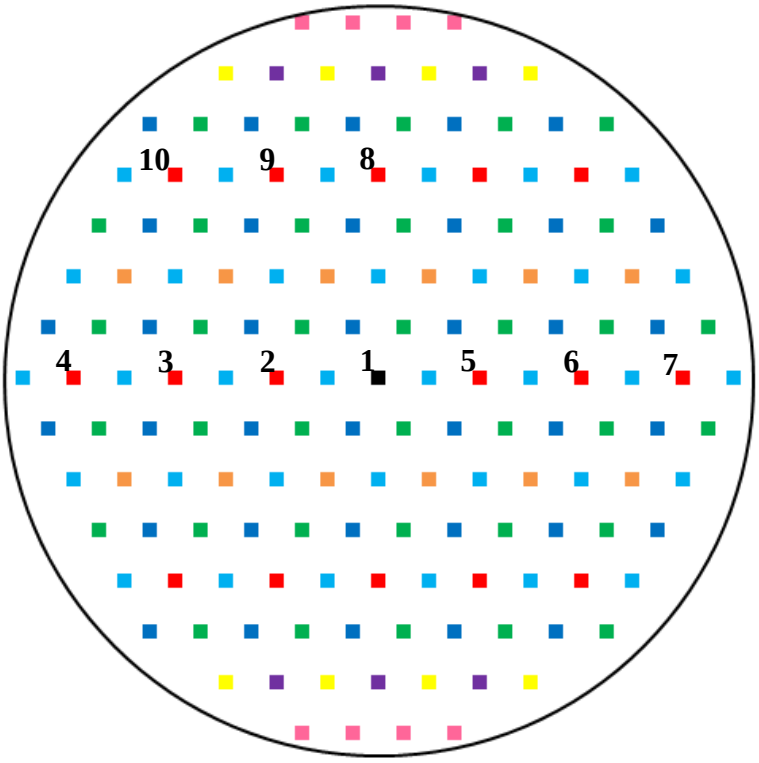

Figure 2.1. *Individual analysis frames for automated SEM-EDX routine. The entire circle represents a 9-mm diameter subsample taken from the center of a 37-mm filter sample. The routine begins in the black (center) frame and then proceeds through the other frames by color (beginning with red) to ensure analysis across a wide area of the subsample. The analysis sequence is numbered for the first 10 frames to illustrate.*

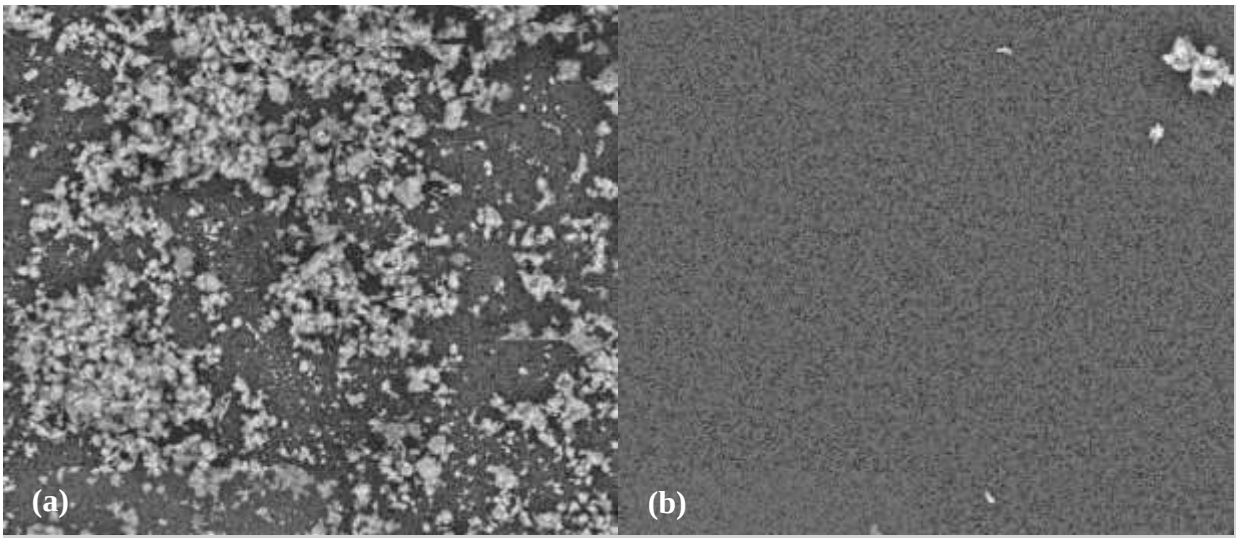

Figure 2.2*. Examples of respirable mine dust samples with (a) very high and (b) very low particle densities.*
These images were both collected at 1,000x magnification.

3. Results and Discussion

Manual SEM-EDX Analysis

The ten respirable mine dust samples shown in Table 2.1 were analyzed manually by three different users, carefully following the methodology established by Sellaro et al., 2015 [25]. Figures 2.3-2.6 summarize the results for distributions of particle size, shape and chemistry, respectively. (Corresponding Tables A.1-A.4 in Appendix A present the results numerically). All results are based on each user's analysis of 100 particles per sample. From the plots, some general inferences can be made. Most importantly, results between different users seem to vary quite a bit across size, shape and chemistry distributions. For instance, User 2 reported more very small (i.e., 0.5-1um) particles for most samples than did Users 1 and 3 (Figure 2.3); and Users 1 and 3 tended to report more "round" particles than did User 2 (Figure 2.4). Substantial variation in the chemistry results is also apparent, although some general trends are noticeable - particularly for fractions of typically minor constituents. For example, all users reported relatively high percentages of heavy minerals in Sample 5, relatively high percentages of quartz in Samples 7 and 9, and significant percentages of carbonate in Samples 1-4 and 10 (Figure 2.6).

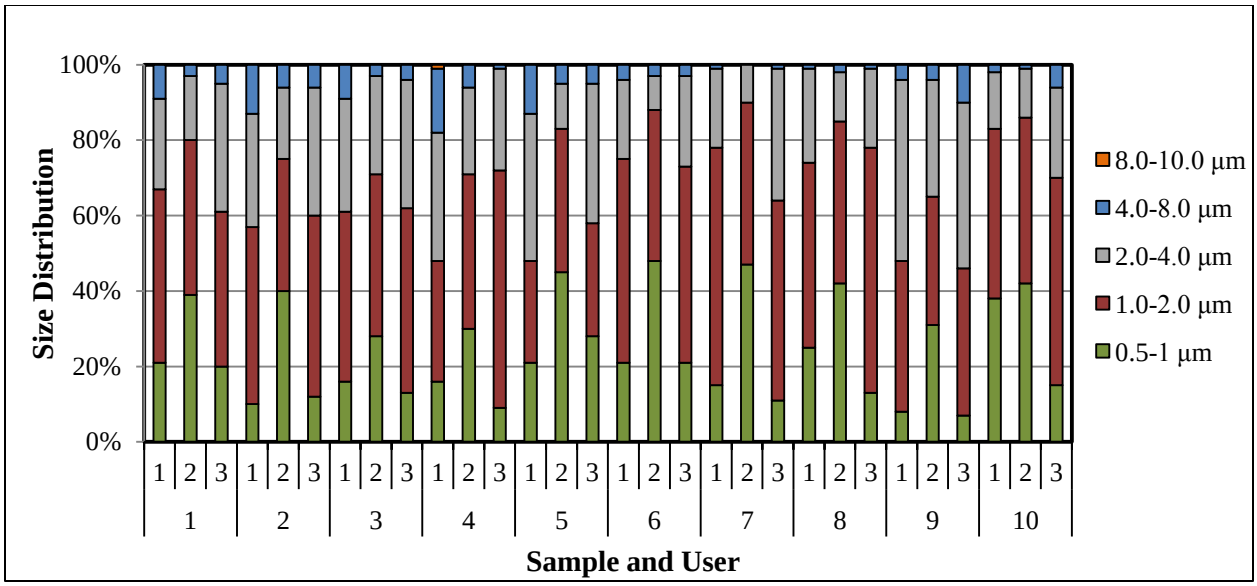

Figure 2.3. *Comparison of particle cross-sectional diameter distributions determined by three different manual users on ten dust samples.*

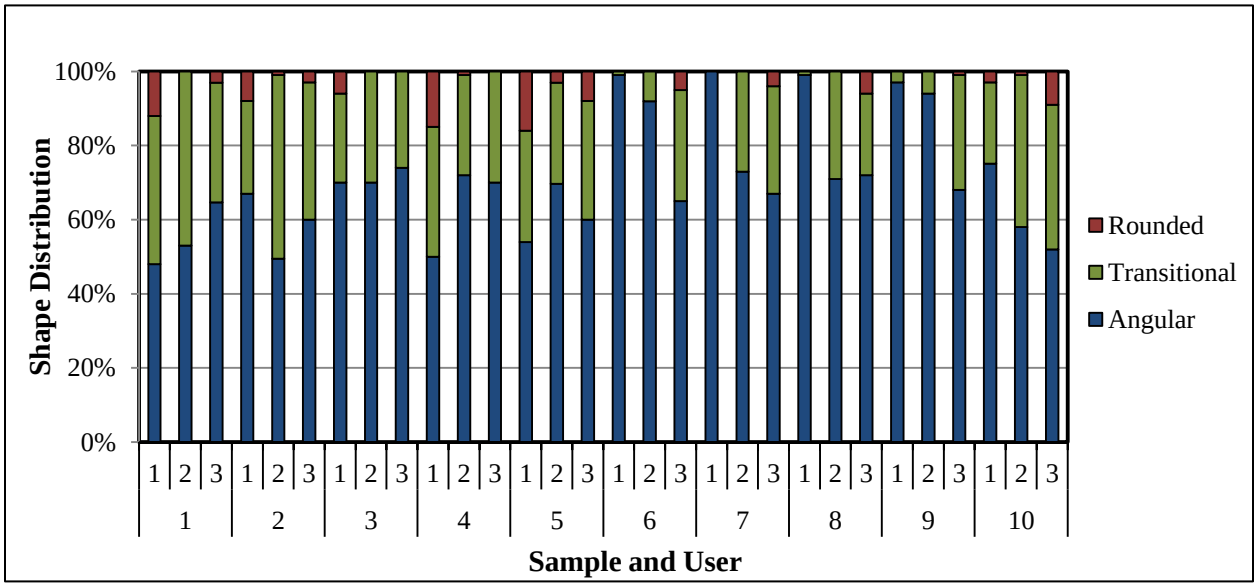

Figure 2.4. *Comparison of particle shape distributions qualitatively determined by three different manual users on ten dust samples.*

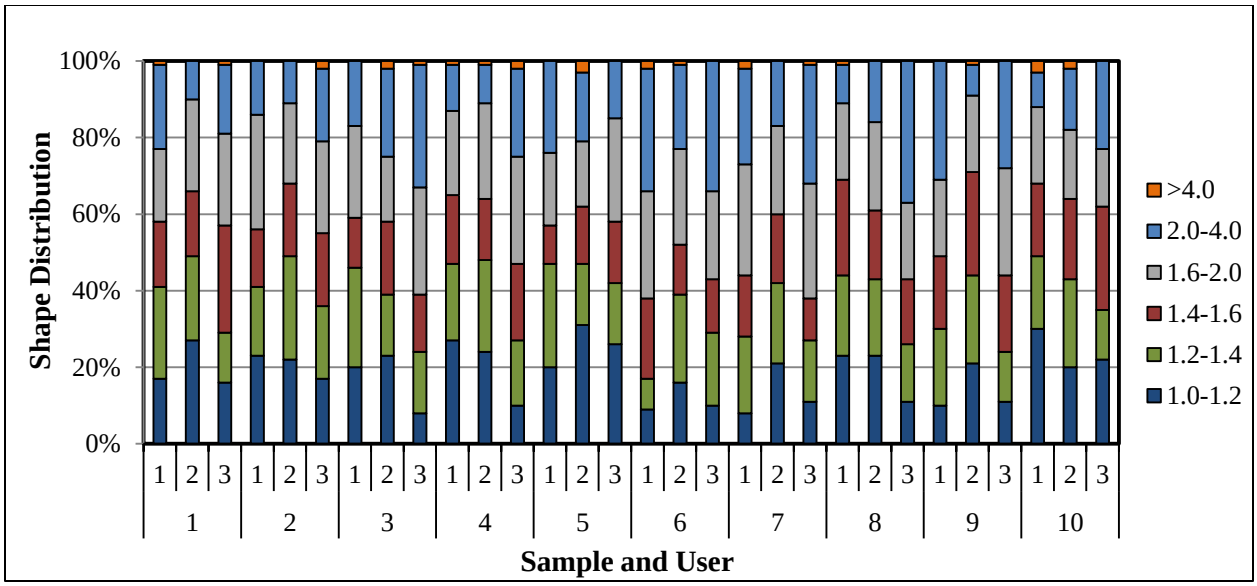

Figure 2.5*. Comparison of particle aspect ratio distributions determined by three different manual users of ten dust samples.*
An aspect ratio of 1.0 indicates a particle has equal long and intermediate dimensions.

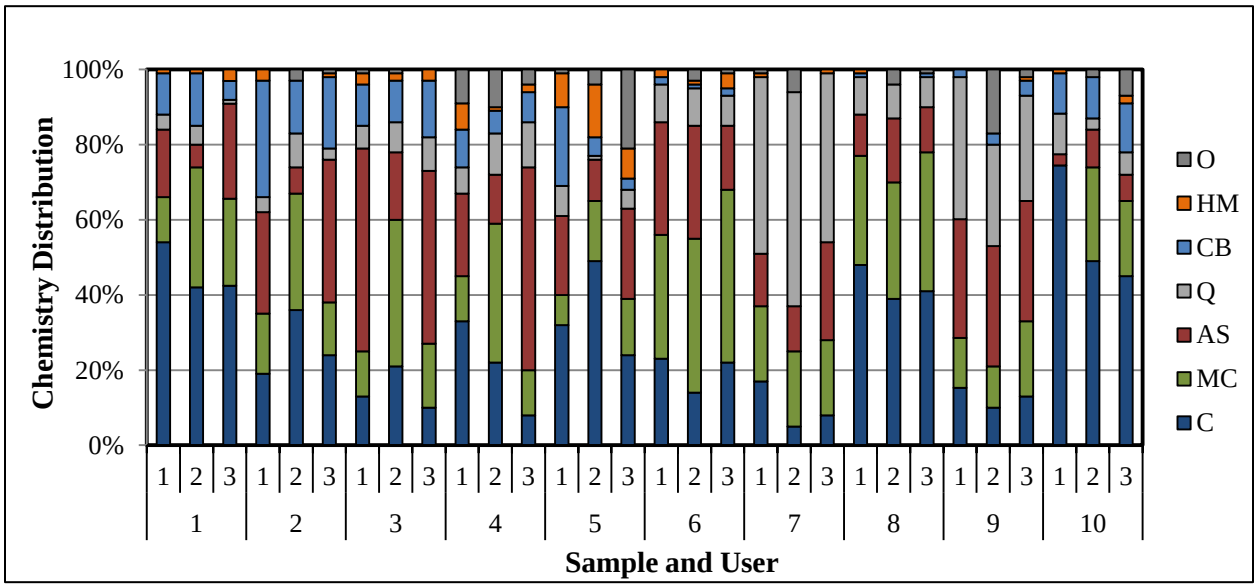

Figure 2.6*. Comparison of particle compositional distributions determined by three different manual users on ten dust samples.*
Chemical composition categories were: Carbonaceous (C), Mixed Carbonaceous (MC), Alumino-silicate (AS), Quartz (Q), Carbonate (CB), Heavy Mineral (HM), Other (O).

To determine whether the data collected by different users was statistically similar, the Freeman-Halton test was performed. This test is a two-sided exact test of independence, which outputs a p-value representing the likelihood of the dependence of two data sets [45]. The test was applied to each pairwise user data set for particle size, shape, and chemistry. Resulting p-

values can be used to determine if, for example, the particle size distribution found for Sample 1 by User 1 agrees with that of User 3. The null hypothesis of each test is that the pair in question agrees (i.e., is statistically similar), and the alternative is that the pair disagrees. At a 95% confidence level, p-values >0.05 indicate pair agreement, while p-values <0.05 indicate disagreement. The results of the Freeman-Halton Test for particle size, shape, and chemistry are displayed in Tables A.5-A.8 in Appendix A, respectively.

Overall, the comparative analysis revealed that results of different users tended to disagree frequently – in terms of size, shape and chemistry. With respect to particle size distributions, only Users 1 and 3 tended to agree often (eight samples). Comparatively, Users 1 and 2 (two samples) and Users 2 and 3 (one sample) mostly disagreed. Similarly, Users 1 and 2 (two samples) and Users 2 and 3 (three samples) were mostly in disagreement with respect to chemistry distributions, while Users 1 and 3 tended to agree more (five samples). For qualitative shape assessments, however, Users 2 and 3 agreed most often (five samples), followed by Users 1 and 3 (three samples) and then Users 1 and 2 (one sample). This may indicate that User 2 and User 3 have a relatively similar perception of particle shape vs. a comparison with User 1. On the other hand, quantitative shape assessments exhibited the most user to user agreement. Users 1 and 2 agreed most often (seven samples), followed by users 1 and 3 (six samples). Users 2 and 3 mostly disagreed (six samples).

Altogether, these results suggest that the number and/or area of filter analyzed by the manual dust characterization method are not sufficient. While the assessment of particle angularity in this method is clearly subjective – and interpretation of EDX spectra can even include some user bias – size and aspect ratio measurements should be largely objective. The fact that distributions of these parameters did not consistently agree well between users most likely indicates that particle deposition on the filter is not completely uniform. Since sample orientation in the SEM undoubtedly changes between users, analysis begins at different locations and different filter areas are ultimately scanned during the analysis. To achieve more reproducible results, which have a higher probability of being representative of an entire sample, particles should be selected for analysis across a larger portion of the filter. Although limited evidence presented by Sellaro et al., 2015 indicated that 100 particles per sample should be sufficient to collect representative data; however, that study did not explicitly consider the issue of substantially different analysis areas on a filter. Given the dramatically increased efficiency

allowed by an automated SEM-EDX routine, analysis of larger number of particles per sample is also prudent.

Automated SEM-EDX Analysis

In order to verify the automated routine described earlier, it was first used to characterize the six known dust samples described earlier. Results are presented in Table 2.3.

Table 2.3*. Chemical composition distribution resulting from the automated SEM-EDX analysis of six known respirable dust samples.*
500 particles were analyzed in each sample.

	Chemical Composition Categories						
Sample	**Carbonaceous**	**Mixed Carbonaceous**	**Alumino-Silicate**	**Quartz**	**Carbonate**	**Heavy Mineral**	**Other**
Coal	92%	3%	1%	1%	2%	1%	0%
Shale	6%	17%	71%	3%	1%	2%	0%
Rock Dust	3%	3%	4%	1%	88%	1%	0%
Quartz	4%	3%	1%	92%	0%	0%	0%
Kaolinite	0%	11%	89%	0%	0%	0%	0%
Calcite	1%	0%	0%	0%	99%	0%	0%

Results for the kaolinite and calcite analysis confirm that respirable-sized particles from these samples are indeed accurately classified by the automated SEM-EDX routine. For the calcite sample, of the 500 particles analyzed, 99% were classified as carbonate and the others were categorized as carbonaceous. This may indicate that a small number of particles were either mis-classified – perhaps due to filter background interference for very thin particles – or that very minor contamination occurred during dust collection. For the kaolinite sample, in which all particles were expected to be alumino-silicates, 100% of particles were classified as either alumino-silicate or mixed carbonaceous. Based on prior work using the manual SEM-EDX method, it was suspected that the mixed carbonaceous category actually represents alumino-silicate particles that are relatively thin or small such that interference from the PC filter background results in relatively high EDX peaks for carbon. These results give further weight to this idea.

For the quartz sample, 92% of the particles were classified as quartz with minor fractions (4% or less) of carbonaceous, mixed carbonaceous, and alumino-silicate. Unlike the kaolinite and calcite materials, which required no size reduction prior to collection of respirable particles, the quartz material had to be pulverized. While care was taken to thoroughly clean the pulverizer

prior to introduction of each new material, it is likely that some contamination of the quartz occurred due to carry over of dust particles from other samples previously prepared in the apparatus.

As mentioned above, the coal, shale, and rock dust product samples were all generated from raw materials, and thus were expected to contain some impurities. For the coal sample, 92% of particles were classified as carbonaceous, with minor fractions (3% or less) showing up in all other defined compositional categories. For the shale sample, 88% of the particles in total were classified in the alumino-silicate and mixed carbonaceous categories, with another 6% coal, 1% carbonate, 3% quartz, and 2% heavy minerals. The presence of carbonaceous and carbonate constituents are consistent with thermogravimetric analysis (TGA) of another sample of this material, which was handpicked and prepared separately. The TGA results showed 5% coal and 8% carbonate by mass. For the rock dust sample, 88% of particles were classified as carbonate. This is in good agreement with mass-based x-ray diffraction (XRD) analysis of this material, which showed 91% carbonate minerals. (XRD results were donated by the mine partner that supplied the rock dust material). From the SEM-EDX analysis, another 7% of the particles were classified as either alumino-silicates or mixed carbonaceous. Assuming the latter category is dominated by relatively small or thin alumino-silicates, these results again agree well with the donated XRD results, which showed 5% alumino-silicate minerals.

Following verification that the automated routine can accurately classify particles into the chemical composition categories of interest, reproducibility of results were also checked. For this, the automated routine was run three separate times on each of the same ten field samples that were previously analyzed by three manual users. For most samples, the automated analysis is completed in less than 20 minutes, which is about 25 times faster than the manual dust characterization method.

Again, results were compared with respect to size, shape and chemistry distributions (Figures 2.7-2.9). (Corresponding Tables A.9-A.11 in Appendix A present the results numerically). All results are based on analysis of 500 particles per sample in each of the three automated scans; and the sample orientation within the SEM was different during each scan (i.e., the sample was either removed from the SEM or rotated between scans).

Based on Figures 2.7-2.9, reproducibility of results is notably better for the automated routine across size, shape and chemistry compared to the manual method. Indeed, for most of the

samples, very little difference is seen between size and shape results from the three different scans. For size (Figure 2.7) and shape (Figure 2.8), all samples appear to show reproducible results. The chemistry distribution results (Figure 2.9) exhibit some slight variability, but comparatively appear much more reproducible than the manual results.

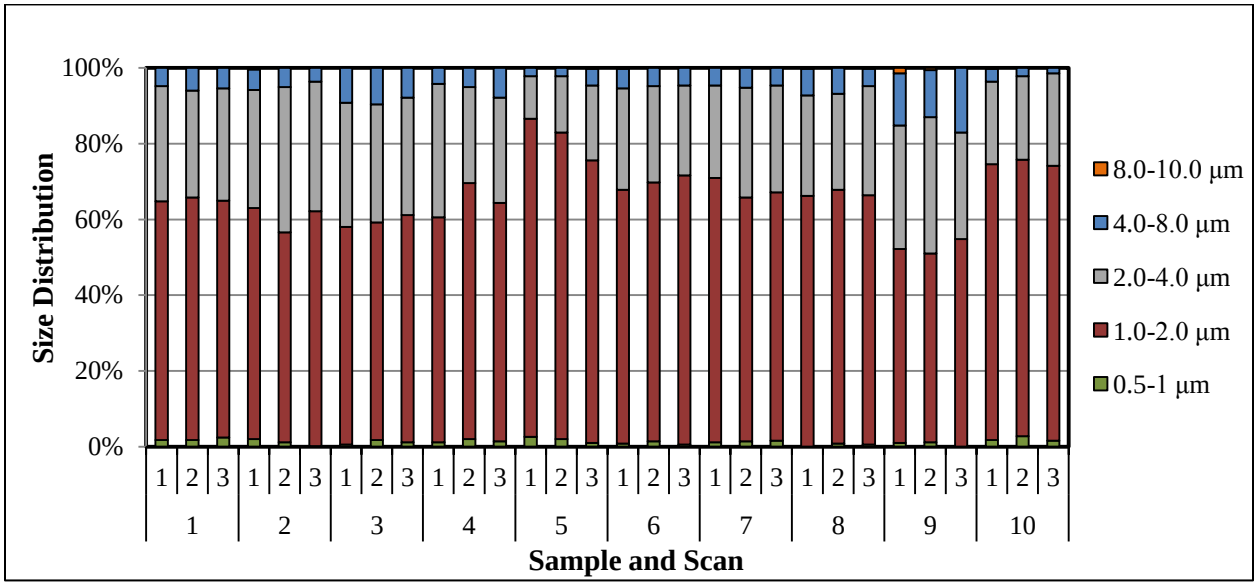

***Figure 2.7**. Comparison of particle cross-sectional diameter distributions determined by three independent automated scans of ten dust samples.*

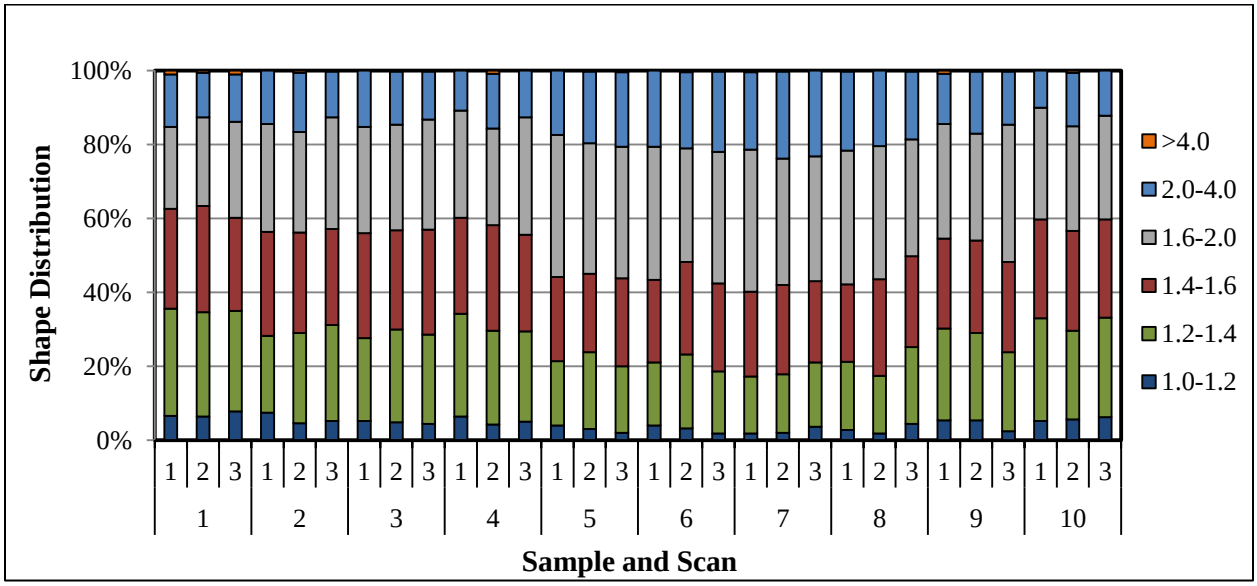

***Figure 2.8**. Comparison of particle aspect ratio distributions determined by three independent automated scans of ten dust samples.*
An aspect ratio of 1.0 indicates a particle has equal long and intermediate dimensions.

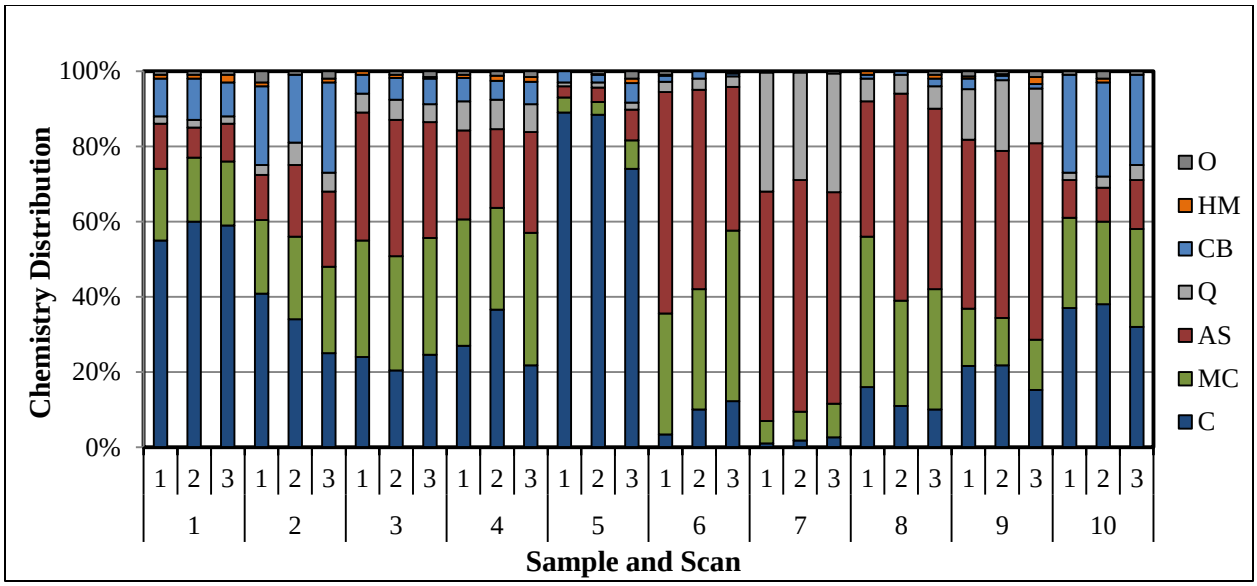

Figure 2.9*. Comparison of particle chemistry distributions determined by three independent automated scans of ten dust samples.*
Chemical composition categories were: Carbonaceous (C), Mixed Carbonaceous (MC), Alumino-silicate (AS), Quartz (Q), Carbonate (CB), Heavy Mineral (HM), Other (O).

To test statistical significance of the results, the Freeman-Halton Test was again performed on each pairwise automation-scan data set for particle size, shape, and chemistry (see Tables A.12-A.14 in Appendix A). All comparisons of particle size and shape distributions from automation-scan to automation-scan were found to be in agreement; and all except one comparison of particle chemistry distributions (Sample 6, Scan 1 vs. Scan 3) were found to be in agreement. This suggests that the automated routine generally analyzes a sufficient number of particles across a sufficient sample area to yield reproducible results.

Direct comparisons between the manual and automated SEM-EDX method results on the ten dust samples are difficult for several reasons. Most importantly, the magnifications differ significantly between the methods (i.e., 10,000x vs. 1,000x) which means that manual users are more likely to include smaller particles (e.g., <1.0μm) in their analysis than does the automated routine. Effectively, the two methods are analyzing a slightly different particle size range. In the ten samples investigated here, the manual characterization results indicate that a relatively large number of smaller particles do exist in the samples – and so these represent a relatively large fraction of the 100 particles included in the analysis. For a direct comparison to the automated results, these particles could be removed, but then some samples may have less than 50 particles on which to determine distribution characteristics.

Analyzing a slightly different size range of particles also makes comparisons of particle shape and chemistry distributions challenging since shape and composition may well vary with size. Also, particle chemistry distributions cannot be directly compared because manual analysis is based on peak heights of elemental spectra while automated analysis is based on elemental atomic percentages. Nevertheless, a qualitative comparison between the manual and automated results shows that, in general, samples found to be relatively high in normally minor constituents (e.g., carbonate or quartz) based on one method also tended to be relatively high in these constituents per the other method.

4. Conclusions

Respirable dust characterization by SEM-EDX can provide new insights into occupational exposures and, potentially, health outcomes for mine workers. Based on a previously developed manual methodology, an automated routine for SEM-EDX analysis of respirable dust samples from coal mines was developed. Operating at just 1,000x magnification, it can accurately classify particles greater than about 1μm into one of six defined chemical composition categories. Compared to manual analysis, it stands to greatly reduce time requirements – typically allowing a scan of 500 particles on a prepared sample in just 20 minutes. Moreover, the automated analysis significantly increases reproducibility of results. This is attributed to both the increased number particles analyzed per sample and the fact that the automated routine guarantees that particles selected for analysis are distributed across a large area of the filter. The routine will next be used to characterize over 200 field samples collected in mines across central and northern Appalachia. To investigate particle distributions in the submicron range, an analogous routine may be developed at higher magnification.

5. Acknowledgements

The authors would like to acknowledge the Alpha Foundation for the Improvement of Mine Safety and Health for funding this work. We would also like to extend thanks to Steve McCartney of Virginia Tech ICTAS-NCFL for operational assistance with SEM-EDX analysis, Ted Juzwak of Bruker Corporation for assistance in learning the Esprit software capabilities, and Dan Baxter of Environmental Analysis Associates for assistance in speeding up the automated routine. We are also grateful to Meredith Scaggs for her efforts to collect and prepare dust

samples, as well as Rachel Sellaro and Patrick Wynne for collecting data via manual SEM-EDX analysis.

References

[1] V. Castranova and V. Vallyathan, Silicosis and coal workers' pneumoconiosis, Environmental Health Perspectives, 108(Suppl 4) (2000) 675-684.

[2] International Agency for Research on Cancer (IARC), Monographs on the evaluation of carcinogenic risks to humans: Silica, some silicates, coal dust and para-aramid fibrils, Geneva, Switzerland: World Health Organization 68 (1997) 41-242, OSHA-2010-0034-1062.

[3] International Organization for Standardization (ISO), Air quality-particle size fraction definitions for health related sampling, ISO Standard 7708 (1995).

[4] World Health Organization (WHO), Hazard Prevention and Control in the Work Environment: Airborne Dust, WHO/SDE/OEH/99.14 (1999).

[5] Occupational Safety and Health Administration (OSHA), Occupational Exposure to Respirable Crystalline Silica -- Review of Health Effects Literature and Preliminary Quantitative Risk Assessment, OSHA-2010-0034 (2010).

[6] J.A. Merchant, G. Taylor, T.K. Hodous, Coal workers' pneumoconiosis and exposure to other carbonaceous dusts, Occupational Respiratory Diseases, NIOSH Publ 86-102 (1986).

[7] J.M. Peters, Silicosis, Occupational Respiratory Diseases, NIOSH Publ 86-102 (1986).

[8] National Institute for Occupational Safety and Health (NIOSH), Criteria for a Recommended Standard – Occupational Exposure to Respirable Coal Mine Dust, DHEW Publication No. 95-106 (1974).

[9] World Health Organization (WHO), Hazard prevention and control in the work environment: airborne dust (1999).

[10] E. Suarthana, A.S. Laney, E. Storey, J.M. Hale, and M.D. Attfield, Coal workers' pneumoconiosis in the United States: regional differences 40 years after implementation of the

1969 Federal Coal Mine Health and Safety Act, Occupational and Environmental Medicine 68 (2011) 908-913.

[11] Centers for Disease Control (CDC), Advanced Cases of Coal Workers' Pneumoconiosis-Two Counties, Virginia, MMWR 55.33 (2006).

[12] Coal Workers' Health Surveillance Program (CWHSP) Data Query System, NIOSH: Centers for Disease Control and Prevention (2016).

[13] V.C. dos S Antao, E.L. Petsonk, L.Z. Sokolow, A.L. Wolfe, G.A. Pinheiro, J.M. Hale, and M.D. Attfield, Rapidly progressive coal workers' pneumoconiosis in the United States: geographic clustering and other factors, Occupational and environmental medicine 62.10 (2005) 670-674.

[14] Mine Safety and Health Administration (MSHA), All Coal Mining Data Table 01. Number of Coal Operations in the United States, by Primary Activity, 1978-2006, Mining Industry Accident, Injuries, Employment, and Production Statistics, US Department of Labor, Retrieved from http://www.msha.gov/STATS/PART50/WQ/1978/ wq78cl01.asp (2008).

[15] A.S. Laney and M.D. Attfield, Coal workers' pneumoconiosis and progressive massive fibrosis are increasingly more prevalent among workers in small underground coal mines in the United States, Occupational and Environmental Medicine 67.6 (2010) 428-431.

[16] J.G. Bennett, J.A. Dick, Y.S. Kaplan, P.A. Shand, D.H. Shennan, D.J. Thomas, and J.S Washington, The relationship between coal rank and the prevalence of pneumoconiosis, British journal of industrial medicine, 36.3 (1979) 206-210.

[17] S. Page and J. Organiscak, Suggestion of a Cause- and-Effect Relationship among Coal Rank, Airborne Dust, and Incidence of Workers' Pneumoconiosis, American Industrial Hygiene Association Journal, 61.6 (2000) 785-787.

[18] D.E. Pollock, J.D. Potts, and G.J. Joy, Investigation into dust exposures and mining practices in mines in the southern Appalachian Region, Mining Engineering, 62.2 (2010) 44-49.

[19] D. Landen, A. Wassel, L. McWilliams, and J. Patel, Coal Dust Exposure and Mortality from Ischemic Heart Disease among a Cohort of U.S. Coal Miners, American Journal of Industrial Medicine, 54.10 (2011) 727-733.

[20] G. Joy, Evaluation of the Approach to Respirable Quartz Exposure Control in U.S. Coal Mines, Journal of Occupational Environmental Hygiene, 9.2 (2012) 65-68.

[21] S.E. Mischler, E.G. Cauda, M. Di Giuseppe, and L.A. Ortiz, A multi-cyclone sampling array for the collection of size-segregated occupational aerosols, Journal of Occupational and Environmental Hygiene 10.12 (2013) 685-93.

[22] J. F. Colinet, J. P. Rider, J. M. Listak, J. A. Organiscak, and A. L. Wolfe, Best Practices for Dust Control in Coal Mining, OMSHR, Information Circular 9517 (2010).

[23] R. Agius, Occupational and Environmental Lung Disease, Health, Environment & Work (2009).

[24] G. Fritz, P. Camus, and D. Rohde, Consideration for Automated Multi-Frame Particle Sizing in the SEM, Microscopy and Microanalysis 12.S02 (2006) 210-211.

[25] R. Sellaro, A Standard Characterization Methodology for Respirable Coal Mine Dust Using SEM-EDX, Resources 4.4 (2015) 939-957.

[26] R. Sellaro and E. Sarver, Preliminary investigation of SEM-EDX as a tool for characterization of coal mine dusts, Mining Engineering 66.8 (2014) 16-40.

[27] R. Sellaro and E. Sarver, Characterization of respirable dust in an underground coal mine in Central Appalachia, Transactions of the Society for Mining, Metallurgy & Exploration 336 (2014) 457-466.

[28] V. Johann and E. Sarver, Considerations for an Automated SEM-EDX Routine for Characterizing Respirable Coal Mine Dust, Proceedings of the 2015 North American Mine Ventilation Symposium (2015).

[29] Z. Cvetkovic, M. Logar, A. Rosic, and A. Ciric, Mineral composition of the airborne particles in the coal dust and fly ash of the Kolubara basin (Serbia), Periodico di Mineralogia 81.2 (2012).

[30] K. Deboudt et al., Mixing state of aerosols and direct observation of carbonaceous and marine coatings on African dust by individual particle analysis, Journal of Geophysical Research 115 (2010) 1-14.

[31] M. Micheletti, L. Murruni, M. Debray, et al., Elemental Analysis of Aerosols Collected at the Pierre Auger Cosmic Ray Observatory with PIXE Technique Complemented with SEM/EDX, Nuclear Instruments and Methods in Physics Research *B288* (2012) 10-17.

[32] K. Suzuki, Characterisation of Airborne Particulates and Associated Trace Metals Deposited on Tree Bark by ICP-OES, ICP-MS, SEM-EDX, and Laser Ablation ICP-MS, Atmospheric Environment 40 (2006) 2626-2634

[33] M. Kasahara, K. Shinoda, K. Yoshida, K. Takahashi, Characterization of Atmospheric Aerosol based on SEM-EDX Analysis of Individual Particles, Journal of Aerosol Science 24(Suppl. 1) (1993) S585-S586.

[34] J. Kasparian, E. Frejafon, P. Rambaldi, et al., Characterization of Urban Aerosols using SEM-Microscopy, X-ray Analysis and Lidar Measurements, Atmospheric Environment 32.17 (1998) 2957-2967.

[35] M. Carpenter, E. Lifshin, R. Gauvin, SEM-EDS Quantative Analysis of Aerosols ≥80 nm: Impact on Atmospheric Aerosol Characterization Campaigns, Microscopy and Microanalysis 8 (Suppl. 2) (2002) 1482CD-1483CD.

[36] A. Wang, B. Luo, Application SEM to Analysis Formation Characteristic of Soot Aerosol Emitted from Lump-Coal Combustion in Fixed-Bed, Proceedings of the Power and Energy Engineering Conference, APPEEC, Asia-Pacific (2009).

[37] E. W. White, P. B. DeNee, Characterization of coal mine dust by computer processing of scanning electron microscope information, Annals of the New York Academy of Sciences 200 (1972) 666-675.

[38] P. DeNee, Mine dust characterization using the scanning electron microscope, American Industrial Hygiene Association Journal 33.10 (1972) 654-660.

[39] K. Terry, Particle Size Distribution of Airborne Dusts Using a Scanning Electron Microscope, Aerosol Science and Technology 23.3 (1995) 475-478.

[40] C. W. Huggins, G.T. Meyers, Particle Size Distribution of Quartz and Other Respirable Dust Particles Collected at Metal Mines, Nonmetal Mines, and Processing Plants, Bureau of Mines Report of Investigations (1986).

[41] M. F. Hoover, E. N. White, J. Lebiedzik, G. G. Johnson, Automated characterization of particulates and inclusions, Microbeam Analysis (1975) 54A-54B.

[42] S. Ekelund, T. Werlefors, A system for the quantitative characterization of microstructures by combined image analysis and Z-ray discrimination in the scanning electron microscope [with minicomputer control], Scanning Electron Microscopy I (1976) 417-424.

[43] A. Worobiec, S. Potgieter-Vermaak, A. Brooker, et al., Interfaced SEM/EDX and Micro-Raman Spectrometry for Characterisation of Heterogeneous Environmental Particles – Fundamental and Practical Challenges, Microchemical Journal 94 (2010) 65-72.

[44] N. Ritchie and V. Filip, SEMantics for High Speed Automated Particle Analysis by SEM/EDX, Microscopy and Microanalysis 17.S2 (2011) 896-897.

[45] A. Agresti, A Survey of Exact Inference for Contingency Tables, Statistical Science 7.1 (1992) 131-153.

Chapter 3. Comparison of Respirable Mine Dust Across Mines in Central and Northern Appalachia

Victoria Johann[a], *Emily Sarver*[a], *Cigdem Keles*[a], *Jeanine Buchanich*[b]
[a]*Virginia Tech, Blacksburg, Virginia, USA*
[b]University of Pittsburgh, *Pittsburgh, Pennsylvania, USA*

Abstract

Increased incidence of coal workers' pneumoconiosis (CWP) and related occupational lung diseases amongst underground coal miners in parts of Appalachia has prompted research on the issue. One focus has been on specific mine dust characteristics that may provide insights into health outcomes. Over 16 months, 210 samples of respirable dust were collected in eight underground coal mines, including two in northern Appalachia, four in mid-central Appalachia, and two in south-central Appalachia. These operations vary in terms of mining method, coal seam thickness, and mined strata geology. Dust samples were taken in various locations within each mine, including in the intake and return, near the feeder or conveyance, and near major production activities such as coal cutting and roof-bolting. An automated SEM-EDX routine was used to characterize up to 500 respirable dust particles per sample such that distributions in size, aspect ratio, and chemistry classification could be determined. This paper evaluates spatial and temporal variation between samples and sample sets. It also compares results between and within mine regions, and examines relationships between the different dust particle characteristics.

Keywords: CWP, Silicosis, Computer-Automated SEM-EDX, Respirable Dust, Particle Cross-Sectional Diameter, Aspect Ratio, and Chemical Composition

1. Introduction

Respirable dust is classified as particulates with aerodynamic diameter less than 10μm, and has long been recognized as a key occupational health hazard for underground coal miners [1-4]. Typically following years of exposure, coal workers' pneumoconiosis (CWP) and silicosis are the most common disease diagnoses. CWP has been generically associated with coal mine dust, while silicosis is associated with exposure to crystalline silica (i.e., quartz) [5]. Although regulatory limits on respirable dust exposures, coupled with better ventilation and dust abatement strategies, resulted in significant declines in CWP and silicosis incidence for several

decades in the US [6-9], since the late 1990s, a resurgence in disease incidence has been noted [8, 10]. The most disconcerting trends have been observed in parts of central Appalachia (e.g., MSHA districts 4 and 12), and many new cases of CWP and silicosis are advanced or are presenting in younger miners [8-10].

While the cause(s) of these recent trends is currently unknown, potential factors include changes in specific dust characteristics, such as particle size, shape, and chemistry (e.g., see [11-19]). For instance, dust characteristics may have changed due to mines in the affected regions extracting increasingly thinner coal seams, thereby increasing the amount of roof and floor rock being cut [13-16]. Because geology in these regions often consists of sandstone layers above the coal seams, miners might also be exposed to higher concentrations of respirable crystalline silica [15, 17]. Likewise, exposure conditions may be significantly different now than in years past. The smaller mine sizes and labor forces common in central Appalachian coal mines could mean that miners are working longer hours and in varying job roles, thus being exposed to higher and/or variable dust concentrations and compositions [3, 9, 14].

Apart from higher dust mass concentrations and higher non-coal fractions, dust particle size and shape may also be important. Recent studies suggest that smaller particle sizes may be more harmful to health than larger, but still respirable-sized particles [18]; and advances in mining equipment have certainly resulted in more powerful cutting (i.e., of coal or rock during mining and drilling), which can yield smaller particles [19]. It is also established that dust particle deposition mechanisms in the lungs (e.g., sedimentation vs. impaction vs. interception vs. diffusion) can be dependent on both size and shape (e.g., elongation, angularity, roughness) [20]. Thus, a better understanding of these characteristics may be key to understanding miner health outcomes.

In order to study respirable mine dust characteristics in central Appalachia where lung disease incidence generally appears to be on the rise, versus northern Appalachia, a total of 210 dust samples were collected in eight underground coal mines over approximately 16 months. The samples were scanned using an automated SEM-EDX routine previously developed by the authors (see Chapter 2). Results were analyzed to specifically: 1) investigate spatial and temporal variability of samples collected in the same location within a mine 2) compare size, shape (i.e., aspect ratio), and chemistry distributions between and within distinct mine regions, and by

general sampling location categories (i.e., intake, feeder, production, return); and 3) examine relationships between different dust particle characteristics.

2. Materials and Methods

Of the eight mines sampled, six were classified as being in central Appalachia (MSHA districts 4 and 12) and two were in northern Appalachia (MSHA districts 2 and 3). Based on field observations and information provided by mine personnel, some general characteristics can be described for each mine region (Table 3.1).

Table 3.1. *General Mine Characteristics*

	MCA				**NA**		**SCA**	
	Mine 1	**Mine 2**	**Mine 3**	**Mine 4**	**Mine 5**	**Mine 6**	**Mine 7**	**Mine 8**
Primary coal seam	Eagle	Powellton	Peerless	Cedar Grove	Pittsburgh #8		#2 gas	Alma
Seam thickness (ft)	3-5	3-4	4.5	2-4	6-8	6.5	5-6	4-4.5
Total mining height (ft)	5	5.5	6	4	8	8	6-7	6
Primary rock strata	sandstone	sandstone	shale and sandstone	sandstone	sandy shale and slate	shale	sandy shale and slate	shale
Number of sections	2 CM	2 CM	2 CM	2 CM	1 LW; 3 CM	1 LW; 5 CM	3 CM	2 CM
Production (10^6 tons/yr)	0.45	0.45	0.84	0.55	2.4	7.5	1.3	0.9
Typical dust conc.[1]	low to moderate	low to moderate	low to moderate	low	low to high	low to moderate	low to moderate	low to moderate
Typical quartz percentage[2]	low to moderate	low to high	low to moderate	low to high	low	low	low to moderate	low to high

[1]based on operator and inspector mine samples collected between 2013-2016; low = <0.6 mg/m^3, moderate = 0.6-1.8 mg/m^3, high = >1.8 mg/m^3

[2]based on operator and inspector mine samples collected between 2013-2016; low = <5.0%, moderate = 5.0-9.0%, high = >9.0%

Northern Appalachian (NA) mines are longwall operations (with continuous miner development sections) generally characterized by: relatively thick coal seams having few

partings of shale, but some pyrite and other heavy mineral content; high production rates; and large workforces. Central Appalachian mines, on the other hand, are continuous miner operations with: relatively thin coal seams having more shale partings, oftentimes a sandstone roof and floor, and less pyrite and other heavy minerals; low production rates; and small workforces. Due to the thin coal seams and usual continuous miner cutting heights, these mines often cut significant floor and/or roof rock. Within central Appalachia, two distinct sub-regions were defined as mid-central Appalachia (MCA) and south-central Appalachia (SCA), which are known to vary somewhat by typical respirable silica (mass) content in compliance dust samples.

Dust samples were collected in various locations within each mine, which can be designated in one of four categories: in the "intake" (including near the headgate of a longwall); near the "feeder" or conveyance system; near major "production" activities (e.g., coal cutting by continuous miner or along the midface of a longwall, and roof-bolting); and in the "return" (including near the tailgate of a longwall), which on occasion had an operating trickle duster (i.e., to apply inert rock dust). In most instances, sampling equipment (described below) was hung from roof bolts toward the center of the airway being sampled; sometimes, this was not possible due to safety concerns or interference with mine activities, so samplers were hung near the rib or on a piece of operating equipment (e.g., roof bolter). In all cases, samples were collected in sets of at least two. For sets containing only two or three samples, they were generally taken side-by-side (i.e., cassettes just a few centimeters apart and oriented in the same direction), simultaneously, such that these samples can be considered true duplicates or triplicates. In some mines, four samples were collected in a set using the collection configuration shown in Figure 3.1.

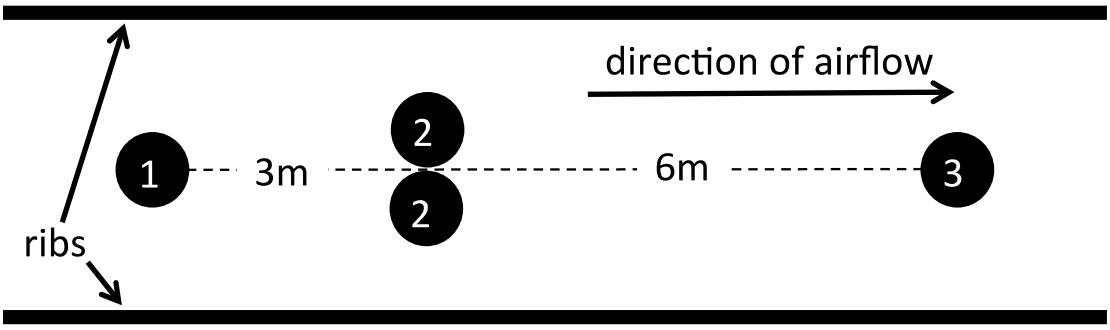

Figure 3.1. *Schematic of sample collection configuration when four samples were collected in a set. In these sets, two (duplicate) samples were collected in position 2, and two additional samples were collected in relatively close proximity at positions 1 and 3, which were up- and down-stream of the duplicate samples, respectively.*

At least one sample set (i.e., 2-4 samples) was collected in each location category in each mine (Table 3.2). In most mines, more than one location in a category was sampled (e.g., roof bolter and continuous miner samples are both categorized as "production"). In several instances, the same mine location was sampled multiple times (i.e., multiple sample sets were collected, each at a different time).

All samples were collected directly onto 37-mm diameter polycarbonate (PC) filters in two-piece cassettes using standard equipment: Escort ELF dust sampling pumps (calibrated to a flow of 1.7 L/min) with nylon Dorr-Oliver cyclones to remove particles larger than respirable size. Sample sets were typically collected over approximately a 2-4 hour timeframe. The samples were prepared for SEM-EDX analysis by mounting a 9-mm filter subsection (cut from the center of each sample) to an aluminum stub, and sputter coating with Au/Pd for electrical conductivity.

A computer-automated SEM-EDX routine (see Chapter 2) was used to characterize approximately 500 respirable dust particles per sample (with the exception of samples having very small particle loading densities), such that distributions in size (i.e., cross-sectional diameter), aspect ratio (i.e., ratio of the long to intermediate particle diameter), and chemistry classification could be determined. Five chemical classification categories were previously defined, which are expected to cover the majority of dust particles from Appalachian coal mines: carbonaceous (C), alumino-silicate (AS), quartz (Q), carbonate (CB), and heavy mineral (HM) (Table 3.3). Particles are classified into these categories based on the atomic percentages of key elements observed in their EDX spectra. For particles that do not meet the classification criteria for one of these five categories, a sixth category called "other" (O) is used. (It should be noted that, in prior work, an additional category called "mixed carbonaceous" was also defined and used. However, particles in that category are thought to be primarily very thin or small alumino-silicates per analysis shown in Chapter 2 and Sellaro et al., 2014 and 2015 [21-23], and so those particles were classified as AS here.)

***Table 3.2**. Respirable dust sample collection summary. Mines are grouped by region: mid-central Appalachia (MCA), northern Appalachia (NA), and south-central Appalachia (SCA). Unless noted, samples were collected as shown in Figure 3.1 for Mines 1-5, and only as duplicates for Mines 6-8. The four general location categories are divided into their more specific sampling locations: H=longwall headgate, I=intake, TR=track, BD=belt drive, C=conveyor, F=feeder, B=roof bolter, M=continuous miner, MF=longwall midface, R=return, T=longwall tailgate, TD=trickle duster.*

Number of Samples/Sample Sets Collected in Specific Location														
Region	**Mine**	**Intake**			**Feeder**			**Production**			**Return**			**Total**
		H	**I**	**TR**	**BD**	**C**	**F**	**B**	**M**	**MF**	**R**	**T**	**TD**	
MCA	1	0/0	4/1	0/0	0/0	0/0	4/1	4/2[1]	6/2[2]	0/0	4/1	0/0	0/0	22
	2	0/0	4/1	0/0	0/0	0/0	4/1	8/2	4/1	0/0	4/1	0/0	0/0	24
	3	0/0	4/1	0/0	0/0	0/0	4/1	4/1	4/1	0/0	4/1	0/0	0/0	20
	4	0/0	4/1	0/0	0/0	0/0	4/1	4/1	0/0	0/0	4/1	0/0	0/0	16
NA	5	3/1[3]	4/1	0/0	0/0	4/1	8/2	4/1	0/0	4/1	8/2	4/1	0/0	39
	6	2/1	8/4	2/1	2/1	0/0	4/2	2/1	2/1	2/1	4/2	2/1	0/0	30
SCA	7	0/0	4/2	0/0	0/0	0/0	6/3	4/2	8/4	0/0	7/3[4]	0/0	0/0	29
	8	0/0	6/3	0/0	0/0	0/0	6/3	4/2	6/3	0/0	6/3	0/0	2/1	30
Total Samples		5	38	2	2	4	40	34	30	6	41	6	2	**210**
Total Sample Sets		2	14	1	1	1	14	12	12	2	14	2	1	**76**
Total Samples in Location Category		45			46			70			49			

[1] two sets of 2 (duplicate) samples
[2] one set of 4 samples (per Figure 3.1 configuration) and one set of 2 (duplicate) samples
[3] one set of 3 samples (no duplicates, one sample collected in each position shown in Figure 3.1)
[4] one set of 3 (triplicate) samples and two sets of 2 (duplicate) samples

***Table 3.3**. Defined chemical composition categories of Appalachian coal mine dust.*

Chemical Composition Category	Carbonaceous (C)	Alumino-Silicate (AS)	Quartz (Q)	Carbonate (CB)	Heavy Mineral (HM)
Example Mineralogy	coal	clays, feldspars	crystalline silica	rock dust, calcite, dolomite	pyrite, Fe/Al/Ti oxides

SEM-EDX work was performed using an FEI Quanta 600 FEG environmental scanning electron microscope (ESEM) (Hillsboro, OR), equipped with a backscatter electron detector (BSD) and a Bruker Quantax 400 EDX spectroscope (Ewing, NJ). Bruker's Esprit software version 1.9.4 (complete with DriftCorr, ImageStitch, Feature, StageControl, and Jobs tools) was used to program and run the automated scanning routine. All work was conducted in high vacuum at 15kV, 12.5mm working distance, 6.5μm spot size, 25,000cps count rate, and 1,000x magnification.

The automated routine collects data on multiple size, shape, and chemistry parameters; however, only cross-sectional diameter, aspect ratio, and chemical classification results were used in the comparative analysis that follows. The automated routine is programmed to output data on a per-particle basis. To make high-level comparisons between and within mines and mine regions, continuous quantitative data was consolidated by binning. Particles were classified into one of three bins based on their cross-sectional diameter: [0.94-2.0)μm, [2.0-3.0)μm, or [3.0-9.0)μm. These size bins represent relatively small, medium, and large respirable-sized particles, respectively. Three bins were also defined for particle aspect ratio: <1.5, [1.5-3), ≥3. As with the size bins, these bins represent particles with relatively low, moderate, and relatively high aspect ratios, respectively. Since the chemistry results are categorical, this data was automatically binned by category: C, AS, Q, CB, HM, O. Results of dust sample characteristics are presented as a percentage of particles classified into the respective size, aspect ratio and chemistry bins.

Statistical Methods

To investigate spatial variability in dust characteristics amongst duplicate samples (i.e., taken side-by-side) and samples collected in close proximity to one another (i.e., as shown in Figure 3.1), comparisons were made between chemistry distribution results from all such sample pairs. For these comparisons, the Freeman-Halton test of independence was used to determine whether statistical differences exist. This test is a two-sided exact test of independence, which outputs a p-value representing the likelihood of the dependence of two data sets [24]. Resulting p-values can be used to determine if, for example, the particle chemistry distribution found for Sample 1 agrees with that of Sample 2. The null hypothesis of each test is that the pair in question agrees (i.e., is statistically similar), and the alternative is that the pair disagrees. At a 95% confidence level, p-values >0.05 indicate pair agreement, while p-values <0.05 indicate disagreement. The Freeman-Halton test was also used to investigate temporal variation in dust characteristics by comparing results from samples collected in the same mine location but at different times (i.e., hours to days apart). Here, the results from all samples in a set were averaged, such that pairs of sample sets could be compared (i.e., the average characteristics from the set taken on day 1 were compared to those from the set taken on day 2).

To investigate differences in dust characteristics between and within regions, between sampling location categories, and between different dust characteristics, one-way Analysis of Variance (ANOVA) testing was performed. In all cases, the null hypothesis was that all

population means were equal and the alternative hypothesis was that at least one mean was different. Resulting F-statistics were compared to the critical F-value corresponding to a 95% confidence level. If the F-statistic was greater than F-critical, then the null hypothesis was rejected, indicating at least one significant difference in particle distributions. In these instances, two-tailed t-tests were performed (also at a 95% confidence level) to pinpoint the detected difference(s).

3. Results and Discussion

All dust characteristic data collected for the entire sample collection is summarized in Table B.1 in Appendix B. For each sample, results represent the percentage of particles in the aforementioned size, aspect ratio, and chemistry bins. Utilizing the automated routine, analysis was on average completed in less than 20 minutes per sample. Of the 210 total samples, 10 samples had fewer than 500 particles analyzed (i.e., due to very low dust particle density on the filter). Those samples were therefore not included in statistical analyses. In general, very few samples appeared to contain an abundance of relatively large particles; and very few contained an abundance of particles with relatively high aspect ratios. The majority of particles in all samples had cross-sectional diameters less than 2μm and moderate aspect ratios. Moreover, all samples had particles classified into multiple chemistry categories, and the most common classifications were carbonaceous (C), alumino-silicate (AS), carbonate (CB), and/or quartz (Q).

Spatial and Temporal Variability

Since all sample sets contained at least two samples, and some sets were replicated by collecting at different times, comparisons of both spatial (i.e., between samples collected side-by-side, or within close proximity as shown in Figure 3.1) and temporal variability are possible. For spatial variation, there were 71 total pairs of true duplicate samples to be compared, and 81 comparisons of samples in close proximity to one another (i.e., 3, 6, or 9 meters apart). For comparisons of samples in close proximity to one another, duplicate samples in position 2 were averaged and then compared with the samples in positions 1 and 3, and samples in positions 1 and 3 were also compared to each other. For temporal variation, there were eight instances where sets of samples were collected in the same mine location under similar mine conditions (i.e., active production), but at different times. For these comparisons, the results from all samples in a

set were averaged, such that pairs of sample sets could be compared (i.e., the average characteristics from the set taken on day 1 were compared to those from the set taken on day 2). Results of these Freeman-Halton test comparisons for both spatial and temporal variability are located in Tables B.2-B.4 in Appendix B.

The comparisons of the 71 true duplicate samples yielded 57 pairs in agreement (80%) and 14 pairs in disagreement (20%). The sampling locations of pairs in disagreement were: one at a continuous miner, one at a roof bolter, five at feeders, two in intakes, three in returns, one at a headgate, and one at a trickle duster. By general mine location category, these pairs correspond to three in *intake*, five in *feeder*, two in *production*, and three in *return*. As discussed in Chapter 2, the automated SEM-EDX routine has been shown to provide reproducible results (i.e., between multiple scans of the same sample) – at least on a limited set of field samples – so variation in duplicate samples reported here suggests that spatial variability even between samples collected side-by-side can be an issue in some cases. It appears that samples nearby the feeder may be more likely to exhibit such variation. In the feeder category, 33% of sample pairs (i.e., 5 of 15 total) were found to be in disagreement.

Comparisons of the 81 pairs of samples collected in close proximity to one another yielded 56 pairs in agreement (69%) and 25 pairs in disagreement (31%). The sampling locations of pairs in disagreement are as follows: one at a continuous miner, five in intakes, five at feeders, six in returns, two at roof bolters, two at a headgate, three at a conveyor, and one at a longwall midface. By mine location category, these pairs correspond to seven in *intake*, eight in *feeder*, four in *production*, and six in *return*. Moreover, out of the disagreeing samples, three groupings of intake sample pairs, two groupings of feeder sample pairs, one grouping of production sample pairs, and three groupings of return sample pairs came from the same sample set. Generally speaking, it thus appears that spatial variability between samples collected in relatively close proximity is not highly associated with production sampling locations; however, it could possibly be associated with intake, feeder, or return categories. In the intake category, 44% of sample pairs (7 of 16 total) were found to be in disagreement; in the feeder category, 42% (8 of 19 total) were in disagreement; and in the return category, 29% (6 of 21 total) were in disagreement.

Temporal comparisons between eight pairs of samples collected in the same location but at different times yielded seven pairs in agreement (88%) and one pair in disagreement (13%).

The samples for the pair in disagreement were collected in a return. Other pairs included one collected in a return, three collected in a feeder, two collected at roof bolters, and one collected near a continuous miner. While only a limited number of sample sets were available for this comparison, the relatively good agreement amongst sets suggests that dust characteristics may not necessarily vary significantly over relatively short time periods (i.e., from shift to shift or day to day) – at least in the specific sampling locations represented here.

Regional Variability

From a cursory visual analysis (e.g., Figure 3.2), some variation in regional dust characteristics is evident. With respect to particle chemistry distributions, there are distinct differences between regions in each locational category. For example, northern Appalachia seems to have consistently lower percentages of AS particles and higher percentages of CB particles than mid-central and south-central Appalachia by sampling location. To investigate regional trends in particle characteristics, all samples were grouped by region and ANOVA and t-tests were performed on each size, shape, and chemistry category. The results of the ANOVA and t-tests for cross-sectional diameter, aspect ratio, and chemistry distributions are presented in Table 3.4. Corresponding t-statistics are provided in Tables B.5-B.15 in Appendix B.

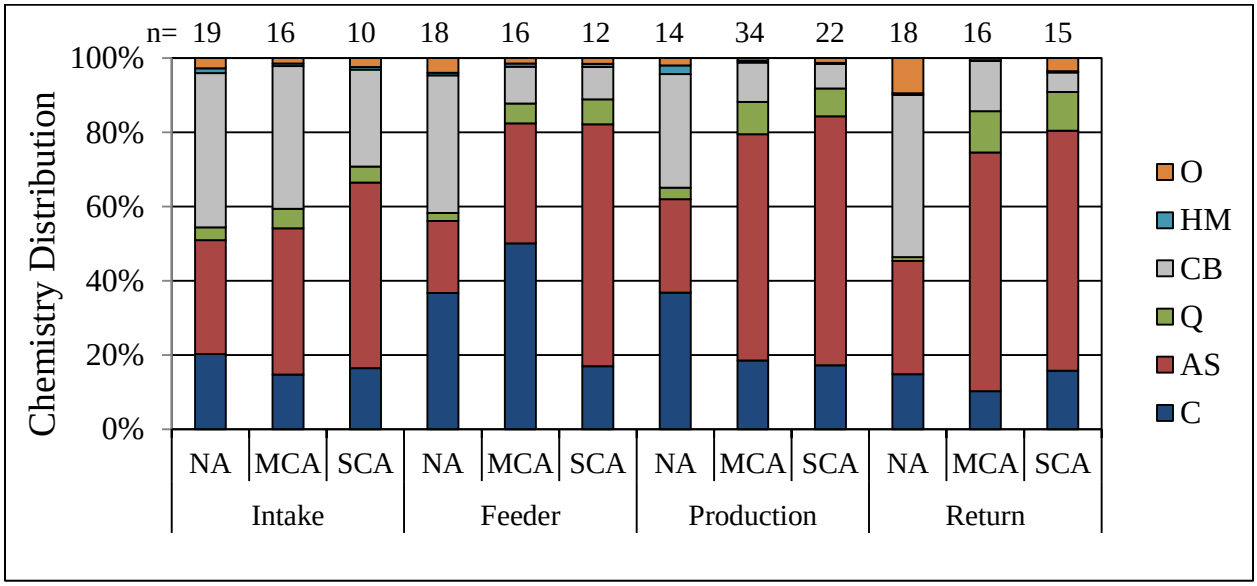

Figure 3.2*. Particle chemistry distributions for each region separated by locational category. Number of samples are provided above the bar for each category.*

***Table 3.4**. ANOVA and t-test results by region. Null hypothesis: all means are equal (i.e., μ NA = μ MCA = μ SCA), Critical F-Value: 3.04.*

	F-value	Differences Observed	Mean Values by Region		
			NA	MCA	SCA
Cross-Sectional Diameter					
[0.94-2.0) μm	17.76	μ MCA > μ NA μ MCA > μ SCA	54.0%	64.4%	56.5%
[2.0-3.0) μm	19.26	μ NA > μ SCA > μ MCA	23.6%	20.1%	21.7%
[3.0-9.0) μm	12.48	μ NA > μ MCA μ SCA > μ MCA	22.4%	15.6%	21.8%
Aspect Ratio					
<1.5	11.79	μ NA > μ SCA μ MCA > μ SCA	40.6%	40.7%	35.6%
[1.5-3)	11.56	μ SCA > μ NA μ SCA > μ MCA	57.1%	57.0%	61.6%
≥3	1.72	no statistical difference between means	2.3%	2.3%	2.7%
Chemistry					
C	4.72	μ NA > μ SCA	26.2%	21.4%	16.6%
AS	39.19	μ SCA > μ MCA > μ NA	27.6%	53.0%	63.6%
Q	11.24	μ MCA > μ NA μ SCA > μ NA	2.3%	6.9%	7.5%
CB	29.10	μ NA > μ MCA > μ SCA	38.3%	17.0%	9.6%
HM	7.52	μ NA > μ MCA μ NA > μ SCA	1.1%	0.5%	0.5%
O	12.72	μ NA > μ SCA > μ MCA	4.6%	1.0%	2.1%

Particle Cross-Sectional Diameter

Significant differences between regions were detected by ANOVA for each size bin. The results of the t-tests indicate that mid-central Appalachia has more small particles than northern and south-central Appalachia; and conversely, northern and south-central Appalachia have more large particles than mid-central Appalachia. Northern Appalachia has the highest percentage of medium-sized particles, followed by south-central Appalachia and then mid-central Appalachia. The finding of significantly more small particles in mid-central Appalachia is an important distinguishing factor for this region relative to the other two regions investigated here. If smaller particles are more harmful to health than larger respirable-sized particles, as recent studies suggest [e.g., 18-19], this finding may help shed light on the possible contributing factors to miner health outcomes in this region.

Particle Aspect Ratio

Significant differences between regions were also detected by ANOVA with respect to particle aspect ratio. The results of the t-tests indicate that northern and mid-central Appalachia have higher percentages of particles with relatively low aspect ratios (i.e., < 1.5) than south-central Appalachia; and conversely south-central Appalachia has a higher fraction of particles with moderate aspect ratios (i.e., 1.5-3) than northern and mid-central Appalachia. The tendency for particles to have relatively higher aspect ratios in south-central Appalachia may be related to the relatively higher fraction of alumino-silicate particles in mines in this region (see next section). Correlation between specific chemistry categories and particle aspect ratio and size is further examined later. No significant differences were detected between regions for particles with relatively high aspect ratio (i.e., ≥3.0).

Particle Chemistry

Significant differences between regions were additionally detected by ANOVA when examining particle chemistry classification. The results of the t-tests indicate that northern Appalachia has a higher fraction of carbonaceous (i.e., coal) particles than south-central Appalachia. This is consistent with expectations based on the relatively thick coal seams in northern Appalachian, which do not necessitate mining significant roof or floor rock. T-test results also indicate that south-central Appalachia has the highest percentage of alumino-silicate particles, followed by mid-central Appalachia and then northern Appalachia. This finding is again consistent with expectations based on coal seam thickness, since the central Appalachian region's thinner seams do require cutting more roof and floor rock that oftentimes is dominated by shale. Moreover, both mid-central and south-central Appalachia were found to have larger fractions of quartz particles than northern Appalachia – and some of the central Appalachian mines are known to have significant sandstone roof and floor rock.

Regarding carbonates, the t-test results indicate that northern Appalachia has the highest percentage of these particles, followed by mid-central Appalachia and then south-central Appalachia. This is consistent with expectations based on anecdotal observations of significant rock dusting in the northern Appalachian mines (e.g., with trickle dusters in the returns) and the fact that these mines have relatively larger surface areas to be covered with rock dust due to their larger (i.e., taller) openings. Very low fractions of heavy mineral particles were found in any

mines, but there were slightly more in northern Appalachia than mid-central or south-central Appalachia. This finding is supported by knowledge of regional geology; northern Appalachian shale and coal contains relatively more heavy minerals than those in central Appalachia.

For the "other" chemistry classification, northern Appalachia had the largest percentage of particles in this category, followed by south-central and then mid-central Appalachia. Upon further review of the chemical spectra associated with many of these particles, it appears that a significant number from samples in northern Appalachian mines and some from south-central Appalachian mines were likely alumino-silicates with relatively high calcium content. Based on the chemical classification criteria for the automated SEM-EDX routine, such particles contained too much calcium to be considered alumino-silicates, and too much aluminum and silicon to be considered carbonates. One possibility is that the source of the calcium-alumino-silicate particles may be the rock dust product being used in some mines. Particularly in the northern Appalachian mines, a large number of those particles were observed in return samples where carbonate particles tended to represent a large fraction of the total dust particles (i.e., due to rock dusting activities).

Mine-to-Mine Variability within Regions

To assess variability between mines within each region, a cursory analysis can again be done by examining the results graphically. Figure 3.3 shows the average distributions of particle chemistry classification in each mine, with results grouped by sampling location category. While some instances are found where mines in the same region have generally similar characteristics (e.g., Mines 5 and 6 in Figure 3.3 appear to have similar fractions of coal, quartz and "other" particles), it is clear that some variability does exist between mines in all regions (e.g., Mines 5 and 6 have different fractions of alumino-silicate and carbonate particles). To investigate further, all samples were grouped by mine and ANOVA and t-tests were performed on each size, aspect ratio, and chemistry category. The results are presented in Tables 3.5-3.7. Corresponding t-statistics are provided in Tables B.16-B.32 in Appendix B.

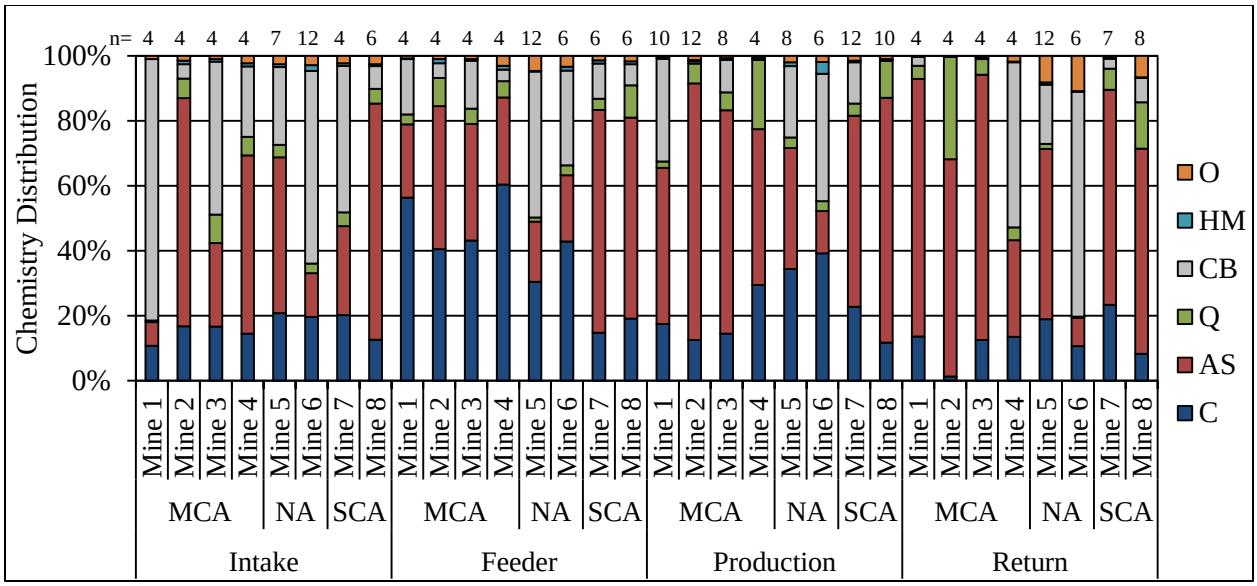

Figure 3.3*. Particle chemistry distributions for each mine separated by locational category. Number of samples are provided above the bar for each category.*

Table 3.5. *ANOVA and t-test results for NA region. Null hypothesis: all means are equal (i.e., μ 5 = μ 6), Critical F-Value: 3.98.*

Northern Appalachia (NA)	**F-value**	**Differences Observed**	**Mean Values by Mine**	
			Mine 5	**Mine 6**
Cross-Sectional Diameter				
[0.94-2.0) μm	3.97	no statistical difference between means	51.7%	57.0%
[2.0-3.0) μm	6.74	μ 5 > μ 6	24.5%	22.5%
[3.0-9.0) μm	1.93	no statistical difference between means	23.8%	20.6%
Aspect Ratio				
<1.5	0.49	no statistical difference between means	40.3%	41.1%
[1.5-3)	0.44	no statistical difference between means	57.4%	56.7%
≥3	1.05	no statistical difference between means	2.4%	2.1%
Chemistry				
C	0.01	no statistical difference between means	26.0%	26.4%
AS	43.52	μ 5 > μ 6	38.2%	13.8%
Q	0.17	no statistical difference between means	2.3%	2.5%
CB	21.50	μ 6 > μ 5	28.3%	51.3%
HM	7.83	μ 6 > μ 5	0.7%	1.7%
O	0.081	no statistical difference between means	4.8%	4.3%

***Table 3.6**. ANOVA and t-test results for MCA region. Null hypothesis: all means are equal (i.e., μ 1 = μ 2 = μ 3 = μ 4), Critical F-Value: 2.72.*

Mid-Central Appalachia (MCA)	**F-value**	**Differences Observed**	**Mean Values by Mine**			
			Mine 1	**Mine 2**	**Mine 3**	**Mine 4**
Cross-Sectional Diameter						
[0.94-2.0) μm	8.60	μ 1 > μ 3 > μ 2 μ 1 > μ 3 > μ 4	72.3%	58.3%	65.2%	61.5%
[2.0-3.0) μm	2.20	no statistical difference between means	19.7%	21.6%	18.6%	20.2%
[3.0-9.0) μm	10.42	μ 2 > μ 1 μ 3 > μ 1 μ 4 > μ 1	8.2%	20.3%	16.0%	18.4%
Aspect Ratio						
<1.5	7.45	μ 1 > μ 2 μ 3 > μ 2 μ 4 > μ 2	45.9%	34.9%	41.7%	41.3%
[1.5-3)	8.41	μ 2 > μ 1 μ 2 > μ 3 μ 2 > μ 4	52.1%	62.5%	56.3%	56.3%
≥3	0.49	no statistical difference between means	2.1%	2.7%	2.0%	2.4%
Chemistry						
C	1.33	no statistical difference between means	22.5%	16.0%	20.3%	29.4%
AS	5.30	μ 2, μ 3 > μ 1, μ 4	41.5%	69.6%	56.2%	39.9%
Q	6.55	μ 2 > μ 3 > μ 1 μ 4 > μ 3 > μ 1	2.2%	10.8%	5.9%	9.0%
CB	6.07	μ 1 > μ 2 μ 3 > μ 2 μ 4 > μ 2	32.5%	1.8%	16.5%	19.1%
HM	2.03	no statistical difference between means	0.2%	0.6%	0.6%	0.8%
O	2.54	no statistical difference between means	0.6%	1.1%	0.7%	1.8%

Table 3.7*. ANOVA and t-test results for SCA region. Null hypothesis: all means are equal (i.e., μ 7 = μ 8), Critical F-Value: 4.01.*

South-Central Appalachia (SCA)	**F-value**	**Differences Observed**	**Mean Values by Mine**	
			Mine 7	**Mine 8**
Cross-Sectional Diameter				
[0.94-2.0) μm	0.27	no statistical difference between means	57.3%	55.7%
[2.0-3.0) μm	0.00	no statistical difference between means	21.7%	21.7%
[3.0-9.0) μm	0.57	no statistical difference between means	20.9%	22.8%
Aspect Ratio				
<1.5	4.61	μ 7 > μ 8	37.0%	34.3%
[1.5-3)	4.21	μ 8 > μ 7	60.3%	62.8%
≥3	0.62	no statistical difference between means	2.6%	2.8%
Chemistry				
C	15.16	μ 7 > μ 8	20.9%	12.5%
AS	5.24	μ 8 > μ 7	58.2%	68.9%
Q	6.69	μ 8 > μ 7	4.4%	10.5%
CB	9.13	μ 7 > μ 8	14.5%	4.9%
HM	2.03	no statistical difference between means	0.6%	0.4%
O	2.75	no statistical difference between means	1.3%	2.9%

Particle Cross-Sectional Diameter

Significant differences between northern Appalachian mines were detected by ANOVA only for the medium-sized particle bin (i.e., 2.0-3.0 μm). The results of the t-tests indicate that the mean percentage of medium-sized particles is slightly higher for Mine 5 compared to Mine 6. Significant differences between mid-central Appalachian mines were detected by ANOVA for the small (i.e., 0.94-2.0 μm) and large particle (i.e., 3.0-9.0 μm) size bins. In this region, Mine 1 is relatively dissimilar from the other mines. It has the highest fraction of relatively small particles, followed by Mine 3 and then Mines 2 and 4. Accordingly, Mines 2, 3, and 4 all have a higher percentage of relatively large particles than Mine 1. No significant differences in the particle size distributions were detected by ANOVA for the south-central Appalachian mines.

Particle Aspect Ratio

No significant differences in the particle shape distributions were detected by ANOVA for the northern Appalachian mines. For the mid-central Appalachian mines, significant differences were detected by ANOVA for the relatively low (i.e., <1.5) and moderate (i.e., 1.5-3) aspect ratio bins. The results of the t-tests indicate that Mines 1, 3, and 4 all have higher fractions of particles with relatively low aspect ratios (with no significant difference between them), while Mine 2 has a higher percentage of particles with moderate aspect ratios. Significant differences between south-central Appalachian mines were also detected by ANOVA for the low and moderate aspect ratio bins – but these differences were fairly small. Mine 7 has a higher percentage of particles with low aspect ratios and Mine 8 has a higher percentage of particles with moderate aspect ratios.

Particle Chemistry

For northern Appalachian mines, significant differences were detected by ANOVA for AS, CB, and HM particle chemistry bins; but no significant differences were found between the C, Q, and O bins. The results of the t-tests indicate that Mine 5 has a larger fraction of AS particles than Mine 6, while Mine 6 has a larger fraction CB and HM particles than Mine 5. Differences in the relative number of carbonate particles may be related to fact that Mine 6 had several samples with very high carbonate content, which appears to be related to heavy rock dusting in the returns. Differences in heavy mineral particle numbers between these two mines could be related to differences in the relative abundance of pyrite and other minerals in the coal and associated shales.

For mid-central Appalachia, significant differences were detected by ANOVA for AS, Q, and CB particle chemistry bins, but not for C, HM, or O. The results of the t-tests indicate that there is no significant difference between the AS distributions for Mines 2 and 3 or for Mines 1 and 4, but Mines 2 and 3 have a higher percentage of AS particles than Mines 1 and 4. Also, the percentage of Q particles in Mines 2 and 4 is the highest, followed by Mine 3 and then Mine 1. Differences in the number of alumino-silicate and quartz particles between these mines is likely related to differences in roof and floor rock geology and also differences in the coal seam thickness. For CB particles, Mines 1, 3, and 4 have a larger fraction than Mine 2. This could be related to differences in rock dust application.

For south-central Appalachia, significant differences were also detected by ANOVA for C, AS, Q, and CB particle chemistry bins. No significant differences were detected for HM or O particle chemistry bins. T-test results suggest that Mine 7 has higher percentages of C and CB particles than Mine 8, while Mine 8 has higher percentages of AS and Q particles. Again, these trends may be due to variations in geology, coal seam thickness, and/or rock dusting practices between these mines.

Variability Between General Sampling Location Categories

Trends in particle characteristics between general sampling location categories (i.e., as can be seen in Figures 3.2 and 3.3) were also investigated. For this, ANOVA and t-tests were performed on each size, aspect ratio, and chemistry category after grouping all samples by collection location category: intake (I), feeder (F), production (P), and return (R). Results are presented in Table 3.8. Corresponding t-statistics are provided in Tables B.33-B.42 in Appendix B.

***Table 3.8**. ANOVA and t-test results by sampling location.*
Null hypothesis: all means are equal (i.e., μ I = μ F = μ P = μ R), Critical F-Value: 2.65.

	F-value	Differences Observed	Mean Values by Location Category			
			I	F	P	R
Cross-Sectional Diameter						
[0.94-2.0) μm	9.68	μ P, μ R > μ I, μ F	52.3%	56.4%	60.9%	63.9%
[2.0-3.0) μm	1.99	no statistical difference between means	21.6%	22.6%	21.8%	20.7%
[3.0-9.0) μm	13.58	μ I > μ F > μ P μ I > μ F > μ R	26.2%	21.1%	17.4%	15.4%
Aspect Ratio						
<1.5	12.57	μ I > μ F > μ P μ I > μ F > μ R	43.8%	40.6%	37.2%	36.8%
[1.5-3)	13.79	μ P > μ F > μ I μ R > μ F > μ I	54.2%	56.7%	60.2%	60.9%
≥3	3.00	μ P > μ I μ F > μ I	1.9%	2.7%	2.6%	2.3%
Chemistry						
C	15.78	μ F > μ I μ F > μ P μ F > μ R μ P > μ R	17.2%	35.4%	20.8%	13.9%
AS	9.55	μ P , μ R > μ I, μ F	37.3%	35.8%	57.2%	54.6%
Q	2.02	no statistical difference between means	4.2%	4.3%	6.0%	7.3%
CB	9.89	μ I > μ F, μ P, μ R	38.2%	21.2%	13.9%	19.0%
HM	3.11	μ I, μ F, μ P > μ R	1.0%	0.7%	0.8%	0.3%
O	5.85	μ I, μ F, μ R > μ P	2.2%	2.5%	1.2%	4.7%

Particle Cross-Sectional Diameter

Significant differences between general sampling location categories were detected by ANOVA for the relatively small and large particle size bins, but not for the medium-sized particle bin. The results of the t-tests indicate that the production and return have a higher percentage of relatively small particles than the intake and feeder location categories. This is consistent with expectations since material is actively being cut or drilled in production areas, generating fine particles that are moved into the returns via the mine ventilation. The t-test results also indicate that the intake has the highest fraction of relatively large particles, followed by the feeder, and then the production and return. This is also expected since the intake should contain the highest percentage of particles associated with the surface environment, and these should be relatively larger than particles generated within the mine. Near the feeder sampling

locations, dust is being generated or aerosolized by dumping or vibrations, but not by active cutting.

Particle Aspect Ratio

Significant differences between particle aspect ratios were also detected by ANOVA between general sampling location categories. The results of the t-tests indicate that the intake has the highest percentage of particles with relatively low aspect ratios, followed by the feeder, and then the production and return. Conversely, the production and return have the highest percentage of particles with moderate aspect ratios, followed by the feeder and then the intake. For the relatively high aspect ratio bin, the production and feeder have a higher fraction of particles than the intake. As previously mentioned and investigated further below, it is suspected that cut rock will produce particles (e.g., alumino-silicates) with relatively higher aspect ratios. In this case, the higher aspect ratios associated with production and return locations make sense.

Particle Chemistry

Significant differences between sampling location categories were additionally detected by ANOVA for all chemistry bins except Q. T-test results suggest that the feeder locations contain the highest percentage of C particles and the production locations contains more C particles than returns. These findings are consistent with expectations since the feeder locations are associated with transport of run-of-mine coal, and the production locations are adjacent to the active coal-cutting face. On the other hand, while the returns are influenced by coal-cutting at the face, they are also subject to heavy rock dusting to mitigate explosibility hazards. The results of the t-tests also indicate that the production and the return have a higher percentage of AS particles than the intake and feeder locations, consistent with cutting roof and floor rock along with the coal. Additionally, intake locations have a higher percentage of CB particles than the feeder, production, and return locations. This result makes sense, considering that rock dusting activities, but little coal or rock cutting is generally taking place in the intakes. One exception is in the northern Appalachian mines, where section development activities should be contributing coal and/or perhaps alumino-silicate particles particularly in the longwall headgate samples; this can generally be seen in Figure 3.4.

Relationships between Particle Chemistry and Size or Aspect Ratio

Finally, the entire sample collection was investigated to determine if any correlations could be found between particle chemistry classifications and size or aspect ratio. Overall, no such correlations were observed. However, when comparing the samples with the highest and lowest percentages of particles in a given chemistry category, significant differences were seen. For the most predominant chemistry categories observed (i.e., C, AS, Q, and CB), the samples were sorted from highest to lowest percentage of particles classified into each category, and then the top ten and bottom ten samples were selected for comparison. (The HM and O categories were not analyzed for size and aspect ratio correlations since relatively few particles tended to be observed in these categories.) In instances where more than ten samples had no particles (i.e., 0%) observed in a particular chemistry category, all such samples were included in the analysis. Likewise, any samples having the same observed percentage of particles for a particular category as the 10^{th} highest percentage were included in the analysis. ANOVA was used to detect significant differences, and then two-tailed t-tests were performed to pinpoint the source of the differences. The results of the t-tests for each comparison by chemistry category are provided in Table 3.9.

Table 3.9*. t-test results for size, shape, and chemistry comparisons. Null hypothesis: all means are equal (i.e., μ Low % Samples = μ High % Samples).*

		t-value	Decision	μ Low % Samples	μ High % Samples	Locations of Low % Samples	Locations of High % Samples
Carbonaceous (C), t-critical two-tail: 2.2, all low values are 0% C, high values are 65±9.5% C							
diameter	*[0.94-2.0) μm*	*3.56*	Rejected	64.1%	53.7%	7 in returns, 7 at roof bolters, and 2 at miners	6 at a feeder, and 4 in production areas
	[2.0-3.0) μm	*-1.67*	Not Rejected	21.6%	23.2%		
	[3.0-9.0) μm	*-3.72*	Rejected	14.3%	23.4%		
aspect ratio	*<1.5*	*-6.66*	Rejected	29.9%	38.7%		
	[1.5-3)	*7.74*	Rejected	66.9%	57.6%		
	≥3	*-1.15*	Not Rejected	3.1%	3.6%		
Alumino-Silicate (AS), t-critical two-tail: 2.1, low values are 5±1.5% AS, high values are 97±2.2% AS							
diameter	*[0.94-2.0) μm*	-0.67	Not Rejected	58.5%	62.9%	8 in intakes, and 2 at tailgates	10 in production areas and 1 in a return
	[2.0-3.0) μm	-0.97	Not Rejected	19.6%	21.4%		
	[3.0-9.0) μm	1.20	Not Rejected	22.0%	15.6%		
aspect ratio	*<1.5*	7.44	Rejected	46.3%	29.6%		
	[1.5-3)	-7.38	Rejected	52.1%	67.3%		
	≥3	-4.19	Rejected	1.4%	2.9%		
Quartz (Q), t-critical two-tail: 2.05, all low values are 0% Q, high values are 32±9.4% Q							
diameter	*[0.94-2.0) μm*	-3.07	Rejected	61.2%	71.2%	4 in intakes, 1 at a feeder, 6 at production areas, 10 in returns	4 at roof bolters and 6 in returns
	[2.0-3.0) μm	2.79	Rejected	21.6%	17.8%		
	[3.0-9.0) μm	2.27	Rejected	17.1%	11.0%		
aspect ratio	*<1.5*	2.74	Rejected	38.9%	31.9%		
	[1.5-3)	-3.25	Rejected	58.7%	66.3%		
	≥3	1.49	Not Rejected	2.5%	1.9%		
Carbonate (CB), t-critical two-tail: 2.2, all low values are 0% CB, high values are 84±6.0% CB							
diameter	*[0.94-2.0) μm*	0.18	Not Rejected	66.9%	65.8%	13 at roof bolters, 11 in returns, and 7 at miners	5 in intakes, 3 in returns, 2 at miners
	[2.0-3.0) μm	-0.04	Not Rejected	19.5%	19.6%		
	[3.0-9.0) μm	-0.21	Not Rejected	13.5%	14.6%		
aspect ratio	*<1.5*	*-5.49*	Rejected	31.7%	48.9%		
	[1.5-3)	*5.27*	Rejected	65.4%	50.1%		
	≥3	*3.17*	Rejected	2.8%	1.2%		

For each chemistry category investigated, most particles tend to be classified into the relatively small particle size bin. With respect to the C category (i.e., expected to represent primarily coal particles), samples with no identified C particles were found to contain significantly higher percentages of relatively small particles compared to samples with the highest C content. Observations of no C particles were also correlated with higher percentages of relatively low aspect ratios. Conversely, samples high in C content had higher fractions of relatively large particles, and higher fractions of particles with moderate aspect ratios. Notably,

two samples were collected (simultaneously) at a continuous miner in south-central Appalachia that contained no C particles, but nearly 100% AS particles.

With respect to the AS category, no significant correlations were found with particle size. However, samples with the highest AS content have larger percentages of particles in the relatively high and moderate aspect ratio bins than samples with low AS content. As mentioned earlier, this is consistent with expectations based on the fact that shale and other clay-rich rocks may contribute platy or sheet-like mineral grains that should have relatively high aspect ratios.

Samples with the highest Q content have relatively high percentages of relatively small particles compared to samples with no identified quartz particles. This finding is of particular interest with respect to potential implications for occupational health – and is deserving of further investigation. High-Q samples also have higher percentages of particles with moderate aspect ratios.

As with the AS category, particle size does not appear to have any correlation with the CB category. However, samples high in CB content tend to have a higher percentage of particles with relatively low aspect ratios; and samples with no identified CB particles have higher percentages of particles with relatively high and moderate aspect ratios.

4. Summary and Conclusions

A total of 210 respirable dust samples were collected from eight mines in central and northern Appalachia and analyzed by an automated SEM-EDX routine to estimate distributions of particle size, aspect ratio and chemistry. Results suggest that distinct trends do exist between and within mine regions as well as between general sampling location categories. These differences between regions, mines, and sampling locations may help provide insights into miner health outcomes, and should be of interest to a variety of stakeholders including mine workers, operators, regulators, and members of the mining, medical and epidemiological research communities. Key findings with respect to respirable dust characteristics in the Appalachian mines examined in this work are summarized as follows:

1) Northern Appalachian mines have relatively higher fractions of coal, carbonate, and heavy mineral particles than the two central Appalachian regions, whereas central Appalachian mines have higher fractions of quartz and alumino-silicate particles.

2) Central Appalachian mines tended to have more mine-to-mine variations in size, shape, and chemistry distributions than northern Appalachian mines.

3) With respect to particle size, samples collected in locations in the production and return categories have the highest percentages of very small particles (i.e., 0.94-2.0μm), followed by the feeder and then the intake locations.

4) With respect to particle shape, samples collected in locations in the production and return categories have higher fractions of particles with moderate (i.e., length is 1.5 to 3x width) to relatively high aspect ratios (i.e., length is greater than 3x width) compared to feeder and intake samples.

5) Samples with relatively high fractions of alumino-silicates have higher fractions of particles with relatively high and moderate aspect ratios than samples with low alumino-silicate fractions.

6) Samples with relatively high fractions of quartz particles have higher fractions of particles with moderate aspect ratios and higher percentages of relatively small particles than samples with no identified quartz particles.

7) Samples with relatively high fractions of carbonates have higher percentages of particles with relatively low aspect ratios (i.e., length and width are similar) than samples with no identified carbonate particles.

Additionally, findings reported here regarding spatial and temporal variations in respirable mine dust should also add to the current understanding on this topic. From the dataset investigated here, it can be concluded that samples collected simultaneously and in close proximity to one another tend to vary somewhat more frequently with respect to particle characteristics than samples collected side-by-side (i.e., true duplicates). While in both instances, sample pairs were in agreement more often than not (i.e., 70% of the time or more), observed variation between true duplicates indicates that analysis of single samples may not always provide accurate representation of dust characteristics.

Finally, it should be noted that the analyses presented here illustrate just a portion of what is possible with the current or similar datasets. The ability to capture detailed particle characteristics via computer-automated SEM-EDX opens the door for a much more comprehensive understanding of respirable dust. This and other analytical methods that can

broaden the present state of knowledge on particle characteristics and exposures should be explored.

5. Acknowledgements

The authors would like to acknowledge the Alpha Foundation for the Improvement of Mine Safety and Health for funding this work. We are grateful to Meredith Scaggs for her extensive efforts to collect and prepare dust samples and for the cooperation of the mines where samples were collected. We would also like to thank Steve McCartney of Virginia Tech ICTAS-NCFL for operational assistance with SEM-EDX analysis, Ted Juzwak of Bruker Corporation for assistance in creating a computer-automated routine to run samples, and Dan Baxter of Environmental Analysis Associates for assistance in speeding up the automated routine.

References

[1] International Agency for Research on Cancer (IARC), Monographs on the evaluation of carcinogenic risks to humans: Silica, some silicates, coal dust and para-aramid fibrils, Geneva, Switzerland: World Health Organization 68 (1997) 41-242, OSHA-2010-0034-1062.

[2] International Organization for Standardization (ISO), Air quality-particle size fraction definitions for health related sampling, ISO Standard 7708 (1995).

[3] World Health Organization (WHO), Hazard Prevention and Control in the Work Environment: Airborne Dust, WHO/SDE/OEH/99.14 (1999).

[4] Occupational Safety and Health Administration (OSHA), Occupational Exposure to Respirable Crystalline Silica -- Review of Health Effects Literature and Preliminary Quantitative Risk Assessment, OSHA-2010-0034 (2010).

[5] V. Castranova and V. Vallyathan, Silicosis and coal workers' pneumoconiosis, Environmental Health Perspectives, 108(Suppl 4) (2000) 675-684.

[6] National Institute for Occupational Safety and Health (NIOSH), Criteria for a Recommended Standard – Occupational Exposure to Respirable Coal Mine Dust, DHEW Publication No. 95-106 (1974).

[7] World Health Organization (WHO), Hazard prevention and control in the work environment: airborne dust (1999).

[8] E. Suarthana, A.S. Laney, E. Storey, J.M. Hale, and M.D. Attfield, Coal workers' pneumoconiosis in the United States: regional differences 40 years after implementation of the 1969 Federal Coal Mine Health and Safety Act, Occupational and Environmental Medicine 68 (2011) 908-913.

[9] Centers for Disease Control (CDC), Advanced Cases of Coal Workers' Pneumoconiosis-Two Counties, Virginia, MMWR 55.33 (2006).

[10] D. Blackley, C. Halldin, and A.S. Laney, Resurgence of a Debilitating and Entirely Preventable Respiratory Disease among Working Coal Miners, American Journal of Respiratory and Critical Care Medicine 190.6 (2014) 708-709.

[11] V.C. dos S Antao, E.L. Petsonk, L.Z. Sokolow, A.L. Wolfe, G.A. Pinheiro, J.M. Hale, and M.D. Attfield, Rapidly progressive coal workers' pneumoconiosis in the United States: geographic clustering and other factors, Occupational and environmental medicine 62.10 (2005) 670-674.

[12] A.S. Laney and M.D. Attfield, Coal workers' pneumoconiosis and progressive massive fibrosis are increasingly more prevalent among workers in small underground coal mines in the United States, Occupational and Environmental Medicine 67.6 (2010) 428-431.

[13] J.G. Bennett, J.A. Dick, Y.S. Kaplan, P.A. Shand, D.H. Shennan, D.J. Thomas, and J.S Washington, The relationship between coal rank and the prevalence of pneumoconiosis, British journal of industrial medicine, 36.3 (1979) 206-210.

[14] S. Page and J. Organiscak, Suggestion of a Cause- and-Effect Relationship among Coal Rank, Airborne Dust, and Incidence of Workers' Pneumoconiosis, American Industrial Hygiene Association Journal, 61.6 (2000) 785-787.

[15] D.E. Pollock, J.D. Potts, and G.J. Joy, Investigation into dust exposures and mining practices in mines in the southern Appalachian Region, Mining Engineering, 62.2 (2010) 44-49.

[16] D. Landen, A. Wassel, L. McWilliams, and J. Patel, Coal Dust Exposure and Mortality from Ischemic Heart Disease among a Cohort of U.S. Coal Miners, American Journal of Industrial Medicine, 54.10 (2011) 727-733.

[17] G. Joy, Evaluation of the Approach to Respirable Quartz Exposure Control in U.S. Coal Mines, Journal of Occupational Environmental Hygiene, 9.2 (2012) 65-68.

[18] S.E. Mischler, E.G. Cauda, M. Di Giuseppe, and L.A. Ortiz, A multi-cyclone sampling array for the collection of size-segregated occupational aerosols, Journal of Occupational and Environmental Hygiene 10.12 (2013) 685-93.

[19] J. F. Colinet, J. P. Rider, J. M. Listak, J. A. Organiscak, and A. L. Wolfe, Best Practices for Dust Control in Coal Mining, OMSHR, Information Circular 9517 (2010).

[20] R. Agius, Occupational and Environmental Lung Disease, Health, Environment & Work (2009).

[21] V. Johann, E. Sarver, and C. Keles, Development of an Automated SEM-EDX Routine for Characterizing Respirable Coal Mine Dust, Virginia Polytechnic Institute and State University, 2016.

[22] R. Sellaro and E. Sarver, Characterization of respirable dust in an underground coal mine in Central Appalachia, Transactions of the Society for Mining, Metallurgy & Exploration 336 (2014) 457-466.

[23] R. Sellaro, A Standard Characterization Methodology for Respirable Coal Mine Dust Using SEM-EDX, Resources 4.4 (2015) 939-957.

[24] A. Agresti, A Survey of Exact Inference for Contingency Tables, Statistical Science 7.1 (1992) 131-153.

Appendix A. Chapter 2 Supplemental Data

Table A.1. *Comparison of particle cross-sectional diameter distributions determined by three different manual users on ten dust samples.*

Sample	User	0.5-1 µm	1.0-2.0 µm	2.0-4.0 µm	4.0-8.0 µm	8.0-10.0 µm
1	1	21%	46%	24%	9%	0%
	2	39%	41%	17%	3%	0%
	3	20%	41%	34%	5%	0%
2	1	10%	47%	30%	13%	0%
	2	40%	35%	19%	6%	0%
	3	12%	48%	34%	6%	0%
3	1	16%	45%	30%	9%	0%
	2	28%	43%	26%	3%	0%
	3	13%	49%	34%	4%	0%
4	1	16%	32%	34%	17%	1%
	2	30%	41%	23%	6%	0%
	3	9%	63%	27%	1%	0%
5	1	21%	27%	39%	13%	0%
	2	45%	38%	12%	5%	0%
	3	28%	30%	37%	5%	0%
6	1	21%	54%	21%	4%	0%
	2	48%	40%	9%	3%	0%
	3	21%	52%	24%	3%	0%
7	1	15%	63%	21%	1%	0%
	2	47%	43%	10%	0%	0%
	3	11%	53%	35%	1%	0%
8	1	25%	49%	25%	1%	0%
	2	42%	43%	13%	2%	0%
	3	13%	65%	21%	1%	0%
9	1	8%	40%	48%	4%	0%
	2	31%	34%	31%	4%	0%
	3	7%	39%	44%	10%	0%
10	1	38%	45%	15%	2%	0%
	2	42%	44%	13%	1%	0%
	3	15%	55%	24%	6%	0%

***Table A.2**. Comparison of particle shape distributions qualitatively determined by three different manual users on ten dust samples.*

Sample	User	Angular	Transitional	Rounded
1	1	48%	40%	12%
	2	53%	47%	0%
	3	65%	32%	3%
2	1	67%	25%	8%
	2	50%	49%	1%
	3	60%	37%	3%
3	1	70%	24%	6%
	2	70%	30%	0%
	3	74%	26%	0%
4	1	50%	35%	15%
	2	72%	27%	1%
	3	70%	30%	0%
5	1	54%	30%	16%
	2	70%	27%	3%
	3	60%	32%	8%
6	1	99%	1%	0%
	2	92%	8%	0%
	3	65%	30%	5%
7	1	100%	0%	0%
	2	73%	27%	0%
	3	67%	29%	4%
8	1	99%	1%	0%
	2	71%	29%	0%
	3	72%	22%	6%
9	1	97%	3%	0%
	2	94%	6%	0%
	3	68%	31%	1%
10	1	75%	22%	3%
	2	58%	41%	1%
	3	52%	39%	9%

***Table A.3**. Comparison of particle aspect ratio distributions determined by three different manual users of ten dust samples. An aspect ratio of 1.0 indicates a particle has equal long and intermediate dimensions.*

Sample	Run	1.0-1.2	1.2-1.4	1.4-1.6	1.6-2.0	2.0-4.0	>4.0
1	1	17%	24%	17%	19%	22%	1%
	2	27%	22%	17%	24%	10%	0%
	3	16%	13%	28%	24%	18%	1%
2	1	23%	18%	15%	30%	14%	0%
	2	22%	27%	19%	21%	11%	0%
	3	17%	19%	19%	24%	19%	2%
3	1	20%	26%	13%	24%	17%	0%
	2	23%	16%	19%	17%	23%	2%
	3	8%	16%	15%	28%	32%	1%
4	1	27%	20%	18%	22%	12%	1%
	2	24%	24%	16%	25%	10%	1%
	3	10%	17%	20%	28%	23%	2%
5	1	20%	27%	10%	19%	24%	0%
	2	31%	16%	15%	17%	18%	3%
	3	26%	16%	16%	27%	15%	0%
6	1	9%	8%	21%	28%	32%	2%
	2	16%	23%	13%	25%	22%	1%
	3	10%	19%	14%	23%	34%	0%
7	1	8%	20%	16%	29%	25%	2%
	2	21%	21%	18%	23%	17%	0%
	3	11%	16%	11%	30%	31%	1%
8	1	23%	21%	25%	20%	10%	1%
	2	23%	20%	18%	23%	16%	0%
	3	11%	15%	17%	20%	37%	0%
9	1	10%	20%	19%	20%	31%	0%
	2	21%	23%	27%	20%	8%	1%
	3	11%	13%	20%	28%	28%	0%
10	1	30%	19%	19%	20%	9%	3%
	2	20%	23%	21%	18%	16%	2%
	3	22%	13%	27%	15%	23%	0%

***Table A.4**. Comparison of particle compositional distributions determined by three different manual users on ten dust samples. Chemical composition categories were: Carbonaceous (C), Mixed Carbonaceous (MC), Alumino-silicate (AS), Quartz (Q), Carbonate (CB), Heavy Mineral (HM), Other (O).*

Sample	User	C	MC	AS	Q	CB	HM	O
1	1	54%	12%	18%	4%	11%	1%	0%
	2	42%	32%	6%	5%	14%	1%	0%
	3	42%	23%	25%	1%	5%	3%	0%
2	1	19%	16%	27%	4%	31%	3%	0%
	2	36%	31%	7%	9%	14%	0%	3%
	3	24%	14%	38%	3%	19%	1%	1%
3	1	13%	12%	54%	6%	11%	3%	1%
	2	21%	39%	18%	8%	11%	2%	1%
	3	10%	17%	46%	9%	15%	3%	0%
4	1	33%	12%	22%	7%	10%	7%	9%
	2	22%	37%	13%	11%	6%	1%	10%
	3	8%	12%	54%	12%	8%	2%	4%
5	1	32%	8%	21%	8%	21%	9%	1%
	2	49%	16%	11%	1%	5%	14%	4%
	3	24%	15%	24%	5%	3%	8%	21%
6	1	23%	33%	30%	10%	2%	2%	0%
	2	14%	41%	30%	10%	1%	1%	3%
	3	22%	46%	17%	8%	2%	4%	1%
7	1	17%	20%	14%	47%	0%	1%	1%
	2	5%	20%	12%	57%	0%	0%	6%
	3	8%	20%	26%	45%	0%	1%	0%
8	1	48%	29%	11%	10%	1%	1%	0%
	2	39%	31%	17%	9%	0%	0%	4%
	3	41%	37%	12%	8%	1%	0%	1%
9	1	15%	13%	32%	38%	2%	0%	0%
	2	10%	11%	32%	27%	3%	0%	17%
	3	13%	20%	32%	28%	4%	1%	2%
10	1	75%	0%	3%	11%	11%	1%	0%
	2	49%	25%	10%	3%	11%	0%	2%
	3	45%	20%	7%	6%	13%	2%	7%

***Table A.5**. Freeman-Halton Test Results for User Particle Size.*

Sample	Comparison	Approximate P-Value	Conclusion
Sample 1	User 1 vs. User 2	0.01954	Disagreement
	User 1 vs. User 3	0.3786	Agreement
	User 2 vs. User 3	0.005368	Disagreement
Sample 2	User 1 vs. User 2	1.019e-05	Disagreement
	User 1 vs. User 3	0.3994	Agreement
	User 2 vs. User 3	5.298e-05	Disagreement
Sample 3	User 1 vs. User 2	0.08947	Agreement
	User 1 vs. User 3	0.4639	Agreement
	User 2 vs. User 3	0.06534	Agreement
Sample 4	User 1 vs. User 2	0.005058	Disagreement
	User 1 vs. User 3	1.911e-06	Disagreement
	User 2 vs. User 3	0.000105	Disagreement
Sample 5	User 1 vs. User 2	1.896e-06	Disagreement
	User 1 vs. User 3	0.1911	Agreement
	User 2 vs. User 3	0.0003305	Disagreement
Sample 6	User 1 vs. User 2	0.0003342	Disagreement
	User 1 vs. User 3	0.9483	Agreement
	User 2 vs. User 3	0.0001448	Disagreement
Sample 7	User 1 vs. User 2	4.062e-06	Disagreement
	User 1 vs. User 3	0.1293	Agreement
	User 2 vs. User 3	2.809e-09	Disagreement
Sample 8	User 1 vs. User 2	0.02189	Disagreement
	User 1 vs. User 3	0.06405	Agreement
	User 2 vs. User 3	2.282e-05	Disagreement
Sample 9	User 1 vs. User 2	0.0002678	Disagreement
	User 1 vs. User 3	0.4362	Agreement
	User 2 vs. User 3	8.868e-05	Disagreement
Sample 10	User 1 vs. User 2	0.877	Agreement
	User 1 vs. User 3	0.001316	Disagreement
	User 2 vs. User 3	6.625e-05	Disagreement

Table A.6*. Freeman-Halton Test Results for Qualitative User Particle Shape (Cross-Sectional Diameter).*

Sample	Comparison	Approximate P-Value	Conclusion
Sample 1	User 1 vs. User 2	0.000783	Disagreement
	User 1 vs. User 3	0.0137	Disagreement
	User 2 vs. User 3	0.02465	Disagreement
Sample 2	User 1 vs. User 2	0.0001942	Disagreement
	User 1 vs. User 3	0.08893	Agreement
	User 2 vs. User 3	0.1936	Agreement
Sample 3	User 1 vs. User 2	0.03464	Disagreement
	User 1 vs. User 3	0.05207	Agreement
	User 2 vs. User 3	0.6368	Agreement
Sample 4	User 1 vs. User 2	8.926e-05	Disagreement
	User 1 vs. User 3	1.921e-05	Disagreement
	User 2 vs. User 3	0.7542	Agreement
Sample 5	User 1 vs. User 2	0.002792	Disagreement
	User 1 vs. User 3	0.2442	Agreement
	User 2 vs. User 3	0.1667	Agreement
Sample 6	User 1 vs. User 2	0.0349	Disagreement
	User 1 vs. User 3	8.829e-11	Disagreement
	User 2 vs. User 3	5.671e-06	Disagreement
Sample 7	User 1 vs. User 2	1.955e-09	Disagreement
	User 1 vs. User 3	9.757e-12	Disagreement
	User 2 vs. User 3	0.1337	Agreement
Sample 8	User 1 vs. User 2	6.202e-09	Disagreement
	User 1 vs. User 3	3.419e-08	Disagreement
	User 2 vs. User 3	0.02763	Disagreement
Sample 9	User 1 vs. User 2	0.4977	Agreement
	User 1 vs. User 3	3.503e-08	Disagreement
	User 2 vs. User 3	3.183e-06	Disagreement
Sample 10	User 1 vs. User 2	0.006357	Disagreement
	User 1 vs. User 3	0.002182	Disagreement
	User 2 vs. User 3	0.03567	Disagreement

Table A.7*. Freeman-Halton Test Results for Quantitative User Particle Shape (Aspect Ratio).*

Sample	Comparison	Approximate P-Value	Conclusion
Sample 1	User 1 vs. User 2	0.1156	Agreement
	User 1 vs. User 3	0.1878	Agreement
	User 2 vs. User 3	0.03943	Disagreement
Sample 2	User 1 vs. User 2	0.3778	Agreement
	User 1 vs. User 3	0.4881	Agreement
	User 2 vs. User 3	0.2938	Agreement
Sample 3	User 1 vs. User 2	0.1733	Agreement
	User 1 vs. User 3	0.01333	Disagreement
	User 2 vs. User 3	0.02412	Disagreement
Sample 4	User 1 vs. User 2	0.9544	Agreement
	User 1 vs. User 3	0.01983	Disagreement
	User 2 vs. User 3	0.01744	Disagreement
Sample 5	User 1 vs. User 2	0.07257	Agreement
	User 1 vs. User 3	0.07762	Agreement
	User 2 vs. User 3	0.3391	Agreement
Sample 6	User 1 vs. User 2	0.01442	Disagreement
	User 1 vs. User 3	0.1312	Agreement
	User 2 vs. User 3	0.3511	Agreement
Sample 7	User 1 vs. User 2	0.01061	Disagreement
	User 1 vs. User 3	0.8553	Agreement
	User 2 vs. User 3	0.03335	Disagreement
Sample 8	User 1 vs. User 2	0.6093	Agreement
	User 1 vs. User 3	0.0001248	Disagreement
	User 2 vs. User 3	0.008492	Disagreement
Sample 9	User 1 vs. User 2	0.0005688	Disagreement
	User 1 vs. User 3	0.5549	Agreement
	User 2 vs. User 3	0.000555	Disagreement
Sample 10	User 1 vs. User 2	0.4441	Agreement
	User 1 vs. User 3	0.01695	Disagreement
	User 2 vs. User 3	0.2207	Agreement

Table A.8*. Freeman-Halton Test Results for User Particle Chemistry.*

Sample	Comparison	Approximate P-Value	Conclusion
Sample 1	User 1 vs. User 2	0.002068	Disagreement
	User 1 vs. User 3	0.04861	Disagreement
	User 2 vs. User 3	0.0003624	Disagreement
Sample 2	User 1 vs. User 2	7.4e-07	Disagreement
	User 1 vs. User 3	0.2488	Agreement
	User 2 vs. User 3	3.215e-07	Disagreement
Sample 3	User 1 vs. User 2	6.707e-07	Disagreement
	User 1 vs. User 3	0.6873	Agreement
	User 2 vs. User 3	5.327e-05	Disagreement
Sample 4	User 1 vs. User 2	0.0004141	Disagreement
	User 1 vs. User 3	1.659e-06	Disagreement
	User 2 vs. User 3	1.361e-09	Disagreement
Sample 5	User 1 vs. User 2	6.165e-05	Disagreement
	User 1 vs. User 3	3.669e-07	Disagreement
	User 2 vs. User 3	1.869e-05	Disagreement
Sample 6	User 1 vs. User 2	0.3669	Agreement
	User 1 vs. User 3	0.2349	Agreement
	User 2 vs. User 3	0.1616	Agreement
Sample 7	User 1 vs. User 2	0.02249	Disagreement
	User 1 vs. User 3	0.1095	Agreement
	User 2 vs. User 3	0.007858	Disagreement
Sample 8	User 1 vs. User 2	0.1895	Agreement
	User 1 vs. User 3	0.7847	Agreement
	User 2 vs. User 3	0.5357	Agreement
Sample 9	User 1 vs. User 2	0.0001924	Disagreement
	User 1 vs. User 3	0.3884	Agreement
	User 2 vs. User 3	0.006151	Disagreement
Sample 10	User 1 vs. User 2	1.101e-09	Disagreement
	User 1 vs. User 3	2.183e-08	Disagreement
	User 2 vs. User 3	0.3369	Agreement

***Table A.9**. Comparison of particle cross-sectional diameter distributions determined by three independent automated scans of ten dust samples.*

Sample	Run	0.5-1 µm	1.0-2.0 µm	2.0-4.0 µm	4.0-8.0 µm	8.0-10.0 µm
1	1	1.8%	63.0%	30.4%	4.8%	0.0%
	2	1.8%	64.0%	28.2%	6.0%	0.0%
	3	2.4%	62.6%	29.6%	5.4%	0.0%
2	1	2.0%	61.0%	31.2%	5.4%	0.4%
	2	1.2%	55.4%	38.4%	5.0%	0.0%
	3	0.2%	62.0%	34.2%	3.6%	0.0%
3	1	0.6%	57.4%	32.8%	9.2%	0.0%
	2	1.8%	57.4%	31.2%	9.6%	0.0%
	3	1.2%	60.0%	31.0%	7.8%	0.0%
4	1	1.2%	59.4%	35.2%	4.2%	0.0%
	2	2.0%	67.6%	25.4%	5.0%	0.0%
	3	1.4%	63.0%	27.8%	7.8%	0.0%
5	1	2.6%	84.0%	11.2%	2.2%	0.0%
	2	2.0%	81.0%	14.8%	2.2%	0.0%
	3	1.0%	74.6%	19.8%	4.4%	0.2%
6	1	0.8%	67.0%	26.8%	5.2%	0.2%
	2	1.4%	68.4%	25.4%	4.8%	0.0%
	3	0.6%	71.0%	23.8%	4.6%	0.0%
7	1	1.2%	69.8%	24.4%	4.6%	0.0%
	2	1.4%	64.4%	29.0%	5.2%	0.0%
	3	1.6%	65.6%	28.2%	4.6%	0.0%
8	1	0.0%	66.2%	26.6%	7.0%	0.2%
	2	0.8%	67.0%	25.4%	6.8%	0.0%
	3	0.6%	65.8%	28.8%	4.6%	0.2%
9	1	1.0%	51.2%	32.6%	13.8%	1.4%
	2	1.2%	49.8%	36.0%	12.4%	0.6%
	3	0.0%	54.8%	28.2%	17.0%	0.0%
10	1	1.8%	72.8%	21.8%	3.4%	0.2%
	2	2.8%	73.0%	22.0%	2.2%	0.0%
	3	1.6%	72.6%	24.4%	1.4%	0.0%

Table A.10. *Comparison of particle aspect ratio distributions determined by three independent automated scans of ten dust samples. An aspect ratio of 1.0 indicates a particle has equal long and intermediate dimensions.*

Sample	Run	1.0-1.2	1.2-1.4	1.4-1.6	1.6-2.0	2.0-4.0	>4.0
1	1	6.6%	29.0%	27.0%	22.2%	14.2%	1.0%
	2	6.4%	28.2%	28.8%	24.0%	12.0%	0.6%
	3	7.8%	27.2%	25.2%	26.0%	12.8%	1.0%
2	1	7.4%	20.8%	28.2%	29.2%	14.4%	0.0%
	2	4.6%	24.4%	27.2%	27.2%	16.0%	0.6%
	3	5.2%	26.0%	26.0%	30.2%	12.4%	0.2%
3	1	5.2%	22.4%	28.4%	28.8%	15.2%	0.0%
	2	4.8%	25.2%	26.8%	28.6%	14.4%	0.2%
	3	4.4%	24.2%	28.4%	29.8%	13.0%	0.2%
4	1	6.4%	27.8%	26.0%	29.0%	10.8%	0.0%
	2	4.2%	25.4%	28.6%	26.2%	14.8%	0.8%
	3	5.0%	24.4%	26.2%	31.8%	12.6%	0.0%
5	1	4.0%	17.4%	22.8%	38.4%	17.4%	0.0%
	2	3.0%	20.8%	21.2%	35.4%	19.4%	0.2%
	3	2.0%	18.0%	23.8%	35.6%	20.2%	0.4%
6	1	4.0%	17.0%	22.4%	36.0%	20.6%	0.0%
	2	3.2%	20.0%	25.0%	30.8%	20.6%	0.4%
	3	1.8%	16.8%	23.8%	35.6%	21.8%	0.2%
7	1	1.8%	15.4%	23.0%	38.4%	21.0%	0.4%
	2	2.0%	15.8%	24.2%	34.2%	23.6%	0.2%
	3	3.6%	17.4%	22.0%	33.8%	23.2%	0.0%
8	1	2.8%	18.4%	21.0%	36.2%	21.4%	0.2%
	2	1.8%	15.6%	26.2%	36.0%	20.4%	0.0%
	3	4.4%	20.8%	24.6%	31.6%	18.4%	0.2%
9	1	5.4%	24.8%	24.4%	31.0%	13.6%	0.8%
	2	5.4%	23.6%	25.0%	29.0%	16.8%	0.2%
	3	2.4%	21.4%	24.4%	37.2%	14.4%	0.2%
10	1	5.2%	27.8%	26.8%	30.2%	10.0%	0.0%
	2	5.6%	24.0%	27.0%	28.4%	14.4%	0.6%
	3	6.2%	27.0%	26.6%	28.0%	12.2%	0.0%

Table A.11. *Comparison of particle chemistry distributions determined by three independent automated scans of ten dust samples. Chemical composition categories were: Carbonaceous (C), Mixed Carbonaceous (MC), Alumino-silicate (AS), Quartz (Q), Carbonate (CB), Heavy Mineral (HM), Other (O).*

Sample	Run	C	MC	AS	Q	CB	HM	O
1	1	54.8%	19.6%	12.0%	2.0%	9.6%	1.2%	0.8%
	2	59.8%	16.6%	7.8%	2.0%	11.4%	1.6%	0.8%
	3	59.2%	16.4%	9.8 %	2.4%	9.2%	1.8%	1.2%
2	1	40.8%	19.6%	12.0%	2.6%	21.0%	1.0%	3.0%
	2	33.8%	21.8%	19.0%	6.0%	17.8%	0.4%	1.2%
	3	24.6%	23.4%	20.4%	4.6%	24.2%	1.2%	1.6%
3	1	23.8%	31.4%	34.0%	5.2%	4.6%	0.6%	0.4%
	2	20.4%	30.4%	36.2%	5.4%	5.8%	0.8%	1.0%
	3	24.6 %	31.0%	30.8%	4.8%	6.8%	0.4%	1.6%
4	1	27.0%	33.6%	23.6%	7.8%	6.2%	0.8%	1.0%
	2	36.6%	27.0%	21.0%	7.8%	5.0%	1.4%	1.2%
	3	21.8%	35.2%	26.8%	7.4%	6.0%	1.2%	1.6%
5	1	89.0%	3.8%	3.2%	1.2%	2.6%	0.2%	0.0%
	2	88.4%	3.4%	3.8%	1.4%	2.0%	0.2%	0.8%
	3	74.0%	7.6%	8.2%	1.8%	5.2%	1.2%	2.0%
6	1	3.4%	32.2%	58.8%	2.8%	1.6%	0.2%	1.0%
	2	10.2%	30.8%	53.2%	3.0%	2.4%	0.0%	0.4 %
	3	12.2%	45.4%	38.2%	2.8%	0.8%	0.4%	0.2%
7	1	1.0%	6.0%	61.0%	31.6%	0.0%	0.0%	0.4 %
	2	1.8%	7.6%	61.6%	28.6%	0.0%	0.2%	0.2%
	3	2.6%	9.0%	56.2%	31.6%	0.0%	0.0%	0.6%
8	1	16.4%	39.8%	35.8%	5.6%	1.0%	1.0%	0.4%
	2	11.0%	27.4%	55.0%	5.2%	0.6%	0.4%	0.4%
	3	10.4%	31.8%	48.4%	6.0%	1.6%	0.8%	1.0%
9	1	21.6%	15.2%	45.0%	13.4%	2.8%	0.6%	1.4%
	2	21.8%	12.6%	44.4%	18.8%	1.2%	0.4%	0.8%
	3	15.2%	13.4%	52.2%	14.6%	1.2%	1.8%	1.6%
10	1	36.8%	23.8%	9.6 %	2.4%	25.6%	0.4%	1.4%
	2	38.0%	22.2%	9.2%	3.0%	25.0%	1.2%	1.4%
	3	32.2%	25.8%	13.6%	3.6%	23.6%	0.0%	1.2%

***Table A.12**. Freeman-Halton Test Results for Automation-Run Particle Size.*

Sample	Comparison	Approximate P-Value	Conclusion
Sample 1	Run 1 vs. Run 2	0.978	Agreement
	Run 1 vs. Run 3	1	Agreement
	Run 2 vs. Run 3	0.978	Agreement
Sample 2	Run 1 vs. Run 2	0.7054	Agreement
	Run 1 vs. Run 3	0.659	Agreement
	Run 2 vs. Run 3	0.7265	Agreement
Sample 3	Run 1 vs. Run 2	0.9656	Agreement
	Run 1 vs. Run 3	0.9528	Agreement
	Run 2 vs. Run 3	0.8987	Agreement
Sample 4	Run 1 vs. Run 2	0.4631	Agreement
	Run 1 vs. Run 3	0.4928	Agreement
	Run 2 vs. Run 3	0.6922	Agreement
Sample 5	Run 1 vs. Run 2	0.887	Agreement
	Run 1 vs. Run 3	0.1858	Agreement
	Run 2 vs. Run 3	0.5939	Agreement
Sample 6	Run 1 vs. Run 2	0.9836	Agreement
	Run 1 vs. Run 3	0.9525	Agreement
	Run 2 vs. Run 3	0.9833	Agreement
Sample 7	Run 1 vs. Run 2	0.8367	Agreement
	Run 1 vs. Run 3	0.8876	Agreement
	Run 2 vs. Run 3	0.9879	Agreement
Sample 8	Run 1 vs. Run 2	0.9718	Agreement
	Run 1 vs. Run 3	0.8644	Agreement
	Run 2 vs. Run 3	0.859	Agreement
Sample 9	Run 1 vs. Run 2	0.9616	Agreement
	Run 1 vs. Run 3	0.6664	Agreement
	Run 2 vs. Run 3	0.3594	Agreement
Sample 10	Run 1 vs. Run 2	1	Agreement
	Run 1 vs. Run 3	0.863	Agreement
	Run 2 vs. Run 3	0.9363	Agreement

***Table A.13**. Freeman-Halton Test Results for Automation-Run Particle Shape (Aspect Ratio).*

Sample	Comparison	Approximate P-Value	Conclusion
Sample 1	Run 1 vs. Run 2	0.9904	Agreement
	Run 1 vs. Run 3	0.9824	Agreement
	Run 2 vs. Run 3	0.9746	Agreement
Sample 2	Run 1 vs. Run 2	0.9497	Agreement
	Run 1 vs. Run 3	0.8978	Agreement
	Run 2 vs. Run 3	0.9356	Agreement
Sample 3	Run 1 vs. Run 2	0.9938	Agreement
	Run 1 vs. Run 3	0.9846	Agreement
	Run 2 vs. Run 3	1	Agreement
Sample 4	Run 1 vs. Run 2	0.8308	Agreement
	Run 1 vs. Run 3	0.9531	Agreement
	Run 2 vs. Run 3	0.9057	Agreement
Sample 5	Run 1 vs. Run 2	0.9263	Agreement
	Run 1 vs. Run 3	0.9263	Agreement
	Run 2 vs. Run 3	0.9573	Agreement
Sample 6	Run 1 vs. Run 2	0.915	Agreement
	Run 1 vs. Run 3	0.9606	Agreement
	Run 2 vs. Run 3	0.9288	Agreement
Sample 7	Run 1 vs. Run 2	0.9736	Agreement
	Run 1 vs. Run 3	0.9047	Agreement
	Run 2 vs. Run 3	0.9522	Agreement
Sample 8	Run 1 vs. Run 2	0.9326	Agreement
	Run 1 vs. Run 3	0.886	Agreement
	Run 2 vs. Run 3	0.8009	Agreement
Sample 9	Run 1 vs. Run 2	0.9875	Agreement
	Run 1 vs. Run 3	0.7304	Agreement
	Run 2 vs. Run 3	0.617	Agreement
Sample 10	Run 1 vs. Run 2	0.8935	Agreement
	Run 1 vs. Run 3	0.9879	Agreement
	Run 2 vs. Run 3	0.9886	Agreement

***Table A.14**. Freeman-Halton Test Results for Automation-Run Particle Chemistry.*

Sample	Comparison	Approximate P-Value	Conclusion
Sample 1	Run 1 vs. Run 2	0.9501	Agreement
	Run 1 vs. Run 3	0.9787	Agreement
	Run 2 vs. Run 3	0.9963	Agreement
Sample 2	Run 1 vs. Run 2	0.4964	Agreement
	Run 1 vs. Run 3	0.2809	Agreement
	Run 2 vs. Run 3	0.754	Agreement
Sample 3	Run 1 vs. Run 2	0.989	Agreement
	Run 1 vs. Run 3	0.8701	Agreement
	Run 2 vs. Run 3	0.9344	Agreement
Sample 4	Run 1 vs. Run 2	0.8414	Agreement
	Run 1 vs. Run 3	0.9779	Agreement
	Run 2 vs. Run 3	0.3632	Agreement
Sample 5	Run 1 vs. Run 2	1	Agreement
	Run 1 vs. Run 3	0.1542	Agreement
	Run 2 vs. Run 3	0.2214	Agreement
Sample 6	Run 1 vs. Run 2	0.3841	Agreement
	Run 1 vs. Run 3	0.007468	Disagreement
	Run 2 vs. Run 3	0.241	Agreement
Sample 7	Run 1 vs. Run 2	0.8624	Agreement
	Run 1 vs. Run 3	0.6436	Agreement
	Run 2 vs. Run 3	0.8852	Agreement
Sample 8	Run 1 vs. Run 2	0.07946	Agreement
	Run 1 vs. Run 3	0.4708	Agreement
	Run 2 vs. Run 3	0.8496	Agreement
Sample 9	Run 1 vs. Run 2	0.8307	Agreement
	Run 1 vs. Run 3	0.7305	Agreement
	Run 2 vs. Run 3	0.61	Agreement
Sample 10	Run 1 vs. Run 2	0.9957	Agreement
	Run 1 vs. Run 3	0.908	Agreement
	Run 2 vs. Run 3	0.8415	Agreement

Appendix B. Chapter 3 Supplemental Data

Table B.1. *Dust Characteristic Data by Sample*

	Cross-Sectional Diameter			Aspect Ratio			Chemical Composition Category					
Sample Name	[0.94-2.0) µm	[2.0-3.0) µm	[3.0-9.0) µm	<1.5	[1.5-3)	≥3	C	AS	Q	CB	HM	O
B-1-F-PC1	72%	19%	9%	28%	65%	7%	95%	1%	3%	1%	0%	0%
B-1-F-PC2	72%	17%	11%	50%	49%	1%	44%	29%	3%	22%	1%	1%
B-1-F-PC3	75%	18%	8%	52%	47%	1%	37%	33%	2%	26%	0%	1%
B-1-F-PC4	76%	19%	5%	49%	50%	2%	49%	27%	4%	19%	0%	1%
B-1-M-PC6	72%	19%	10%	31%	67%	2%	5%	93%	1%	0%	0%	0%
B-1-M-PC7	73%	17%	10%	38%	60%	2%	24%	69%	4%	1%	1%	1%
B-1-I-PC8	79%	14%	7%	57%	42%	0%	15%	13%	0%	71%	0%	1%
B-1-I-PC9	86%	12%	2%	57%	43%	0%	7%	8%	1%	83%	0%	1%
B-1-I-PC11	85%	11%	4%	58%	41%	1%	10%	3%	1%	85%	0%	1%
B-1-I-PC12	86%	10%	4%	57%	42%	1%	11%	5%	0%	83%	0%	1%
B-1-R-PC13	67%	25%	8%	38%	60%	2%	14%	76%	4%	4%	1%	0%
B-1-R-PC14	75%	18%	7%	42%	57%	1%	15%	76%	5%	3%	0%	0%
B-1-R-PC16	72%	20%	8%	41%	57%	2%	11%	81%	5%	3%	0%	0%
B-1-R-PC17	71%	20%	10%	36%	62%	2%	14%	81%	2%	1%	0%	0%
B-1-B-PC19	68%	20%	12%	33%	65%	2%	3%	91%	3%	2%	0%	1%
B-1-B-PC21	73%	17%	10%	36%	53%	12%	84%	6%	1%	7%	0%	1%
B-1-M-PC23	56%	29%	16%	55%	44%	1%	9%	25%	2%	63%	1%	0%
B-1-M-PC24	64%	30%	6%	59%	41%	0%	5%	8%	0%	85%	0%	1%
B-1-M-PC26	65%	31%	4%	57%	43%	1%	6%	10%	0%	83%	0%	1%
B-1-M-PC27	64%	29%	7%	61%	38%	1%	17%	9%	2%	71%	0%	0%
B-1-B-PC37	68%	20%	12%	37%	60%	3%	8%	87%	2%	2%	0%	1%
B-1-B-PC38	72%	18%	10%	37%	60%	3%	13%	81%	4%	1%	1%	0%
B-2-I-PC28	33%	22%	45%	46%	53%	2%	4%	86%	4%	3%	1%	1%
B-2-I-PC29	54%	21%	25%	47%	52%	2%	25%	60%	9%	4%	1%	1%
B-2-I-PC31	51%	21%	29%	37%	61%	2%	33%	48%	9%	7%	1%	2%
B-2-I-PC32	39%	26%	35%	40%	58%	2%	5%	86%	2%	4%	1%	2%
B-2-R-PC33	65%	22%	12%	27%	71%	2%	1%	71%	28%	0%	0%	0%
B-2-R-PC34	70%	20%	10%	32%	66%	3%	1%	59%	39%	0%	0%	0%
B-2-R-PC36	71%	16%	13%	33%	66%	1%	1%	67%	32%	0%	0%	0%
B-2-R-PC39	65%	20%	15%	28%	70%	3%	2%	70%	27%	0%	0%	1%
B-2-B-PC41	62%	24%	13%	31%	66%	3%	0%	97%	3%	0%	0%	0%
B-2-B-PC42	64%	22%	14%	30%	66%	3%	0%	95%	3%	0%	0%	1%
B-2-B-PC51	63%	21%	17%	31%	66%	3%	0%	88%	11%	0%	0%	1%
B-2-B-PC59	61%	22%	17%	25%	63%	13%	92%	0%	1%	0%	0%	7%
B-2-M-PC43	44%	22%	34%	36%	61%	2%	9%	76%	12%	1%	2%	1%
B-2-M-PC46	43%	22%	35%	37%	62%	1%	19%	63%	13%	3%	1%	1%

B-2-M-PC52	52%	20%	28%	46%	52%	3%	22%	60%	13%	3%	1%	1%
B-2-M-PC53	49%	25%	26%	29%	68%	3%	8%	76%	11%	1%	1%	3%
B-2-F-PC61	69%	19%	13%	41%	58%	1%	59%	37%	3%	1%	0%	0%
B-2-F-PC63	70%	17%	13%	40%	58%	1%	38%	44%	13%	2%	1%	2%
B-2-F-PC64	58%	23%	20%	40%	59%	1%	28%	49%	11%	7%	3%	1%
B-2-F-PC66	63%	24%	14%	40%	58%	2%	37%	46%	8%	8%	1%	1%
B-2-B-PC62	63%	24%	13%	33%	65%	2%	0%	97%	2%	0%	0%	0%
B-2-B-PC68	65%	19%	16%	28%	68%	3%	0%	97%	3%	0%	0%	0%
B-2-B-PC69	61%	20%	19%	28%	67%	5%	0%	100 %	0%	0%	0%	0%
B-2-B-PC71	63%	26%	12%	33%	65%	2%	0%	98%	1%	0%	0%	0%
B-3-I-PC72	69%	16%	15%	51%	47%	1%	10%	35%	8%	46%	1%	0%
B-3-I-PC73	77%	14%	9%	55%	44%	1%	17%	11%	7%	64%	0%	1%
B-3-I-PC74	64%	14%	21%	47%	53%	0%	13%	24%	8%	54%	1%	1%
B-3-I-PC76	60%	20%	19%	47%	51%	2%	27%	33%	12%	25%	1%	2%
B-3-R-PC77	66%	21%	13%	37%	60%	3%	5%	91%	4%	1%	0%	0%
B-3-R-PC78	72%	16%	12%	36%	62%	1%	23%	69%	7%	0%	1%	0%
B-3-R-PC79	68%	17%	15%	39%	58%	3%	16%	78%	4%	1%	0%	0%
B-3-R-PC81	59%	19%	22%	37%	60%	2%	6%	88%	4%	0%	0%	1%
B-3-B-PC87	44%	22%	33%	32%	66%	2%	2%	93%	2%	3%	0%	0%
B-3-B-PC89	67%	20%	12%	47%	52%	1%	20%	39%	8%	27%	3%	2%
B-3-B-PC91	68%	20%	12%	47%	51%	2%	13%	45%	9%	32%	1%	1%
B-3-B-PC94	67%	20%	13%	43%	55%	3%	28%	48%	7%	16%	0%	2%
B-3-M-PC83	65%	21%	14%	35%	64%	1%	16%	80%	3%	0%	0%	0%
B-3-M-PC86	68%	17%	15%	36%	62%	2%	16%	76%	6%	1%	1%	0%
B-3-M-PC88	68%	19%	13%	33%	65%	2%	10%	84%	5%	1%	0%	0%
B-3-M-PC92	70%	17%	12%	35%	63%	2%	11%	85%	4%	0%	0%	0%
B-3-F-PC82	53%	19%	28%	42%	54%	4%	55%	33%	4%	7%	0%	1%
B-3-F-PC84	66%	21%	13%	51%	48%	2%	36%	36%	5%	20%	1%	2%
B-3-F-PC93	64%	20%	16%	40%	57%	3%	43%	43%	5%	8%	1%	1%
B-3-F-PC96	69%	18%	13%	44%	53%	3%	39%	32%	5%	24%	0%	0%
B-4-I-PC97	46%	29%	25%	44%	55%	2%	13%	69%	9%	6%	2%	1%
B-4-I-PC99	49%	19%	31%	42%	56%	2%	16%	72%	6%	4%	2%	1%
B-4-I-PC104	41%	22%	37%	38%	60%	2%	10%	69%	7%	12%	0%	2%
B-4-I-PC106	68%	16%	16%	49%	49%	2%	19%	10%	1%	65%	0%	5%
B-4-R-PC98	73%	19%	9%	56%	43%	1%	11%	13%	2%	73%	0%	1%
B-4-R-PC101	66%	20%	14%	52%	46%	2%	12%	12%	2%	74%	0%	1%
B-4-R-PC102	69%	18%	13%	47%	51%	2%	17%	25%	8%	46%	1%	2%
B-4-R-PC103	38%	23%	39%	43%	55%	2%	14%	69%	4%	10%	0%	3%
B-4-B-PC107	73%	17%	11%	35%	63%	2%	29%	53%	17%	1%	0%	0%
B-4-B-PC108	80%	15%	5%	35%	64%	1%	30%	45%	25%	0%	0%	0%
B-4-B-PC109	79%	13%	8%	38%	60%	1%	28%	48%	22%	0%	1%	0%

B-4-B-PC111	73%	18%	8%	40%	58%	1%	31%	46%	21%	0%	2%	1%
B-4-F-PC112	69%	21%	10%	31%	61%	8%	67%	7%	10%	3%	3%	10%
B-4-F-PC113	52%	25%	23%	35%	62%	3%	55%	35%	5%	3%	0%	1%
B-4-F-PC114	52%	24%	25%	36%	59%	4%	63%	32%	2%	3%	1%	0%
B-4-F-PC116	56%	24%	20%	39%	58%	3%	56%	33%	3%	5%	1%	1%
A-5-R-PC1	60%	22%	18%	42%	56%	2%	30%	63%	2%	3%	1%	2%
A-5-R-PC2	57%	22%	21%	41%	57%	2%	23%	65%	1%	5%	2%	4%
A-5-R-PC3	61%	20%	19%	41%	57%	2%	32%	60%	2%	4%	0%	2%
A-5-R-PC4	67%	19%	14%	35%	63%	2%	28%	61%	2%	4%	1%	3%
A-5-I-PC6	34%	29%	37%	45%	54%	1%	10%	71%	4%	12%	2%	2%
A-5-I-PC8	38%	25%	38%	46%	53%	1%	16%	44%	5%	32%	1%	2%
A-5-I-PC9	38%	24%	38%	35%	63%	2%	6%	73%	8%	9%	0%	4%
A-5-I-PC11	49%	23%	28%	45%	53%	2%	32%	38%	3%	23%	1%	4%
A-5-H-PC12	48%	26%	26%	40%	57%	3%	31%	31%	3%	31%	1%	2%
A-5-H-PC13	49%	29%	23%	45%	53%	2%	31%	28%	2%	37%	1%	2%
A-5-H-PC14	34%	29%	37%	44%	54%	2%	20%	52%	2%	24%	0%	2%
A-5-C-PC16	40%	25%	35%	40%	58%	2%	4%	32%	2%	49%	0%	13%
A-5-C-PC17	46%	27%	26%	48%	51%	1%	14%	16%	2%	66%	1%	1%
A-5-C-PC18	50%	25%	25%	50%	49%	1%	24%	16%	2%	55%	2%	2%
A-5-C-PC19	45%	24%	31%	43%	55%	2%	8%	15%	1%	67%	0%	9%
A-5-MF-PC21	49%	28%	23%	37%	59%	3%	52%	30%	2%	16%	0%	1%
A-5-MF-PC22	51%	25%	24%	35%	63%	2%	42%	43%	2%	11%	1%	2%
A-5-MF-PC23	45%	26%	28%	41%	56%	3%	29%	54%	3%	11%	1%	2%
A-5-MF-PC24	41%	28%	31%	36%	61%	4%	43%	39%	2%	14%	1%	2%
A-5-T-PC26	55%	22%	23%	38%	59%	3%	21%	57%	4%	12%	1%	5%
A-5-T-PC27	60%	25%	15%	38%	58%	4%	24%	55%	2%	18%	0%	1%
A-5-T-PC28	59%	21%	20%	36%	62%	2%	31%	53%	2%	12%	1%	1%
A-5-T-PC29	63%	20%	17%	35%	64%	1%	36%	48%	5%	10%	1%	1%
A-5-B-PC31	46%	25%	29%	43%	55%	2%	22%	31%	9%	30%	3%	4%
A-5-B-PC32	50%	26%	24%	41%	57%	2%	32%	31%	1%	34%	0%	2%
A-5-B-PC33	57%	25%	18%	46%	53%	1%	35%	27%	3%	32%	2%	2%
A-5-B-PC34	46%	27%	28%	45%	53%	2%	21%	44%	4%	29%	1%	1%
A-5-F-PC36	62%	26%	12%	46%	53%	2%	34%	9%	1%	54%	0%	1%
A-5-F-PC37	66%	20%	15%	49%	50%	1%	38%	13%	1%	47%	0%	1%
A-5-F-PC38	66%	19%	15%	45%	54%	1%	45%	14%	1%	37%	0%	3%
A-5-F-PC39	56%	24%	20%	47%	51%	2%	28%	27%	2%	41%	0%	2%
A-5-F-PC41	41%	28%	30%	35%	61%	4%	54%	25%	1%	17%	0%	2%
A-5-F-PC42	45%	26%	29%	36%	60%	4%	20%	21%	1%	47%	0%	10%
A-5-F-PC43	41%	27%	32%	32%	62%	6%	78%	9%	1%	10%	0%	2%
A-5-F-PC44	48%	28%	24%	35%	61%	4%	18%	25%	0%	48%	0%	9%
A-5-R-PC46	69%	19%	11%	34%	62%	4%	1%	59%	0%	25%	0%	15%

A-5-R-PC47	62%	23%	15%	33%	63%	4%	0%	40%	0%	36%	0%	24%
A-5-R-PC48	62%	24%	14%	34%	64%	2%	0%	46%	0%	34%	1%	20%
A-5-R-PC49	62%	23%	14%	33%	65%	3%	1%	23%	0%	56%	0%	20%
A-6-I-PC1	65%	20%	16%	35%	63%	2%	23%	49%	5%	19%	4%	0%
A-6-I-PC2	60%	21%	19%	36%	63%	1%	27%	29%	2%	36%	1%	6%
A-6-R-PC3	68%	19%	13%	29%	68%	3%	0%	15%	0%	44%	0%	41%
A-6-R-PC4	66%	21%	13%	34%	64%	3%	0%	9%	0%	75%	0%	17%
A-6-F-PC5	56%	19%	25%	38%	60%	2%	19%	27%	2%	45%	1%	7%
A-6-F-PC6	65%	23%	12%	42%	56%	2%	29%	31%	2%	31%	1%	5%
A-6-H-PC7	63%	22%	16%	46%	53%	1%	26%	6%	3%	61%	2%	1%
A-6-H-PC8	34%	20%	46%	45%	54%	1%	4%	6%	0%	86%	0%	4%
A-6-T-PC9	69%	18%	13%	38%	60%	2%	2%	2%	0%	95%	0%	2%
A-6-T-PC10	68%	20%	12%	41%	58%	1%	3%	5%	0%	90%	0%	2%
A-6-MF-PC11	40%	25%	35%	39%	58%	3%	72%	13%	0%	12%	1%	2%
A-6-MF-PC12	50%	23%	28%	39%	57%	4%	81%	9%	0%	7%	1%	1%
A-6-I-PC13	35%	26%	39%	45%	53%	1%	25%	4%	1%	68%	0%	2%
A-6-I-PC14	35%	23%	42%	43%	55%	2%	17%	5%	0%	75%	0%	4%
A-6-R-PC15	54%	28%	19%	46%	53%	1%	29%	10%	1%	57%	1%	1%
A-6-R-PC16	57%	29%	14%	44%	55%	1%	30%	11%	1%	55%	0%	2%
A-6-F-PC17	76%	15%	9%	41%	57%	2%	42%	25%	9%	21%	3%	1%
A-6-F-PC18	34%	25%	41%	38%	58%	4%	36%	15%	1%	43%	1%	4%
A-6-B-PC19	63%	27%	10%	41%	57%	2%	24%	18%	5%	44%	7%	2%
A-6-B-PC20	65%	20%	16%	39%	58%	3%	23%	15%	4%	53%	4%	1%
A-6-TR-PC21	75%	19%	6%	48%	52%	0%	19%	18%	3%	54%	5%	1%
A-6-TR-PC22	63%	22%	15%	44%	55%	1%	17%	17%	4%	54%	7%	2%
A-6-M-PC23	53%	27%	20%	39%	58%	2%	18%	11%	5%	58%	5%	3%
A-6-M-PC24	58%	25%	17%	51%	47%	2%	17%	12%	4%	61%	4%	2%
A-6-I-PC25	42%	23%	35%	39%	58%	3%	14%	9%	3%	67%	0%	7%
A-6-I-PC26	62%	24%	14%	39%	58%	2%	21%	6%	6%	64%	1%	1%
A-6-BD-PC27	62%	24%	14%	44%	51%	5%	68%	11%	2%	18%	0%	1%
A-6-BD-PC28	62%	22%	16%	40%	57%	3%	64%	14%	2%	18%	1%	2%
A-6-I-PC29	63%	22%	15%	49%	50%	1%	16%	6%	6%	68%	1%	3%
A-6-I-PC30	47%	24%	29%	41%	55%	3%	27%	7%	3%	61%	0%	3%
C-7-R-PC1	61%	22%	17%	36%	60%	3%	26%	63%	7%	4%	0%	0%
C-7-R-PC2	66%	19%	14%	36%	62%	2%	27%	58%	5%	8%	1%	0%
C-7-I-PC3	68%	21%	11%	45%	51%	4%	24%	8%	2%	61%	2%	3%
C-7-I-PC4	38%	25%	37%	38%	60%	2%	8%	55%	4%	29%	1%	4%
C-7-R-PC5	66%	18%	16%	34%	63%	3%	30%	64%	3%	2%	0%	1%
C-7-R-PC6	70%	17%	13%	41%	57%	2%	25%	67%	4%	3%	0%	0%
C-7-R-PC7	70%	19%	11%	35%	63%	2%	34%	55%	6%	3%	0%	1%
C-7-I-PC8	59%	22%	19%	43%	52%	5%	26%	26%	7%	40%	0%	1%

C-7-I-PC51	62%	20%	18%	44%	55%	2%	23%	21%	4%	51%	0%	1%
C-7-F-PC9	42%	25%	32%	46%	52%	2%	17%	59%	5%	16%	1%	2%
C-7-F-PC43	52%	27%	21%	42%	55%	3%	26%	36%	3%	33%	0%	2%
C-7-M-PC11	60%	22%	18%	45%	53%	2%	36%	48%	2%	13%	0%	0%
C-7-M-PC12	50%	25%	25%	38%	59%	2%	30%	53%	3%	11%	1%	1%
C-7-M-PC13	56%	22%	21%	40%	60%	1%	29%	51%	5%	13%	1%	1%
C-7-M-PC14	58%	19%	24%	31%	66%	3%	24%	59%	7%	9%	1%	2%
C-7-F-PC15	44%	25%	31%	36%	61%	2%	9%	79%	3%	6%	1%	1%
C-7-F-PC16	54%	24%	22%	38%	59%	2%	17%	75%	5%	2%	1%	1%
C-7-B-PC10	61%	23%	16%	34%	64%	2%	27%	36%	2%	32%	0%	2%
C-7-B-PC18	62%	20%	18%	34%	63%	3%	24%	50%	2%	20%	1%	2%
C-7-R-PC20	59%	21%	20%	30%	67%	3%	8%	83%	8%	0%	1%	0%
C-7-R-PC21	63%	21%	16%	35%	61%	4%	13%	71%	13%	1%	1%	1%
C-7-M-PVC17	61%	18%	20%	36%	62%	3%	27%	45%	4%	23%	0%	1%
C-7-M-PC19	56%	25%	19%	35%	61%	3%	26%	50%	3%	19%	0%	2%
C-7-B-PC49	57%	20%	23%	31%	67%	2%	14%	79%	3%	2%	0%	2%
C-7-B-PC50	54%	22%	23%	31%	67%	2%	12%	81%	3%	2%	0%	2%
C-7-F-PC30	50%	20%	30%	35%	62%	3%	10%	81%	4%	4%	1%	1%
C-7-F-PC31	52%	24%	24%	35%	62%	3%	10%	82%	1%	4%	2%	1%
C-7-M-PC23	58%	22%	20%	35%	63%	2%	10%	77%	6%	5%	0%	1%
C-7-M-PC25	52%	22%	27%	35%	61%	4%	14%	75%	5%	4%	1%	2%
C-8-TD-PC24	63%	23%	15%	28%	69%	3%	0%	40%	0%	36%	0%	23%
C-8-TD-PC22	66%	20%	13%	27%	70%	3%	0%	70%	0%	11%	0%	20%
C-8-M-PC39	73%	16%	12%	36%	62%	2%	23%	62%	11%	2%	0%	1%
C-8-M-PC40	79%	14%	7%	39%	59%	1%	30%	54%	14%	0%	0%	1%
C-8-I-PC51	37%	23%	40%	34%	62%	3%	6%	83%	6%	4%	0%	1%
C-8-I-PC52	38%	23%	39%	40%	59%	2%	12%	67%	5%	9%	1%	6%
C-8-F-PC32	45%	27%	28%	44%	55%	1%	20%	66%	5%	7%	1%	2%
C-8-F-PC47	48%	23%	29%	42%	56%	2%	17%	71%	5%	5%	0%	1%
C-8-I-PC27	29%	25%	46%	40%	57%	3%	15%	72%	4%	7%	1%	1%
C-8-I-PC28	33%	22%	45%	38%	59%	3%	19%	69%	2%	7%	1%	2%
C-8-F-PC37	50%	19%	31%	36%	61%	3%	18%	63%	8%	8%	1%	2%
C-8-F-PC38	42%	25%	34%	40%	56%	5%	24%	54%	5%	12%	2%	3%
C-8-R-PC41	65%	20%	15%	27%	70%	3%	0%	97%	1%	0%	0%	2%
C-8-R-PC42	57%	24%	19%	34%	64%	3%	9%	82%	7%	0%	0%	2%
C-8-R-PC29	71%	17%	12%	33%	65%	2%	15%	36%	48%	0%	0%	1%
C-8-R-PC26	69%	17%	14%	29%	70%	1%	9%	43%	47%	0%	0%	1%
C-8-I-PC35	32%	27%	41%	35%	59%	5%	16%	68%	5%	8%	1%	2%
C-8-I-PC36	36%	26%	39%	34%	62%	3%	8%	77%	5%	7%	0%	3%
C-8-R-PC33	47%	24%	29%	37%	62%	1%	15%	73%	3%	6%	0%	3%
C-8-R-PC34	50%	25%	25%	46%	51%	3%	18%	65%	9%	7%	1%	1%

C-8-F-PC53	58%	20%	22%	35%	63%	2%	12%	64%	19%	3%	1%	1%
C-8-F-PC54	61%	26%	14%	33%	64%	3%	24%	53%	18%	4%	0%	1%
C-8-M-PC44	61%	25%	15%	31%	65%	4%	3%	89%	6%	1%	0%	1%
C-8-M-PC46	59%	19%	22%	29%	65%	6%	5%	86%	8%	0%	0%	1%
C-8-M-PC21	65%	20%	15%	27%	70%	3%	0%	97%	1%	0%	0%	2%
C-8-M-PC58	68%	19%	12%	26%	70%	4%	0%	99%	0%	0%	1%	0%
C-8-B-PC55	60%	23%	17%	34%	63%	3%	10%	80%	7%	1%	0%	2%
C-8-B-PC56	68%	21%	12%	31%	66%	3%	13%	75%	11%	0%	0%	1%
C-8-B-PC48	71%	19%	11%	31%	67%	2%	17%	59%	23%	1%	0%	1%
C-8-B-PC54	71%	19%	10%	33%	64%	3%	16%	52%	32%	0%	0%	0%

Spatial and Temporal Variability

Table B.2*. Freeman-Halton test results for spatial variation between pairs of duplicate or samples (i.e., taken side-by-side in position 2 per Figure 3.1).*

Sample Group	Comparison	Approximate P-Value	Conclusion
Mine 1, Feeder	B-1-F-PC2 vs. B-1-F-PC3	0.8593	Agreement
Mine 1, Intake	B-1-I-PC9 vs. B-1-I-PC11	0.5887	Agreement
Mine 1, Return	B-1-R-PC14 vs. B-1-R-PC16	0.8512	Agreement
Mine 1, Continuous Miner	B-1-M-PC23 vs. B-1-M-PC24	0.0008334	Disagreement
Mine 1, Roof Bolter	B-1-B-PC37 vs. B-1-B-PC38	0.5352	Agreement
Mine 2, Intake	B-2-I-PC29 vs. B-2-I-PC31	0.5869	Agreement
Mine 2, Return	B-2-R-PC34 vs. B-2-R-PC36	0.6488	Agreement
Mine 2, Roof Bolter	B-2-B-PC42 vs. B-2-B-PC51	0.04892	Disagreement
Mine 2, Continuous Miner	B-2-M-PC46 vs. B-2-M-PC52	0.9894	Agreement
Mine 2, Feeder	B-2-F-PC61 vs. B-2-F-PC63	0.003464	Disagreement
Mine 2, Roof Bolter	B-2-B-PC69 vs. B-2-B-PC71	0.4975	Agreement
Mine 3, Intake	B-3-I-PC72 vs. B-3-I-PC76	0.00195	Disagreement
Mine 3, Return	B-3-R-PC78 vs. B-3-R-PC79	0.2759	Agreement
Mine 3, Roof Bolter	B-3-B-PC89 vs. B-3-B-PC94	0.1542	Agreement
Mine 3, Continuous Miner	B-3-M-PC83 vs. B-3-M-PC86	0.6392	Agreement
Mine 3, Feeder	B-3-F-PC82 vs. B-3-F-PC84	0.01953	Disagreement
Mine 4, Intake	B-4-I-PC97 vs. B-4-I-PC99	0.9289	Agreement
Mine 4, Return	B-4-R-PC98 vs. B-4-R-PC102	0.002727	Disagreement
Mine 4, Roof Bolter	B-4-B-PC107 vs. B-4-B-PC109	0.6483	Agreement
Mine 5, Return	A-5-R-PC2 vs. A-5-R-PC3	0.4888	Agreement
Mine 5, Intake	A-5-I-PC8 vs. A-5-I-PC11	0.1023	Agreement
Mine 5, Conveyor	A-5-C-PC17 vs. A-5-C-PC18	0.4998	Agreement
Mine 5, Midface	A-5-MF-PC22 vs. A-5-MF-PC23	0.5229	Agreement
Mine 5, Tailgate	A-5-T-PC27 vs. A-5-T-PC28	0.7076	Agreement

Mine 5, Roof Bolter	A-5-B-PC32 vs. A-5-T-PC33	0.7155	Agreement
Mine 5, Feeder	A-5-F-PC37 vs. A-5-F-PC38	0.5845	Agreement
Mine 5, Feeder	A-5-F-PC42 vs. A-5-F-PC43	5.575e-16	Disagreement
Mine 5, Return	A-5-R-PC47 vs. A-5-R-PC48	0.671	Agreement
Mine 6, Intake	A-6-I-PC1 vs. A-6-I-PC2	0.0006551	Disagreement
Mine 6, Return	A-6-R-PC3 vs. A-6-R-PC4	5.251e-05	Disagreement
Mine 6, Feeder	A-6-F-PC5 vs. A-6-F-PC6	0.3356	Agreement
Mine 6, Headgate	A-6-H-PC7 vs. A-6-H-PC8	3.905e-06	Disagreement
Mine 6, Tailgate	A-6-T-PC9 vs. A-6-T-PC10	0.6326	Agreement
Mine 6, Midface	A-6-MF-PC11 vs. A-6-MF-PC12	0.5602	Agreement
Mine 6, Intake	A-6-I-PC13 vs. A-6-I-PC14	0.4788	Agreement
Mine 6, Return	A-6-R-PC15 vs. A-6-R-PC16	0.9871	Agreement
Mine 6, Feeder	A-6-F-PC17 vs. A-6-F-PC18	0.0006586	Disagreement
Mine 6, Roof Bolter	A-6-B-PC19 vs. A-6-B-PC20	0.7977	Agreement
Mine 6, Continuous Miner	A-6-M-PC23 vs. A-6-M-PC24	0.9896	Agreement
Mine 6, Belt Drive	A-6-BD-PC27 vs. A-6-BD-PC28	0.9494	Agreement
Mine 6, Intake	A-6-I-PC29 vs. A-6-I-PC30	0.3602	Agreement
Mine 7, Return	C-7-R-PC1 vs. C-7-R-PC2	0.6108	Agreement
Mine 7, Return	C-7-R-PC5 vs. C-7-R-PC6	0.8324	Agreement
	C-7-R-PC5 vs. C-7-R-PC7	0.6981	Agreement
	C-7-R-PC6 vs. C-7-R-PC7	0.3955	Agreement
Mine 7, Intake	C-7-I-PC8 vs. C-7-I-PC51	0.5556	Agreement
Mine 7, Feeder	C-7-F-PC9 vs. C-7-F-PC43	0.00476	Disagreement
Mine 7, Continuous Miner	C-7-M-PC11 vs. C-7-M-PC12	0.7606	Agreement
Mine 7, Continuous Miner	C-7-M-PC13 vs. C-7-M-PC14	0.7898	Agreement
Mine 7, Feeder	C-7-F-PC15 vs. C-7-F-PC16	0.3531	Agreement
Mine 7, Roof Bolter	C-7-B-PC10 vs. C-7-B-PC18	0.2411	Agreement
Mine 7, Return	C-7-R-PC20 vs. C-7-R-PC21	0.2831	Agreement
Mine 7, Continuous Miner	C-7-M-PC17 vs. C-7-M-PC19	0.8824	Agreement
Mine 7, Roof Bolter	C-7-B-PC49 vs. C-7-B-PC50	0.9924	Agreement
Mine 7, Feeder	C-7-F-PC30 vs. C-7-F-PC31	0.8741	Agreement
Mine 7, Continuous Miner	C-7-M-PC23 vs. C-7-M-PC25	0.9088	Agreement
Mine 8, Trickle Duster	C-8-TD-PC22 vs. C-8-TD-PC24	1.57e-05	Disagreement
Mine 8, Continuous Miner	C-8-M-PC39 vs. C-8-M-PC40	0.4635	Agreement
Mine 8, Intake	C-8-I-PC51 vs. C-8-I-PC52	0.05533	Agreement
Mine 8, Feeder	C-8-F-PC32 vs. C-8-F-PC47	0.893	Agreement
Mine 8, Intake	C-8-I-PC27 vs. C-8-I-PC28	0.9092	Agreement
Mine 8, Feeder	C-8-F-PC37 vs. C-8-F-PC38	0.6122	Agreement

Mine 8, Return	C-8-R-PC41 vs. C-8-R-PC42	0.0002474	Disagreement
Mine 8, Return	C-8-R-PC26 vs. C-8-R-PC29	0.5405	Agreement
Mine 8, Intake	C-8-I-PC35 vs. C-8-I-PC36	0.4756	Agreement
Mine 8, Return	C-8-R-PC33 vs. C-8-R-PC34	0.3253	Agreement
Mine 8, Feeder	C-8-F-PC53 vs. C-8-F-PC54	0.2195	Agreement
Mine 8, Continuous Miner	C-8-M-PC44 vs. C-8-M-PC46	0.8256	Agreement
Mine 8, Continuous Miner	C-8-M-PC21 vs. C-8-M-PC58	0.3712	Agreement
Mine 8, Roof Bolter	C-8-B-PC55 vs. C-8-B-PC56	0.605	Agreement
Mine 8, Roof Bolter	C-8-B-PC48 vs. C-8-B-PC54	0.3756	Agreement

Table B.3*. Freeman-Halton test results for spatial variation of samples collected in proximity to one another at the same time. The average results for duplicate samples were used in this comparison.*

Sample Group	Comparison	Sample Position	Approximate P-Value	Conclusion
Mine 1, Feeder	B-1-F-PC2/3 vs. B-1-F-PC4	2 vs. 3	0.7965	Agreement
Mine 1, Intake	B-1-I-PC9/11 vs. B-1-I-PC8	2 vs. 1	0.1147	Agreement
	B-1-I-PC9/11 vs. B-1-I-PC12	2 vs. 3	0.9567	Agreement
	B-1-I-PC8 vs. B-1-I-PC12	1 vs. 3	0.1156	Agreement
Mine 1, Return	B-1-R-PC14/16 vs. B-1-R-PC13	2 vs. 1	0.9431	Agreement
	B-1-R-PC14/16 vs. B-1-R-PC17	2 vs. 3	0.554	Agreement
	B-1-R-PC13 vs. B-1-R-PC17	1 vs. 3	0.5088	Agreement
Mine 1, Continuous Miner	B-1-M-PC23/24 vs. B-1-M-PC26	2 vs. 3	0.4745	Agreement
	B-1-M-PC23/24 vs. B-1-M-PC27	2 vs. 1	0.0551	Agreement
	B-1-M-PC26 vs. B-1-M-PC27	3 vs. 1	0.03338	Disagreement
Mine 2, Intake	B-2-I-PC29/31 vs. B-2-I-PC28	2 vs. 3	7.297e-07	Disagreement
	B-2-I-PC29/31 vs. B-2-I-PC32	2 vs. 1	1.159e-06	Disagreement
	B-2-I-PC28 vs. B-2-I-PC32	3 vs. 1	0.9664	Agreement
Mine 2, Return	B-2-R-PC34/36 vs. B-2-R-PC33	2 vs. 1	0.5234	Agreement
	B-2-R-PC34/36 vs. B-2-R-PC39	2 vs. 3	0.4136	Agreement
	B-2-R-PC33 vs. B-2-R-PC39	1 vs. 3	1	Agreement
Mine 2, Roof Bolter	B-2-B-PC42/51 vs. B-2-B-PC41	2 vs. 1	0.2134	Agreement
Mine 2, Continuous Miner	B-2-M-PC46/52 vs. B-2-M-PC43	2 vs. 1	0.1231	Agreement
	B-2-M-PC46/52 vs. B-2-M-PC53	2 vs. 3	0.058	Agreement
	B-2-M-PC43 vs. B-2-M-PC53	1 vs. 3	0.9437	Agreement
Mine 2, Feeder	B-2-F-PC61/63 vs. B-2-F-PC64	2 vs. 1	0.03716	Disagreement
	B-2-F-PC61/63 vs. B-2-F-PC66	2 vs. 3	0.2735	Agreement
	B-2-F-PC64 vs. B-2-F-PC66	1 vs. 3	0.7366	Agreement
Mine 2, Roof Bolter	B-2-B-PC69/71 vs. B-2-B-PC62	2 vs. 1	0.6212	Agreement
	B-2-B-PC69/71 vs. B-2-B-PC68	2 vs. 3	0.6212	Agreement
	B-2-B-PC62 vs. B-2-B-PC68	1 vs. 3	1	Agreement

Mine 3, Intake	B-3-I-PC72/76 vs. B-3-I-PC73	2 vs. 3	0.0001665	Disagreement
	B-3-I-PC72/76 vs. B-3-I-PC74	2 vs. 1	0.1689	Agreement
	B-3-I-PC73 vs. B-3-I-PC74	3 vs.1	0.1367	Agreement
Mine 3, Return	B-3-R-PC78/79 vs. B-3-R-PC77	2 vs. 1	0.004727	Disagreement
	B-3-R-PC78/79 vs. B-3-R-PC81	2 vs. 3	0.008411	Disagreement
	B-3-R-PC77 vs. B-3-R-PC81	1 vs. 3	0.9343	Agreement
Mine 3, Roof Bolter	B-3-B-PC89/94 vs. B-3-B-PC87	2 vs. 3	9.102e-14	Disagreement
	B-3-B-PC89/94 vs. B-3-B-PC91	2 vs. 1	0.2958	Agreement
	B-3-B-PC87 vs. B-3-B-PC91	3 vs. 1	4.406e-13	Disagreement
Mine 3, Continuous Miner	B-3-M-PC83/86 vs. B-3-M-PC88	2 vs. 1	0.7063	Agreement
	B-3-M-PC83/86 vs. B-3-M-PC92	2 vs. 3	0.4752	Agreement
	B-3-M-PC88 vs. B-3-M-PC92	1 vs. 3	1	Agreement
Mine 3, Feeder	B-3-F-PC82/84 vs. B-3-F-PC93	2 vs. 3	0.7079	Agreement
	B-3-F-PC82/84 vs. B-3-F-PC96	2 vs. 1	0.2708	Agreement
	B-3-F-PC93 vs. B-3-F-PC96	3 vs. 1	0.01782	Disagreement
Mine 4, Intake	B-4-I-PC97/99 vs. B-4-I-PC104	2 vs. 1	0.2884	Agreement
Mine 4, Return	B-4-R-PC98/102 vs. B-4-R-PC101	2 vs. 3	0.3007	Agreement
	B-4-R-PC98/102 vs. B-4-R-PC103	2 vs. 1	2.785e-15	Disagreement
	B-4-R-PC101 vs. B-4-R-PC103	3 vs. 1	2.2e-16	Disagreement
Mine 4, Roof Bolter	B-4-B-PC107/109 vs. B-4-B-PC108	2 vs. 1	0.6485	Agreement
	B-4-B-PC107/109 vs. B-4-B-PC111	2 vs. 3	0.8895	Agreement
	B-4-B-PC108 vs. B-4-B-PC111	1 vs. 3	0.641	Agreement
Mine 4, Feeder	B-4-F-PC114 vs. B-4-F-PC113	2 vs. 1	0.6052	Agreement
	B-4-F-PC114 vs. B-4-F-PC116	2 vs. 3	0.8802	Agreement
	B-4-F-PC113 vs. B-4-F-PC116	1 vs. 3	0.9054	Agreement
Mine 5, Return	A-5-R-PC2/3 vs. A-5-R-PC1	2 vs. 1	0.9774	Agreement
	A-5-R-PC2/3 vs. A-5-R-PC4	2 vs. 3	1	Agreement
	A-5-R-PC1 vs. A-5-R-PC4	1 vs. 3	0.9895	Agreement
Mine 5, Intake	A-5-I-PC8/11 vs. A-5-I-PC6	2 vs. 1	0.0002713	Disagreement
	A-5-I-PC8/11 vs. A-5-I-PC9	2 vs. 3	9.199e-07	Disagreement
	A-5-I-PC6 vs. A-5-I-PC9	1 vs. 3	0.4087	Agreement
Mine 5, Headgate	A-5-H-PC13 vs. A-5-H-PC12	2 vs. 1	0.967	Agreement
	A-5-H-PC13 vs. A-5-H-PC14	2 vs. 3	0.007472	Disagreement
	A-5-H-PC12 vs. A-5-H-PC14	1 vs. 3	0.04986	Disagreement
Mine 5, Conveyor	A-5-C-PC17/18 vs. A-5-C-PC16	2 vs. 1	1.594e-05	Disagreement
	A-5-C-PC17/18 vs. A-5-C-PC19	2 vs. 3	0.02848	Disagreement
	A-5-C-PC16 vs. A-5-C-PC19	1 vs. 3	0.01579	Disagreement
Mine 5, Midface	A-5-MF-PC22/23 vs. A-5-MF-PC21	2 vs. 1	0.04337	Disagreement
	A-5-MF-PC22/23 vs. A-5-MF-PC24	2 vs. 3	0.7998	Agreement
	A-5-MF-PC21 vs. A-5-MF-PC24	1 vs. 3	0.6365	Agreement
Mine 5, Tailgate	A-5-T-PC27/28 vs. A-5-T-PC26	2 vs. 1	0.4406	Agreement
	A-5-T-PC27/28 vs. A-5-T-PC29	2 vs. 3	0.5813	Agreement

	A-5-T-PC26 vs. A-5-T-PC29	1 vs. 3	0.1453	Agreement
Mine 5, Roof Bolter	A-5-T-PC32/33 vs. A-5-T-PC31	2 vs. 1	0.1089	Agreement
	A-5-T-PC32/33 vs. A-5-T-PC34	2 vs. 3	0.1369	Agreement
	A-5-T-PC31 vs. A-5-T-PC34	1 vs. 3	0.2346	Agreement
Mine 5, Feeder	A-5-F-PC37/38 vs. A-5-F-PC36	2 vs. 1	0.4068	Agreement
	A-5-F-PC37/38 vs. A-5-F-PC39	2 vs. 3	0.09208	Agreement
	A-5-F-PC36 vs. A-5-F-PC39	1 vs. 3	0.007114	Disagreement
Mine 5, Feeder	A-5-F-PC42/43 vs. A-5-F-PC41	2 vs. 1	0.07031	Agreement
	A-5-F-PC42/43 vs. A-5-F-PC44	2 vs. 3	4.516e-05	Disagreement
	A-5-F-PC41 vs. A-5-F-PC44	1 vs. 3	1.454e-08	Disagreement
Mine 5, Return	A-5-R-PC47/48 vs. A-5-R-PC46	2 vs. 1	0.0677	Agreement
	A-5-R-PC47/48 vs. A-5-R-PC49	2 vs. 3	0.004015	Disagreement
	A-5-R-PC46 vs. A-5-R-PC49	1 vs. 3	7.401e-07	Disagreement

Table B.4*. Freeman-Halton test results for temporal variation of samples collected in the same general area at different times.*

Sample Group	**Comparison**	**Approximate P-Value**	**Conclusion**
Mine 1, Roof Bolter	B-1-B-PC-19 vs. B-1-B-PC37/38	0.2403	Agreement
Mine 2, Roof Bolter	B-2-B-PC41/42/51 vs. B-2-B-PC62/68/69/71	0.1697	Agreement
Mine 5, Return	A-5-R-PC1/2/3/4 vs. A-5-R-PC46/47/48/49	2.2e-16	Disagreement
Mine 5, Feeder	A-5-F-PC36/37/38/39 vs. A-5-F-PC41/42/43/44	0.1906	Agreement
Mine 7, Return	C-7-R-PC1/2 vs. C-7-R-PC5/6/7	0.7003	Agreement
Mine 7, Feeder	C-7-F-PC15/16 vs. C-7-F-PC30/31	0.9548	Agreement
Mine 7, Continuous Miner	C-7-M-PC13/14 vs. C-7-M-PC17/19	0.402	Agreement
Mine 8, Feeder	C-8-F-PC32/47 vs. C-8-F-PC37/38	0.7507	Agreement

Regional Variability

Particle Cross-Sectional Diameter

Table B.5*. t-critical two-tail: 1.98*

[0.94-2.0) µm	NA	MCA	SCA
NA	-	5.72	-1.23
MCA	5.72	-	4.10
SCA	-1.23	4.10	-

Table B.6*. t-critical two-tail: 1.98*

[2.0-3.0) µm	NA	MCA	SCA
NA	-	-6.02	3.49
MCA	-6.02	-	-2.77
SCA	3.49	-2.77	-

***Table B.7**. t-critical two-tail: 1.98*

[≥3.0) µm	NA	MCA	SCA
NA	-	-4.51	0.33
MCA	-4.51	-	-3.93
SCA	0.33	-3.93	-

Particle Aspect Ratio

***Table B.8**. t-critical two-tail: 1.98*

<1.5	NA	MCA	SCA
NA	-	0.12	5.62
MCA	0.12	-	4.33
SCA	5.62	4.33	-

***Table B.9**. t-critical two-tail: 1.98*

[1.5-3.0)	NA	MCA	SCA
NA	-	-0.15	-5.39
MCA	-0.15	-	-4.24
SCA	-5.39	-4.24	-

Particle Chemistry

***Table B.10**. t-critical two-tail: 1.98*

C	NA	MCA	SCA
NA	-	-1.48	3.83
MCA	-1.48	-	1.82
SCA	3.83	1.82	-

Table B.11. *t-critical two-tail: 1.98*

AS	NA	MCA	SCA
NA	-	6.24	-10.73
MCA	6.24	-	-2.58
SCA	-10.73	-2.58	-

Table B.12. *t-critical two-tail: 1.98*

Q	NA	MCA	SCA
NA	-	5.26	-4.14
MCA	5.26	-	-0.40
SCA	-4.14	-0.40	-

***Table B.13**. t-critical two-tail: 1.98*

CB	NA	MCA	SCA
NA	-	-5.22	8.72
MCA	-5.22	-	2.18
SCA	8.72	2.18	-

***Table B.14**. t-critical two-tail: 1.98*

HM	NA	MCA	SCA
NA	-	-2.82	3.10
MCA	-2.82	-	0.44
SCA	3.10	0.44	-

***Table B.15**. t-critical two-tail: 1.98*

O	NA	MCA	SCA
NA	-	-4.40	2.61
MCA	-4.40	-	-2.17
SCA	2.61	-2.17	-

Mine-to-Mine Variability within Regions

Particle Cross-Sectional Diameter

***Table B.16**. t-critical two-tail: 2.00*

NA **[2.0-3.0) µm**	Mine 5	Mine 6
Mine 5	-	-2.57
Mine 6	-2.57	-

***Table B.17**. t-critical two-tail: 2.02*

MCA [0.94-2.0) µm	Mine 1	Mine 2	Mine 3	Mine 4
Mine 1	-	5.34	3.20	2.88
Mine 2	5.34	-	2.63	-0.81
Mine 3	3.20	2.63	-	0.98
Mine 4	2.88	-0.81	0.98	-

***Table B.18**. t-critical two-tail: 2.05*

MCA **[3.0-9.0) µm**	Mine 1	Mine 2	Mine 3	Mine 4
Mine 1	-	-5.89	-5.22	-3.70
Mine 2	-5.89	-	-1.84	0.59
Mine 3	-5.22	-1.84	-	-0.80
Mine 4	-3.70	0.59	-0.80	-

Particle Aspect Ratio

Table B.19. *t-critical two-tail: 2.03*

MCA **<1.5**	Mine 1	Mine 2	Mine 3	Mine 4
Mine 1	-	4.15	1.53	1.61
Mine 2	4.15	-	3.41	-2.92
Mine 3	1.53	3.41	-	0.20
Mine 4	1.61	-2.92	0.20	-

Table B.20. *t-critical two-tail: 2.03*

MCA [1.5-3)	Mine 1	Mine 2	Mine 3	Mine 4
Mine 1	-	-4.50	-1.68	-1.64
Mine 2	-4.50	-	-3.41	3.26
Mine 3	-1.68	-3.41	-	-5.3E-15
Mine 4	-1.64	3.26	-5.3E-15	-

Table B.21. *t-critical two-tail: 2.00*

SCA <1.5	Mine 7	Mine 8
Mine 7	-	-2.15
Mine 8	-2.15	-

***Table B.22**. t-critical two-tail: 2.00*

SCA **[1.5-3)**	Mine 7	Mine 8
Mine 7	-	2.06
Mine 8	2.06	-

Particle Chemistry

***Table B.23**. t-Critical two-tail: 2.00*

NA **AS**	Mine 5	Mine 6
Mine 5	-	-7.08
Mine 6	-7.08	-

***Table B.24**. t-Critical two-tail: 2.00*

NA **CB**	Mine 5	Mine 6
Mine 5	-	4.49
Mine 6	4.49	-

***Table B.25**. t-Critical two-tail: 2.03*

NA **HM**	Mine 5	Mine 6
Mine 5	-	2.53
Mine 6	2.53	-

Table B.26*. t-Critical two-tail: 2.02*

MCA **AS**	Mine 1	Mine 2	Mine 3	Mine 4
Mine 1	-	-3.09	-1.53	0.17
Mine 2	-3.09	-	-1.74	3.92
Mine 3	-1.53	-1.74	-	2.00
Mine 4	0.17	3.92	2.00	-

***Table B.27**. t-Critical two-tail: 2.05*

MCA **Q**	Mine 1	Mine 2	Mine 3	Mine 4
Mine 1	-	-3.89	-5.68	-3.38
Mine 2	-3.89	-	-2.20	0.60
Mine 3	-5.68	-2.20	-	-1.54
Mine 4	-3.38	0.60	-1.54	-

***Table B.28**. t-Critical two-tail: 2.05*

MCA **CB**	Mine 1	Mine 2	Mine 3	Mine 4
Mine 1	-	3.97	1.81	1.30
Mine 2	3.97	-	3.30	-2.46
Mine 3	1.81	3.30	-	-0.31
Mine 4	1.30	-2.46	-0.31	-

***Table B.29**. t-Critical two-tail: 2.00*

SCA C	Mine 7	Mine 8
Mine 7	-	-3.89
Mine 8	-3.89	-

***Table B.30**. t-Critical two-tail: 2.00*

SCA AS	Mine 7	Mine 8
Mine 7	-	2.28
Mine 8	2.28	-

Table B.31. *t-Critical two-tail: 2.04*

SCA **Q**	Mine 7	Mine 8
Mine 7	-	2.63
Mine 8	2.63	-

Table B.32. *t-Critical two-tail: 2.02*

SCA **CB**	Mine 7	Mine 8
Mine 7	-	-2.99
Mine 8	-2.99	-

Locational Variability

Particle Cross-Sectional Diameter

Table B.33. *t-critical two-tail: 1.99*

[0.94-2.0) µm	Intake	Feeder	Production	Return
Intake	-	-1.39	-3.15	-4.33
Feeder	-1.39	-	-2.23	-3.88
Production	-3.15	-2.23	-	-1.95
Return	-4.33	-3.88	-1.95	-

***Table B.34**. t-critical two-tail: 1.99*

[3.0-9.0) µm	Intake	Feeder	Production	Return
Intake	-	2.18	4.09	5.12
Feeder	2.18	-	2.36	3.77
Production	4.09	2.36	-	1.62
Return	5.12	3.77	1.62	-

Particle Aspect Ratio

***Table B.35**. t-critical two-tail: 1.98*

<1.5	Intake	Feeder	Production	Return
Intake	-	2.54	5.15	5.41
Feeder	2.54	-	2.84	3.12
Production	5.15	2.84	-	0.27
Return	5.41	3.12	0.27	-

***Table B.36**. t-critical two-tail: 1.98*

[1.5-3)	Intake	Feeder	Production	Return
Intake	-	-2.24	-5.08	-5.56
Feeder	-2.24	-	-3.33	-3.90
Production	-5.08	-3.33	-	-0.65
Return	-5.56	-3.90	-0.65	-

***Table B.37**. t-critical two-tail: 1.98*

≥3	Intake	Feeder	Production	Return
Intake	-	-2.85	-2.58	-1.88
Feeder	-2.85	-	0.22	1.61
Production	-2.58	0.22	-	1.32
Return	-1.88	1.61	1.32	-

Particle Chemistry

***Table B.38**. t-critical two-tail: 1.99*

C	Intake	Feeder	Production	Return
Intake	-	-5.53	-1.39	1.60
Feeder	-5.53	-	3.79	6.19
Production	-1.39	3.79	-	2.43
Return	1.60	6.19	2.43	-

***Table B.39**. t-critical two-tail: 1.99*

AS	Intake	Feeder	Production	Return
Intake	-	0.29	-3.66	-3.14
Feeder	0.29	-	-4.55	-3.92
Production	-3.66	-4.55	-	0.52
Return	-3.14	-3.92	0.52	-

***Table B.40**. t-critical two-tail: 1.99*

CB	Intake	Feeder	Production	Return
Intake	-	3.37	4.99	3.39
Feeder	3.37	-	1.91	0.46
Production	4.99	1.91	-	-1.11
Return	3.39	0.46	-1.11	-

***Table B.41**. t-critical two-tail: 1.99*

HM	Intake	Feeder	Production	Return
Intake	-	1.08	0.94	3.08
Feeder	1.08	-	-0.09	2.83
Production	0.94	-0.09	-	2.50
Return	3.08	2.83	2.50	-

***Table B.42**. t-critical two-tail: 1.99*

O	Intake	Feeder	Production	Return
Intake	-	-0.64	3.74	-1.96
Feeder	-0.64	-	2.90	-1.63
Production	3.74	2.90	-	-2.82
Return	-1.96	-1.63	-2.82	-